AD-A031 292 COLORADO UNIV BOULDER DEPT OF ASTRO-GEOPHYSICS F/G 20/9
PUMP WAVENUMBER DEPENDENT EFFECTS IN THE PARAMETRIC INSTABILITI--ETC(U)
JUL 76 S J BARDWELL F44620-73-C-0003
UNCLASSIFIED CU-1019-A5 AFOSR-TR-76-1116-ATTACH-5 NL

1 OF 2
ADA031292

DEPARTMENT OF ASTRO-GEOPHYSICS

UNIVERSITY OF COLORADO, BOULDER, COLORADO 80302

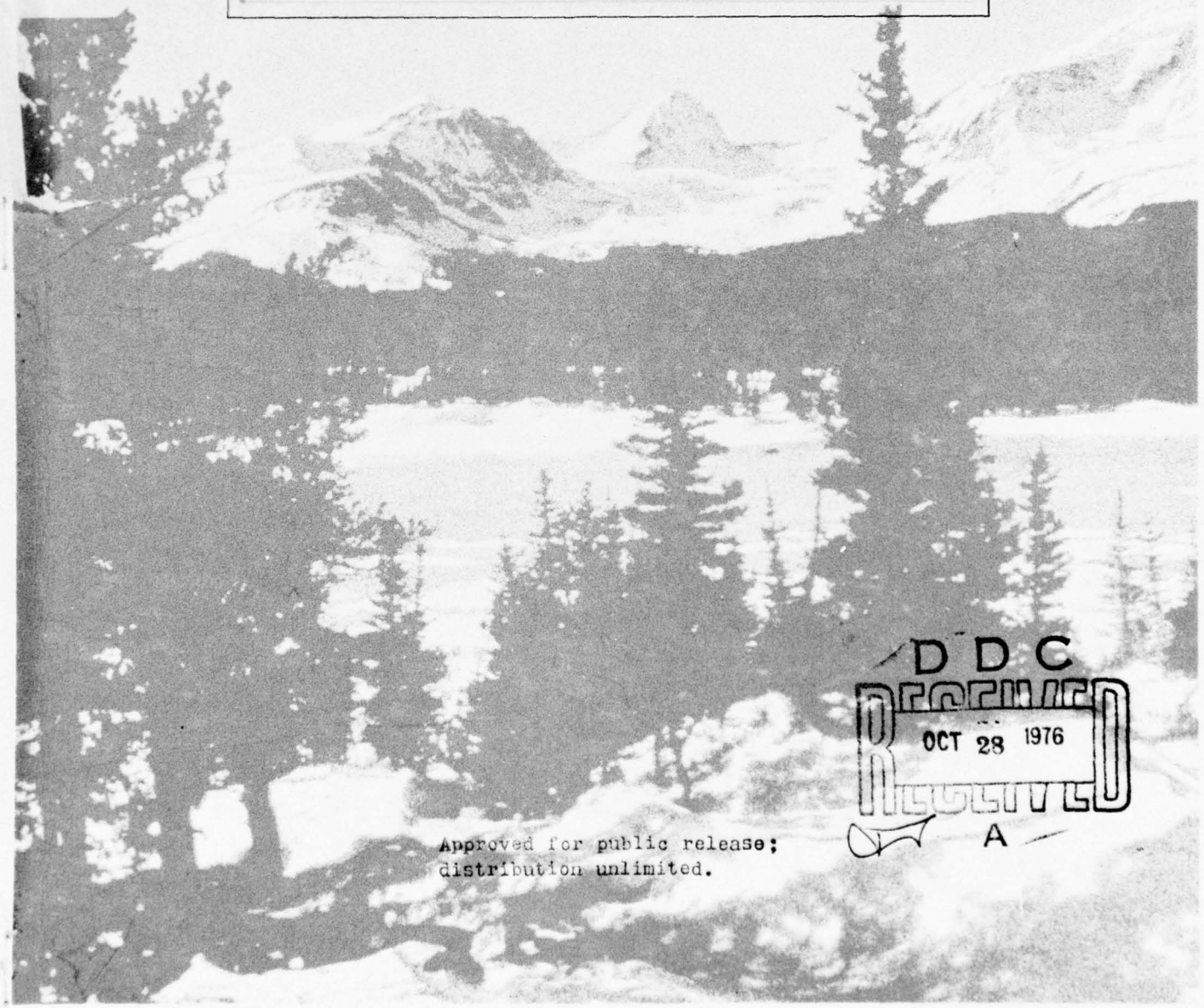

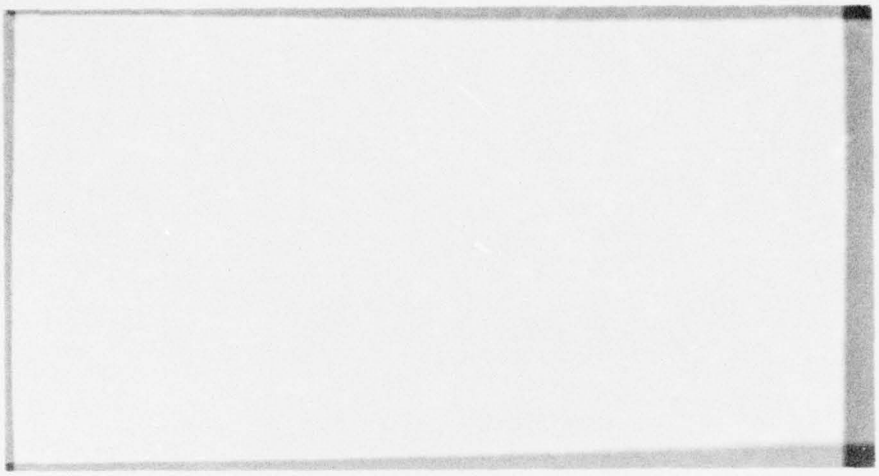

AIR FORCE OFFICE OF SCIENTIFIC RESEARCH (AFSC)
NOTICE OF TRANSMITTAL TO DDC
This technical report has been reviewed and is
approved for publication IAW AFR 190-12 (7b).
Distribution is unlimited.
A. D. BLOSE
Technical Information Officer

(9)

AFOSR - TR - 76 - 1116 Atch 5

Air Force Office of Scientific Research

FINAL REPORT - Attachment A5

#F44620-73-C-0003

PUMP WAVENUMBER DEPENDENT EFFECTS IN THE PARAMETRIC INSTABILITIES OF A PLASMA

Steven J. Bardwell

June 1976 (Ph.D. Thesis) CU #1019-A5

UNCLASSIFIED

SECURITY CLASSIFICATION OF THIS PAGE (When Data Entered)

REPORT DOCUMENTATION PAGE	READ INSTRUCTIONS BEFORE COMPLETING FORM
1. REPORT NUMBER: AFOSR - TR - 76 - 1116 Atch 5	2. GOVT ACCESSION NO. / 3. RECIPIENT'S CATALOG NUMBER (9)
4. TITLE (and Subtitle): PUMP WAVENUMBER DEPENDENT EFFECTS IN THE PARAMETRIC INSTABILITIES OF A PLASMA. (6)	5. TYPE OF REPORT & PERIOD COVERED: FINAL REPORT, - ATTACH.
	6. PERFORMING ORG. REPORT NUMBER: CU -1019-A5 (14)
7. AUTHOR(s): Steven J. Bardwell (10)	8. CONTRACT OR GRANT NUMBER(s): F44620-73-C-0003 (15)
9. PERFORMING ORGANIZATION NAME AND ADDRESS: University of Colorado, Department of Astro-Geophysics, Boulder, Colorado 80309	10. PROGRAM ELEMENT, PROJECT, TASK AREA & WORK UNIT NUMBERS: 9751-03
11. CONTROLLING OFFICE NAME AND ADDRESS: AFOSR/NP, Bolling AFB, D.C. 20332 (11)	12. REPORT DATE: 31 July 1976; 13. NUMBER OF PAGES: 155
14. MONITORING AGENCY NAME & ADDRESS (if different from Controlling Office) (12) 156p.	15. SECURITY CLASS. (of this report): UNCLASSIFIED; 15a. DECLASSIFICATION/DOWNGRADING SCHEDULE
16. DISTRIBUTION STATEMENT (of this Report): (16) AF-9751; Approved for Public Release; Distribution Unlimited (17) 9751-03	
17. DISTRIBUTION STATEMENT (of the abstract entered in Block 20, if different from Report): (18) AFOSR (19) TR-76-1116-ATCH 5	
18. SUPPLEMENTARY NOTES: TECH, OTHER	
19. KEY WORDS (Continue on reverse side if necessary and identify by block number)	

20. ABSTRACT (Continue on reverse side if necessary and identify by block number)

THIS PAPER DERIVES

We have derived a linear kinetic theory of parametric instabilities in an infinite, homogeneous, fully ionized plasma, with no magnetic field. Our derivation relaxes three assumptions usually made in the linear theory of certain parametric instabilities:

1) We do not assume that k_o, the wavenumber of the pump (the driving field of the instability), is much smaller than any other inverse distance in the plasma; → cont.

DD FORM 1 JAN 73 1473 EDITION OF 1 NOV 65 IS OBSOLETE

UNCLASSIFIED

088425

AB

20. Abstract, continued

2) We do not restrict ourselves growth of the instability in one dimension; and,

3) We consider a standing-wave pump, in addition to the usual travelling-wave pump.

Using this generalized formalism, we have studied the important problem of the parametric instabilities, in three dimensions, pumped by a monochromatic, longitudinal pump or arbitrary wavevector. By solving a dispersion relation derived for these instabilities, numerically and analytically, we have found a number of new, three-dimensional effects.

1) Only under quite restrictive conditions on $\underline{k}_o$ does the oscillating two stream (OTS) instability have its fastest growing daughter waves with wavenumbers that are parallel to $\underline{k}_o$: when $k_o \gtrsim k$, these daughter waves can grow at as much of an angle to k_o as 20^o.

2) The Langmuir-pumped electron-ion decay (EID) instability, for arbitrary $\underline{k}_o$, has regimes in which it is a forward scattering instability (as well as the usual back-scattering regimes in the case that $k_o > \sqrt{2\alpha/3}$).

3) A new instability, which is only seen in three dimensions, is possible. This instability, the stimulated modulational (SM) instability, can produce daughter waves at an angle to k_o, with wavenumbers slightly larger than k_o.

PUMP WAVENUMBER DEPENDENT EFFECTS IN THE PARAMETRIC INSTABILITIES OF A PLASMA

by

Steven Jack Bardwell

B.A., Swarthmore College, 1971

A thesis submitted to the Faculty of the Graduate School of the University of Colorado in partial fulfillment of the requirements for the degree of Doctor of Philosophy

Department of Physics and Astrophysics

1976

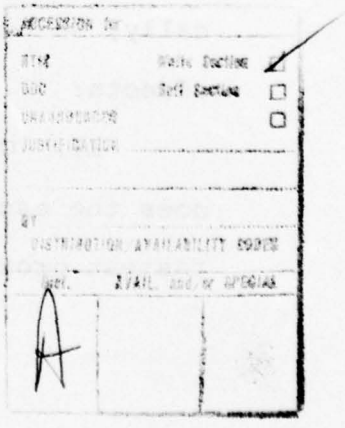

Bardwell, Steven Jack (Ph.D., Physics)

Pump Wavenumber Dependent Effects in the Parametric Instabilities of a Plasma

Thesis directed by Professor Martin V. Goldman

We have derived a linear kinetic theory of parametric instabilities in an infinite, homogeneous, fully ionized plasma, with no magnetic field. Our derivation relaxes three assumptions usually made in the linear theory of certain parametric instabilities:

1). We do not assume that $\underline{k}_o$, the wavenumber of the pump (the driving field of the instability), is much smaller than any other inverse distance in the plasma;

2). We do not restrict ourselves growth of the instability in one dimension; and,

3). We consider a standing-wave pump, in addition to the usual travelling-wave pump.

Using this generalized formalism, we have studied the important problem of the parametric instabilities, in three dimensions, pumped by a monochromatic, longitudinal pump of arbitrary wavevector. By solving a dispersion relation derived for these instabilities, numerically and analytically, we have found a number of new, three-dimensional effects:

1). Only under quite restrictive conditions on $\underline{k}_o$ does the oscillating two stream (OTS) instability have its fastest growing daughter waves with wavenumbers that are

parallel to $\underline{k}_o$; when $k_o \gtrsim k$, these daughter waves can grow at as much of an angle to k_o as 20°.

2). The Langmuir-pumped electron-ion decay (EID) instability, for arbitrary $\underline{k}_o$, has regimes in which it is a forward scattering instability (as well as the usual backscattering regimes in the case that $k_o > \sqrt{2\alpha/3}$).

3). A new instability, which is only seen in three dimensions, is possible. This instability, the stimulated modulational (SM) instability, can produce daughter waves at an angle to k_o, with wavenumbers slightly larger than k_o.

We have applied these results to three physical situations modelled on an electron stream quasilinearly generating a Langmuir spectrum of sufficient intensity to act as a pump:

1). Type III solar radio bursts. We find that three dimensional effects are critical in understanding the relaxation of Langmuir waves at distances less than 450 $R_\odot$.

2). Auroral streams. Our results show a one-dimensional treatment is sufficient in this case, although three dimensional effects are very likely to be important in determining the saturated state of the instability.

3). Laboratory electron beams. We conclude here that parametric effects dominate the wave dynamics for a "slow" beam, but that this is not the case for faster beams.

In none of these cases do we find parametric processes that

greatly affect the quasilinear decay of the beam, contrary to the findings of several authors who have examined similar applications of parametric instabilities.

We have also studied the effects of a standing-wave pump of arbitrary $\underline{k}_o$ for two parametric instabilities, the $2\omega_{pe}$ and EID instabilities. The most important result of a standing-wave pump for these instabilities is a reduction of the effective power of the pump. This is a result of different modes of the plasma being excited by each of the two components of the standing-wave pump; these excited modes are coupled more strongly (raising the effective pump power) as the (k_o-dependent) frequency separation of the modes decreases relative to the growth rate of the instability. As k_o goes to zero, and a standing-wave becomes indistinguishable from a travelling-wave, we recover the travelling-wave results. When we apply our results for the EID instability to ionospheric modification data, we find the decrease in the effective pump power resulting from a standing-wave pump, lowers the theoretical predictions for the Langmuir turbulence produced in these experiments.

TABLE OF CONTENTS

LIST OF TABLES

LIST OF FIGURES

CHAPTER TWO

LIST OF TABLES

FIGURE PAGE

CHAPTER I

INTRODUCTION

The coupling of normal modes of a linear system by a time-dependent interaction is a phenomenon first noted by Faraday[1] in 1831 and studied theoretically by Lord Rayleigh[2] in 1883. Now called parametric excitation, the study of these processes provides a general and powerful framework for studying linear responses of a system. In this dissertation, the theory of the parametric excitations of an infinite, homogeneous, fully-ionized plasma is extended to include two effects dependent on the wavevector, $\underset{\sim}{k}_o$, of the driving field of the instability:

1). The effects of this driving field (the "pump") being a standing-wave field rather than the usual travelling-wave field.

2). Three dimensional effects of a longitudinally polarized pump with arbitrary wavevector.

We have found that in a large number of physical situations the spatial dependence of the parametric coupling, dependent on $\underset{\sim}{k}_o$, is important in determining both qualitative and quantitative features of this plasma interaction.

The first systematic observations of parametric excitation were done by Michael Faraday, when he noted that

he could maintain water waves at half the frequency of the vibrating support which generated them. In 1859, F. Melde[3] published results of an exhaustive study he had carried out of the excitation of transverse modes of a vibrating wire which could be amplified by a longitudinal vibration of the wire at twice the transverse frequency. Lord Rayleigh made several theoretical studies of this problem, and his results exhibited the two characteristic features of parametric excitation: the existence of approximate frequency matching (in the examples given above, the excited disturbances occurred at half the frequency of the driver, or "pump"), and a threshold power for the pump, above which the normal modes of the system begin to be amplified.

A much more commonplace example of this phenomenon is the energy transfer that occurs in a child's pumping a swing. The time-varying element in this otherwise simple pendulum is the raising and lowering of the effective length of the pendulum; the child raises his center of gravity as the swing goes up and lowers it as the swing comes down. The frequency of this variation is twice that of the natural frequency of the swing. This "pumping" couples together the two, here degenerate, normal modes of the pendulum, with the frequency matching condition:

$$\omega_{pump} = |\omega_1| + |\omega_2| = |\omega| + |-\omega| = 2\omega.$$

And, if this pumping is of sufficient amplitude, then both normal modes become unstable and energy is transferred to these modes.

In general, parametric excitation occurs when several otherwise independent resonances of a system are coupled together by some time-varying parameter of the system. If amplification of these normal modes is to occur, the time variation of this parameter is not arbitrary, but rather is fixed by a condition, dependent on the frequencies of the normal modes which are being amplified. When there is dissipation in the uncoupled modes, then a "threshold" power of the time-varying parameter exists, above which energy is transferred to the now-coupled normal modes. Notice that we have made the implicit assumption that the energy transfer is small enough that the pump remains essentially unaffected by the excitation of modes in the system; this is the origin of the term "parametric," the time-varying parameter being treated as having constant amplitude over many periods, and entering the calculations as a parameter in the growth rates of the excited modes. Current application of this principle is being made in many fields, including circuit design[4], non-linear optics[5], and several areas of plasma physics.

In the case of a plasma, parametric couplings occur in amazing variety, as a result of the multitude of waves possible in a plasma and the richness of the interactions among them. If we restrict ourselves to an infinite, homogeneous, unmagnetized, fully-ionized plasma, there are only three linear resonances possible, each with a well-known dispersion relation:

1). the electromagnetic wave, $\hat{e}\cdot\hat{k} = 0$ (see page 12 for our notation):

$$\frac{\omega_e}{\omega_{pe}} = \left[1 + (c^2k^2/v_e^2 k_{De}^2)\right]^{1/2}, \quad v_e^2 k_{De}^2 = \omega_{pe}^2 = 4\pi ne^2/m_e;$$

2). the Langmuir wave, $\hat{e}\cdot\hat{k} = 1$,

$$\frac{\omega_L}{\omega_{pe}} = \left(1 + 3k^2/k_{De}^2\right)^{1/2}, \quad k_{De}^2 = 4\pi ne^2/\theta_e;$$

3). the ion-acoustic wave, $\hat{e}\cdot\hat{k} = 1$,

$$\frac{\omega_A}{\omega_{pe}} = \begin{cases} 1.7\,(m_e/m_i)^{1/2}\, k/k_{De}, & \theta_e \approx \theta_i, \\ (m_e/m_i)^{1/2}\, k/k_{De}, & \theta_e >> \theta_i. \end{cases}$$

Each of these waves has a well-understood dissipation which we list here as the imaginary part of the above frequencies:

1). the electromagnetic wave,[6]

$$\frac{\mathrm{Im}\,\omega_E}{\omega_E} \approx k_{De}^3 \ln(\theta_e/k\omega_{pe})/\left[6\sqrt{2}\,n\pi^{3/2}\omega_E\right];$$

2). the Langmuir wave,[6]

$$\frac{\mathrm{Im}\,\omega_L}{\omega_L} \approx \left(\frac{\pi}{2}\right)^{1/2} e^{-3/2}\left(\frac{k_{De}^3}{k^3}\right)\exp\left(-k_{De}^2/k^2\right) + k_{De}^3 \ln(\theta_e/k\omega_{pe})/(6\sqrt{2}\,n\pi^{3/2});$$

3). the ion-acoustic wave,[7]

$$\frac{\mathrm{Im}\,\omega_A}{\omega_A} = \begin{cases} 0.41, & \theta_e \approx \theta_i; \\ (m_e/m_i)^{1/2}(\pi/8)^{1/2}, & \theta_e >> \theta_i. \end{cases}$$

In a quiescent plasma, these three waves are independent; however, an intense high frequency field can parametrically couple together various combinations of these modes.[8] Physically, this high-frequency field acts as the pump, by setting up currents in the plasma. These currents change the susceptibility of the plasma, nonlinearly, in

such a way that the equations describing the resultant fields in the plasma have source terms which depend on a power series in the pump power. Thus, for example, the equation describing the amplitude of a low-frequency ion-acoustic wave contains a term due to the beating of a high-frequency pump and a high-frequency daughter field. Given that the appropriate frequency-matching condition is satisfied, both the high-frequency daughter field and the ion-acoustic wave can be amplified. The frequency matching condition for all parametric interactions which depend on the lowest power of the pump is:

$$\omega_{pump} \approx |\omega_{daughter\text{-}one}| + |\omega_{daughter\text{-}two}| .$$

These lowest order interactions couple the pump wave to two other waves and are called three-wave interactions. Table I lists the possible three-wave couplings in an homogeneous, unmagnetized plasma.

In addition to these three-wave processes, the pump can couple modes of the plasma through interactions in which two pump waves are involved. These processes are frequently called second-order in the pump, even though the physics of the interaction is similar to the first-order processes which lead to the three-wave interactions. These "four-wave" interactions couple together two pump waves and two high frequency modes of the plasma through a low frequency response of the plasma. This low frequency response of the plasma has the effect of making the expected frequency

TABLE I

THREE-WAVE PARAMETRIC INSTABILITIES

Pump	Daughter Wave	Name	Diagram
L or T	L, L	$2\omega_{pe}$[9]	
L or T	L, A	Electron-ion decay[8]	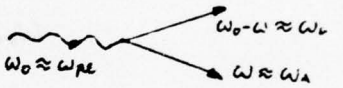
T	L, T	Stimulated Raman scattering[10]	
T	T, A	Stimulated Brillouin scattering[11]	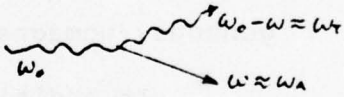
T	T, T	Degenerate electro-magnetic	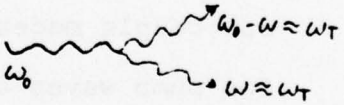

matching condition:

$$2\omega_{pump} \approx |\omega_{daughter\text{-}one}| + |\omega_{daughter\text{-}two}| .$$

hold only approximately. In contrast to the three-wave case, the greatest amplification does not occur when this condition is satisfied. These four-wave interactions are tabulated in Table II. In both Tables I and II, the diagrams that are used to schematically represent these interactions are taken from an analogy with quantum mechanics. Thus, the frequency matching condition becomes a condition guaranteeing energy conservation in the wave interaction.

The general formalism for parametric interactions in a plasma is well-known for the case that the pump field is homogeneous, i.e., has a wavevector, $\underline{k}_o$, equal to zero. In the following two chapters, we present a generalization of a kinetic formalism of parametric instabilities to the case of pumps with more complicated dependence on the wavenumber of the pump. As we will show, the most striking of the results of this generalization come from the wavevector matching condition that must be satisfied:

$$\underline{k}_o = \underline{k}_{daughter\text{-}one} + \underline{k}_{daughter\text{-}two} .$$

In our quantum analogy, this is a requirement for conservation of momentum. In general, this results in important changes in the character of the parametric instabilities, which now have a sensitive dependence on the vector character of the pump wavenumber. We have restricted our study

TABLE II

FOUR-WAVE PARAMETRIC INSTABILITIES

Pump	Daughter Waves	Name	Diagram
T	L, L	Oscillating two-stream[12]	
T	T, T	Filamentation[13]	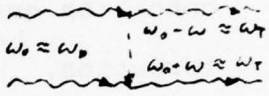
T	T, L		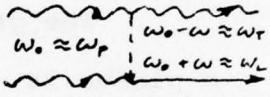
L	L, L	Modulational	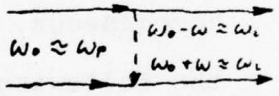
L	L, T		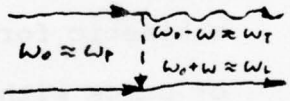
L	T, T		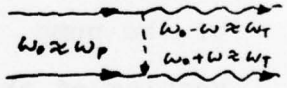

of arbitrary $\underline{k}_o$ effects to two general types: the effects of a standing-wave pump, and the three-dimensional aspects (in a cylindrical symmetry about $\underline{k}_o$). As will be shown, both of these situations are frequently applicable in astrophysical and laboratory plasmas in which parametric instabilities play a role.

In Chapter II, the general formalism for a kinetic theory analysis of parametric mode coupling is derived for a pump of more general form: the pump can be a standing wave (or travelling-wave) with arbitrary wavevector, $\underline{k}_o$. This more general pump introduces two general kinds of effects:

1). Effects due to qualitative changes in the mode couplings possible with a standing wave pump, and

2). Three dimensional effects due to the finite size of $\underline{k}_o$ and its vector character (independent of the standing-wave character of the pump).

The problem of a standing-wave pump driving parametric instabilities arises in several important plasma configurations; whenever a transversely polarized pump wave is reflected from a critical surface in a plasma, for example, a standing-wave pump field is set up by the superposition of the incident and reflected waves. A longitudinally polarized standing-wave pump field can arise from the decay products of another parametric instability if these daughter products have almost equal and opposite wavenumbers, and equal frequencies. This is sometimes the case for a

four-wave instability known as the oscillating two-stream (OTS) instability (see Table II). At the end of Chapter II we apply our general formalism to the specific case of the $2\omega_{pe}$ and electron-ion decay (EID) instabilities driven by a standing-wave pump. The most important effect here is a lowering of the effective power of the pump when the pump is a standing-wave. This reduction is a result of different modes of the plasma being excited by each of the two components of the standing-wave. We find, in addition, the these modes are coupled more strongly (raising the effective pump power) as the separation in frequency of these waves decreases (with smaller k_o), relative to the growth rate of the instability. As k_o goes to zero, and a standing-wave becomes indistinguishable from a travelling-wave, we are able to recover the travelling-wave results. When we apply our results for the EID instability to ionospheric modification data, we find the decrease in the effective pump power with a standing wave pump lowers the theoretical predictions of the Langmuir turbulence produced in these experiments.

After this application of our general formalism, the third chapter is devoted to the more complicated, and more important, problem of the parametric instabilities driven by a longitudinally polarized pump. The dispersion relation we have derived makes possible a unified treatment of all Langmuir pumped instabilities which have longitudinally polarized daughter waves. We find that the

parametric processes in this case are of three types, all of which demand a treatment in three dimensions with arbitrary wavenumber pump:

1). A non-oscillatory process, which we have called the oscillating two-stream instability after Nishikawa.[12] For non-zero k_o, the OTS instability is one dimensional only under quite restrictive conditions, and, in many cases, has its fastest growing daughter waves at a large angle to $\underline{k}_o$.

2). The well-known electron-ion decay (EID) instability. For k_o on the order of the mass ratio, we find that the EID instability can be a forward scattering process.

3). A new instability, which is only seen in three dimensions, called the stimulated modulational (SM) instability. This instability produces daughter waves at an angle to k_o, which can have wavenumbers slightly larger than k_o.

The third chpater concludes with an application of these results to three physical situations in which the longitudinal pump is modelled on the quasilinear decay of an electron beam. In all three of the situations examined, Type III solar radio bursts, auroral arcs, and non-relativistic laboratory electron beams, we have concluded that parametric effects do not substantially affect the beam relaxation, which still proceeds quasilinearly. Other aspects of these situations, however, do require the parametric processes of a Langmuir pump for their understanding:

the electromagnetic radiation associated with solar bursts, the anomalous resistivity encountered by the auroral streams, and the low frequency spectra observed in laboratory electron experiments.

Notation

We have attempted to follow conventional notation whenever possible. All wavenumbers and wavevectors are represented by lower case, Latin k's; all frequencies are denoted by lower case, Greek omega. In every case, a subscript zero refers to the pump (for example, k_o is the pump wavenumber). We use a system of units in which time is given in terms of the inverse plasma frequency and distance in units of the inverse Debye wavenumber, k_{De}, defined above (note that this gives velocity units of the electron thermal velocity). Finally, n_e always is the ambient electron number density per cm^3 and θ_s the temperature, in ergs, of the s species. Vectors are denoted by underscoring, and unit vectors by a circumflex; thus, the electric field of the pump is $\underline{E}_o$ and has direction $\hat{e}_o$ or $\hat{e}_{k_o}$ (this is not to be confused with an unsubscripted e, standing for the electronic charge).

NOTES TO CHAPTER ONE

[1]M. Faraday, Phil. Trans. Royal Soc., 121, 299 (1831).

[2]Lord Rayleigh, John William Strutt, Phil. Mag., series 5, 16, 50 (1883).

[3]F. Melde, Ann. Physik Chemie, series 2, 109, 193 (1859).

[4]W. H. Louisell, Coupled Modes and Parametric Electronics, New York, John Wiley and Sons, Inc. (1960).

[5]N. Bloembergen, Nonlinear Optics, New York, W. A. Benjamin, Inc. (1965).

[6]D. F. DuBois, V. Gilinsky, M. G. Kivelson, Phys. Rev., 129, 2376 (1963).

[7]B. D. Fried, R. W. Gould, Phys. Fluids, 4, 139 (1961).

[8]V. P. Silin, Soviet Physics--JETP, 21, 1127 (1965). D. F. DuBois, M. V. Goldman, Phys. Rev. Lett., 14, 544 (1965).

[9]M. V. Goldman, Annals of Physics (N. Y.), 38, 95 (1966). E. A. Jackson, Phys. Rev., 153, 235 (1967).

[10]M. V. Goldman, D. F. DuBois, Phys. Fluids, 8, 1404 (1965). N. Bloembergen, Y. K. Shen, Phys. Rev., 141, 298 (1966).

[11]L. M. Gorbunov, Soviet Physics--JETP, 28, 1220 (1969). L. M. Gorbunov, V. P. Silin, Tech. Physics, 14, 1 (1969).

[12]K. Nishikawa, J. Phys. Soc. Japan, 24, 916, 1152 (1968).

[13]A. Yu. Kuri, Soviet Physics--JETP, 31, 538 (1970).

CHAPTER II

THE GENERAL FORMALISM

The first studies of parametric instabilities were done using three simplifying assumptions:[1,2]

1). The pump wavenumber is much less than any other wavenumber in the plasma;

2). A one-dimensional treatment is sufficient to determine the fastest growing modes; and,

3). The pump is a monochromatic, travelling wave field.

Assumption one sometimes implies that the pump is homogeneous, the so-called "dipole approximation," and frequently is applicable to parametric instabilities. From the frequency matching condition for the EID instability, (see Table I, page 6), to take one example, we can derive the following relation between k_o and k, the daughter wavenumber, for a transversely polarized pump:

$$c^2 k_o^2 \approx 3 v_e^2 k^2$$

so that $k_o \ll k$. If the pump is a travelling wave, this allows us to ignore k_o. (As we shall see, assumptions one and three are related, and the condition $k_o \ll k$ is not sufficient to guarantee a dipole pump if the pump is a standing-wave). In the derivation of a kinetic theory of

parametric instabilities in this chapter, we have relaxed this assumption. The necessity of studying more general pump field is clear if we repeat the above calculation for a longitudinally polarized pump, a Langmuir wave. In this case we have:

$$k = 2\underline{k}\cdot\underline{k}_o - 2c_s/3 ,$$

where c_s is the sound speed in the plasma. Clearly, k and k_o can be comparable in magnitude. We have found the most important effects of a finite k_o pump do occur for longitudinally polarized pumps. In Chapter III we will derive detailed results for the k_o dependent effects in parametric effects pumped by a Langmuir wave field.

Furthermore, when $k_o \ll k$, we would expect that the parametric processes would not depend on the direction of k_o (except as this is determined by the polarization of the pump), and hence, that a one dimensional treatment would be sufficient. This is the content of assumption two. However, to be consistent, if we relax assumption one, we must be ready to examine possible three dimensional effects. Indeed, our formalism, especially in the regimes when $k_o \approx k$, predicts important three dimensional effects for all parametric instabilities. These will be examined in detail in Chapter III, for the case of a Langmuir pump. For the EID instability, to compare with our example above, driven by a Langmuir pump, not only are k and k_o comparable, but, in addition, the angle between $\underline{k}$ and $\underline{k}_o$

enters critically into the condition for maximum growth. Our general formalism is derived in a three dimensional geometry in which we have assumed a cylindrical symmetry about $\underline{k}_o$.

Finally, our motivation for relaxing the assumption concerning a travelling wave pump field (assumption three--although we have kept the assumption of a monochromatic pump) is the evidence that in many experimental situations the pump is not a simple travelling-wave. It is frequently the case, for example, that the theory of parametric instabilities is applied to experiments in an inhomogeneous plasma. In this situation, one approximation to a treatment of the problem which take the density variation into account, is based on the observation that an electromagnetic pump will be reflected in the region of any critical density surfaces in the plasma (where the local plasma frequency equals the frequency of the pump wave), and, the superposition of the reflected and incident waves will create a standing-wave electromagnetic field in the plasma. If the absorption of energy from the pump is small enough, this standing-wave will double the local amplitude of the pump field, but with a new wavenumber and frequency dependence. This is thought to be the case for the plasma-radiation systems occurring in ionospheric modification experiments and in laser-irradiated pellets.[3] The other general class of problems in which a standing-wave pump

arises is that of the saturation of parametric instabilities. One example of this, which will be examined in more detail in the next chapter, is the non-oscillatory interaction of a small wavenumber pump whose daughter waves are a pair of Langmuir-like waves with almost equal frequencies and equal, but opposite, wavenumbers. The superposition of these two daughter waves sets up a standing-wave field, and the saturation of the process depends then on the dynamics of the standing-wave pump generated by the original daughter waves.

In this chapter, we begin with a kinetic theory derivation of parametric excitation in an homogeneous, infinite magnetic field-free plasma. Our derivation relaxes assumptions one, two and three. We have divided our applications of this formalism into two parts:

1). At the end of this chapter, we study the effects dependent on the standing-wave pump. The most striking effect we find is a lowering of the effective power of the pump. This is an effect we explain by a detailed consideration of the new mode couplings that a standing-wave allows. These new couplings arise from the different wavenumber matching conditions possible with each component of the standing-wave. The key concept concerning these phenomena is that of the "closeness" of modes; that is, the separation in frequency of two modes compared to the growth rate of the instability. Using this idea, we have derived relations between k_o, the number of modes coupled in the plasma,

and the effective power of the pump These results are applied to ionospheric modification experiments, where our predictions of a lowered effective pump power changes the theoretical predictions made of the observed Langmuir turbulence.

2). All of Chapter III is devoted to a study of the three dimensional and finite k_o effects of parametric instabilities driven by a Langmuir wave pump.

THE NORMAL MODE EQUATION[4]

Maxwell's equations in a medium are efficiently solved beginning with the equation relating the ensemble-averaged electric field, $\underline{E}$, the external currents, and that part of the internal current which has a higher than linear dependence on the field, $\underline{j}^{NL}$:

$$\underline{\underline{m}}(\underline{k},\omega)\cdot\underline{E}(\underline{k},\omega) = -4\pi i\left[\underline{j}^{ext}(\underline{k},\omega) + \underline{j}^{NL}(\underline{k},\omega)\right], \tag{1}$$

where $\underline{\underline{m}}(\underline{k},\omega)$ is the generalized susceptibility, related to the linear dielectric function, $\underline{\underline{\epsilon}}(\underline{k},\omega)$ through the relation:

$$m_{lm}(\underline{k},\omega) = \frac{c^2 k_l k_m}{\omega} - \frac{c^2 k^2}{\omega} + \omega\,\epsilon_{lm}(\underline{k},\omega). \tag{2}$$

The dielectric function itself is derivable from the equations describing the plasma. Our strategy in solving this equation is as follows:

1). By limiting ourselves to linear stability analysis, to look at the solutions to the equation when there

are no external currents, $\underline{j}^{ext} = 0$, and concern ourselves only with the normal modes of the system, whose dispersion relation is given by roots of:

$$\underline{\underline{m}}(\underline{k},\omega)\cdot\underline{E}(\underline{k},\omega) = -4\pi i\,\underline{j}^{NL}(\underline{k},\omega); \tag{3}$$

2). To find an expansion of the non-linear current in powers of the field; and,

3). To introduce an ordering among the contributions to the field, distinguishing between the pump field, an externally applied field which is assumed to be of fixed amplitude, frequency, and wavenumber, and the much smaller fields that the pump drives up (this is the so-called parametric approximation).

The solution to (3), using only the internal current which is first order in the pump, i.e., second-order in the total field, gives the three-wave parametric interactions; the current which is third-order in the total field (second order in the pump) gives rise to the four-wave processes. To solve equation (3), we must evaluate the internal current; in general, we can write the current in terms of the non-linear susceptibilities and the fields in the plasma. The linear susceptibility is given by the linear dielectric function:

$$j_l^{(1)}(\underline{k},\omega) = -i\omega\chi_{lm}(\underline{k},\omega)E_m(\underline{k},\omega), \tag{4}$$

where:

$$\epsilon_{lm}(\underline{k},\omega) = \delta_{lm} + 4\pi\chi_{lm}(\underline{k},\omega).$$

The non-linear currents can likewise be written in a series expansion which comes out of a Fourier transform of an expansion of the current in terms of the electric field:

$$\underline{j}^{NL}(\underline{k},\omega) = \underline{j}^{(2)}(\underline{k},\omega) + \underline{j}^{(3)}(\underline{k},\omega) + \ldots$$

where:

$$(5) \qquad j_\ell^{(2)}(\underline{k},\omega) = -i\omega \int dK_{12}\, \chi_{\ell mn}(\underline{k},\omega;\underline{k}_1,\omega_1;\underline{k}_2,\omega_2)\, E_m(\underline{k}_1,\omega_1)\, E_n(\underline{k}_2,\omega_2),$$

and:

$$(6) \qquad j_\ell^{(3)}(\underline{k},\omega) = -i\omega \int dK_{123}\, \chi_{\ell mnp}(\underline{k},\omega;\underline{k}_1,\omega_1;\underline{k}_2,\omega_2;\underline{k}_3,\omega_3) \cdot E_m(\underline{k}_1,\omega_1)\, E_n(\underline{k}_2,\omega_2)\, E_p(\underline{k}_3,\omega_3).$$

with the definitions:

$$(7) \qquad dK_{12} = \frac{d^3k_1\, d\omega_1\, d^3k_2\, d\omega_2}{(2\pi)^8}\, \delta^3(\underline{k}-\underline{k}_1-\underline{k}_2)\, \delta(\omega-\omega_1-\omega_2),$$

$$(8) \qquad dK_{123} = \frac{d^3k_1\, d\omega_1\, d^3k_2\, d\omega_2\, d^3k_3\, d\omega_3}{(2\pi)^{12}}\, \delta^3(\underline{k}-\underline{k}_1-\underline{k}_2-\underline{k}_3)\, \delta(\omega-\omega_1-\omega_2-\omega_3).$$

It is important to note that the model of the plasma-field interactions used to derive the susceptibilities is separate from the model used to evaluate the dielectric function in equation (2). We have, in the Appendix, evaluated $\chi_{\ell mn}$ and $\chi_{\ell mnp}$ for several important cases using a fluid model.[4] From equations (A.7) and (A.8) in the Appendix, we have explicit forms for the non-linear susceptibilities, and we use them with the definition:

$$(9) \qquad \chi(\underline{k},\omega;\underline{k}_1,\omega_1;\underline{k}_2,\omega_2) = \hat{e}_\ell\, \hat{e}_m\, \hat{e}_n\, \chi_{\ell mn}(\underline{k},\omega;\underline{k}_1,\omega_1;\underline{k}_2,\omega_2),$$

where $\hat{e}_1 = \hat{e}_k$, $\hat{e}_m = \hat{e}_{k1}$, etc. are the unit polarization vectors of the $\underline{E}(k)$, $\underline{E}(k_1)$, etc. The next step is to make

the parametric approximation:

$$\underline{E}(\underline{k},\omega) = \underline{E}_0(\underline{k}_0,\omega_0) + \underline{E}'(\underline{k},\omega), \tag{10}$$

where E_0 is the pump field amplitude and E' the amplitude of the self-consistent fields generated by the plasma. We require that the following condition hold on these amplitudes:

$$\int |E_0|^2 d^3k \gg \int |E'|^2 d^3k ,$$

and that E_0 still be small enough to ensure the convergence of the current expansion (a sufficient condition for this convergence is that:

$$\int |E_0|^2 d^3k \ll n\theta_e ,$$

whose details are discussed in reference 5). Physically, our zero order (in E') state is that of a large amplitude known field interacting with a plasma. Our object is to calculate the effects linear in E'. In general, E_0 has the effect of coupling together previously independent modes of the plasma (resonances in E') and, in some cases amplifying these now coupled resonances. This is a parametric process since we take $|E_0|^2$ as fixed, and the time and space variation of E_0 provide the coupling mechanism.

We now relax the assumptions listed in the beginning of this chapter, on the form of the pump, and write:

$$\begin{aligned}\underline{E}_0(\underline{r},t) &= |E_0|\,\hat{e}_0\left[(1-\alpha)\sin(\underline{k}_0\cdot\underline{r}+\omega_0 t+\varphi)+\alpha\sin(-\underline{k}_0\cdot\underline{r}+\omega_0 t+\varphi)\right] \\ &= |E_0|\,\hat{e}_0\,\mathrm{Im}\left[(1-\alpha)e^{i(\underline{k}_0\cdot\underline{r}+\omega_0 t+\varphi)}+\alpha e^{i(-\underline{k}_0\cdot\underline{r}+\omega_0 t+\varphi)}\right].\end{aligned} \tag{11}$$

where φ is an arbitrary phase factor. This pump is a standing-wave of arbitrary k_o when $\alpha = \frac{1}{2}$ and a travelling-wave when $\alpha = 1$ or 0. The local amplitude of this pump is always $|E_o|$ for any value of α. We write the Fourier transform in space and time of the pump as:

$$E(\underline{k}_o,\omega_o) = \frac{(2\pi)^4}{2} \sum_{s=1,-1} \left[\left(\frac{s+1}{2} - \alpha\right) E_o^* \delta^3(\underline{k}+s\underline{k}_o)\delta(\omega-\omega_o) + \left(\frac{s+1}{2} - \alpha\right) E_o\, \delta^3(\underline{k}+s\underline{k}_o)\delta(\omega+\omega_o) \right].$$

Substitution of this expression for E_o in (10) and then into (5), (6), and their higher order analogues, immediately gives the various currents in (4). The second order current is, for example:

$$(12)\quad j_\ell^{(2)}(\underline{k},\omega) = i\omega \sum_{s=1,-1} \left[\left(\frac{s+1}{2} - \alpha\right) E_{om}^* E_n'(\underline{k}+s\underline{k}_o, \omega-\omega_o) \chi_{\ell mn}(\underline{k}, \omega; -s\underline{k}_o, \omega; \underline{k}+s\underline{k}_o, \omega-\omega_o) \right.$$
$$\left. + \left(\frac{s+1}{2} - \alpha\right) E_{om} E_n(\underline{k}+s\underline{k}_o, \omega+\omega_o) \chi_{\ell mn}(\underline{k}, \omega; -s\underline{k}_o, -\omega_o; \underline{k}+s\underline{k}_o, \omega+\omega_o) \right].$$

In an isotropic plasma ($B_o = 0$), we can choose $\underline{\underline{m}}(\underline{k},\omega)$ diagonal, and equation (3) becomes:

$$(13)\quad \epsilon(\underline{k},\omega) E_\ell'(\underline{k},\omega) = -\frac{4\pi i}{\omega} \left[j_\ell^{(2)}(\underline{k},\omega) + \cdots \right].$$

This equation generates a system of equations connecting fields at various values of the wavenumber and frequency, shifted in their arguments by letting k go into $k \pm k_o$ and ω go into $\omega \pm \omega_o$. The result is an infinite, homogeneous set of coupled equations for $E'(\underline{k} \pm n\underline{k}_o, \omega \pm \omega_o)$.

Physically, the pump has coupled previously independent modes of the plasma; there is, for example, the term in these equations proportional to $E_o \chi_{\ell mn}$ which couples the mode at $(\underline{k}, \omega)$ with the four modes at $(\underline{k} \pm \underline{k}_o, \omega \pm \omega_o)$

and $(\underline{k}\pm\underline{k}_o, \omega\mp\omega_o)$. Our object is to solve this system of equations. Given that we know the susceptibilities, substitution of (12) and the like expressions for $\underline{j}^{(3)}$, etc. into (13) gives a homogeneous set of equations for the $\underline{E}'$ fields at different wavenumber and frequency, and the determinant of the coefficient matrix of this set of equations gives us a dispersion relation which describes the new normal modes of the plasma. We now turn to an evaluation of the dispersion relation.

THE DISPERSION RELATION

The fundamental difficulty in solving the matrix equation that follows from (13) is that it is infinite. The infinite number of variables that we have are the fields E': $E'(\underline{k}, \omega)$, $E'(\underline{k}\pm\underline{k}_o, \omega\pm\omega_o)$, $E'(\underline{k}\pm\underline{k}_o, \omega\mp\omega_o)$, $E'(\underline{k}\pm 2\underline{k}_o, \omega)$, etc. We must find a way to truncate this doubly infinite group of variables in wavenumber and frequency, if we are to get a finite set of equations. We will show that truncation in frequency and wavenumber is provided by a restriction that allows us to take into account only modes that fall near a resonance of the unperturbed system. However, our ability to truncate the series of variables in wavenumber will be a sensitive function of $\underline{k}_o$, which is not the case for the truncation in frequency. In this section we will reduce our infinite equation to an m x m determinant, where m is a function of k_o. We then will apply this m x m determinental dispersion

relation to several parametric instabilities driven by a standing-wave pump.

We now turn to the problem of truncating the infinite matrix equation that follows from (13). We first make the convention that $0 < \omega < \omega_0$. This guarantees that all the arguments in frequency, $\omega \pm n\omega_0$ are different for different values of n. One consequence of the condition that

$$\int |E_0|^2 d^3k \ll n\theta_e ,$$

is that the predominate response of the plasma, E', will be very near the normal modes of the unperturbed plasma. It is in this sense that the pump is said to couple the normal modes of a plasma; that is, if ω_a is a high frequency normal mode of the plasma, so that:

$$\epsilon(\underline{k}_a, \omega_a) = 0,$$

and, if $\omega(\underline{k})$ is a solution to our new dispersion relation, then:

$$|\omega - \omega_a| \ll \omega_0 .$$

This is easily verified a posteriori. Now the normal modes of the unperturbed plasma are well known, and we can conclude that we need only keep fields, E', which have a frequency near a normal mode of the plasma. Since we will choose the pump frequency, ω_0, to be a high frequency (on the order of the plasma frequency), it is easy to verify that, for the responses of a homogeneous plasma, Table I (page 6) gives the possible excited fields for the couplings allowed by $\underline{j}^{(2)}$. Let us call, for such a three- wave

process, $\omega_a(\underline{k}_a)$ and $\omega_b(\underline{k}_b) = \omega_b(\underline{k}_a - \underline{k}_o)$, the normal modes of the unpumped plasma; the daughter waves of the instability must be near these two frequencies. Thus, for example, to excite the $2\omega_{pe}$ instability (see Table I), we must satisfy the frequency matching condition, at least approximately:

$$\omega \approx \omega_L(\underline{k}_a) \equiv \omega_a(\underline{k}_a),$$

$$\omega - \omega_o \approx -\omega_L(\underline{k}_a - \underline{k}_o) \equiv \omega_b(\underline{k}_a - \underline{k}_o)$$

(In the case of the $2\omega_{pe}$ instability, ω_a and ω_b, the natural resonances of the plasma that the pump excites, are both Langmuir waves). We can choose $\underline{k}_a$ so that these equations are satisfied. But, the other modes, at:

$$\omega + \omega_o \approx 3\omega_{pe},$$

$$\omega - 2\omega_o \approx -2\omega_{pe},$$

will never be near a resonance of the unpumped plasma. The more exact meaning of "near a resonance" is straightforward. Physically, we want $\omega(k)$, the new normal mode, to be within a growth rate of the "old" normal mode of the system. Expressing this in terms of the dielectric functions, which are more properly a measure of the plasma response:

$$|\mathrm{Re}\,\epsilon(\underline{k},\omega) - \mathrm{Re}\,\epsilon(\underline{k}_a,\omega_a)| < |\mathrm{Im}\,\epsilon(\underline{k},\omega)|,$$

$$|\mathrm{Re}\,\epsilon(\underline{k}',\omega-\omega_o) - \mathrm{Re}\,\epsilon(\underline{k}_b,\omega_b)| < |\mathrm{Im}\,\epsilon(\underline{k}',\omega-\omega_o)|.$$

Figure one a) shows schematically what is required. These inequalities allow us to truncate our equation in frequency.

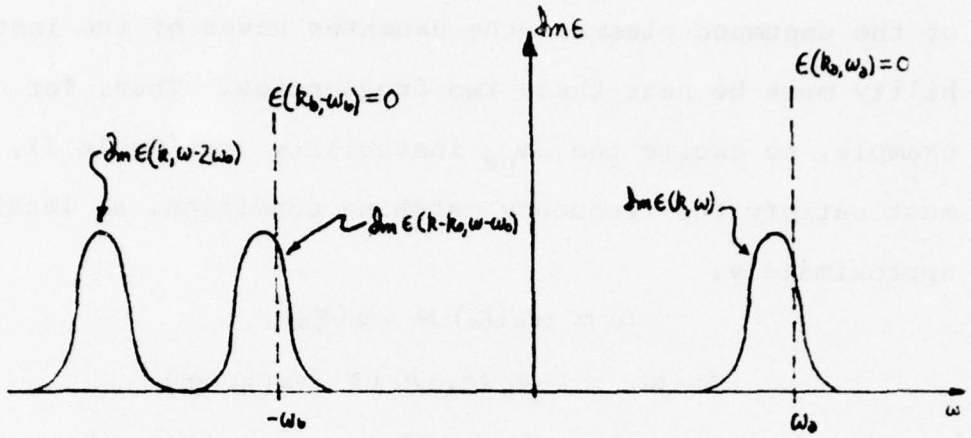

a)

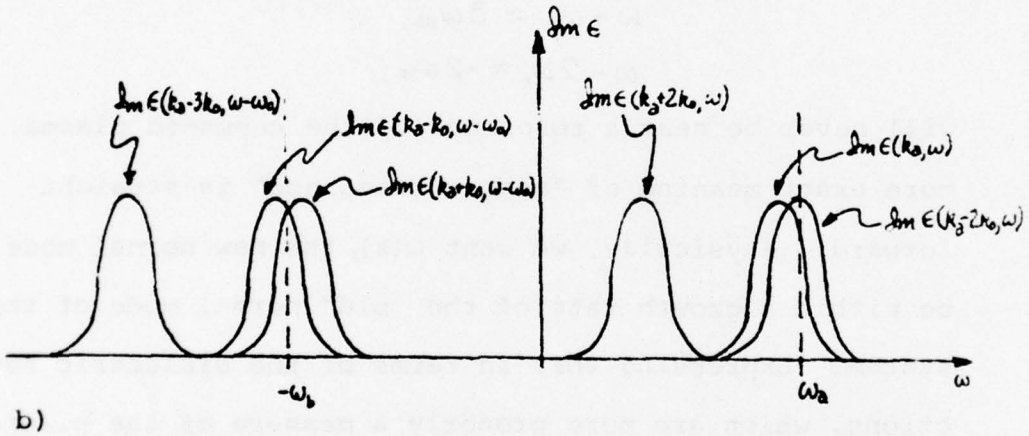

b)

Figure one. Qualitative diagram of the plasma response as a function of wavenumber and frequency. In a) we have the criterion for determination of which frequencies are "close enough" to a natural resonance of the plasma (shown by the dotted lines at $\omega_a(k_a)$ and $-\omega_b(k_b)$). The mode at $\omega-\omega_o$ is close enough; the mode at $\omega-2\omega_o$ is not. In b) the criterion for determination of which wavenumbers will be excited. Modes at $(k_a \pm k_o, \omega-\omega_o)$, (k_a, ω), and (k_a-2k_o, ω) are "close enough" to a natural resonance, but the modes at $(k_a-3k_o, \omega-\omega_o)$ and (k_a+2k_o, ω) are not.

Notice that if ω is a low frequency, that it is possible to have three daughter frequencies near resonance:

$$\omega - \omega_o \approx -\omega_{pe} \ , \quad \omega + \omega_o \approx \omega_{pe} \ , \quad \omega \approx \omega_A .$$

This enables $E'(\underline{k}, \omega)$, $E'(\underline{k}+\underline{k}_o, \omega+\omega_o)$ and $E'(\underline{k}-\underline{k}_o, \omega-\omega_o)$ all to be excited. We shall see that is the case for the four-wave instabilities (see Table II, page 8). In the remainder of this chapter, however, we assume:

$$|Re\ \epsilon(\omega-\omega_o) - Re\ \epsilon(\omega_o)| < Im\ \epsilon(\omega-\omega_o) < |Re\ \epsilon(\omega+\omega_o) - Re\ \epsilon(\omega_o)|,$$

and we will defer discsssion of four-wave effects to Chapter III.

We now specialize our results to this case, and make the related assumption that only $\underline{j}^{(2)}$ needs to be considered. This is admissible as long as we can neglect small corrections to Re ω,[4] and are interested only in three-wave effects. In chapter III we will include effects due to both the up-shifted wave at $E'(\underline{k}+\underline{k}_o, \omega+\omega_o)$ and due to couplings introduced by $\underline{j}^{(3)}$. This leaves us with the following equations, obtained from a substitution of (12) into (13):

$$(14)\quad \frac{\epsilon(k,\omega)\,E_\ell'(k,\omega)}{4\pi} = \alpha\,\chi_{\ell mn}(k-k_o,\omega-\omega_o;-k_o,-\omega_o;k,\omega)\,E_n'(k-k_o,\omega-\omega_o)E_{om} + (1-\alpha)\,\chi_{\ell mn}(k+k_o,\omega-\omega_o;k_o,-\omega_o;k,\omega)\,E_n'(k+k_o,\omega-\omega_o)E_{om};$$

$$(15)\quad \frac{\epsilon(k-k_o,\omega-\omega_o)E_\ell'(k-k_o,\omega-\omega_o)}{4\pi} = \alpha\,\chi_{\ell mn}(k,\omega;k_o,\omega_o;k-k_o,\omega-\omega_o)E_n'(k,\omega)E_{om}^* + (1-\alpha)\,\chi_{\ell mn}(k-2k_o,\omega;-k_o,\omega_o;k-k_o,\omega-\omega_o)\,E_n'(k-2k_o,\omega)E_{om};$$

$$(16)\quad \frac{\epsilon(k+k_o,\omega-\omega_o)E_\ell'(k+k_o,\omega-\omega_o)}{4\pi} = \alpha\,\chi_{\ell mn}(\omega,k+2k_o;k_o,\omega_o;k+k_o,\omega-\omega_o)\,E_n'(k+2k_o,\omega)E_{om} + (1-\alpha)\,\chi_{\ell mn}(k,\omega;-k_o,\omega_o;k+k_o,\omega-\omega_o)\,E_n'(k,\omega)\,E_{om}^*;$$

$$(17)\quad \frac{\epsilon(k-2k_o,\omega)\,E_\ell'(k-2k_o,\omega)}{4\pi} = \alpha\,\chi_{\ell mn}(k-3k_o,\omega-\omega_o;-k_o,-\omega_o;k-2k_o,\omega)\,E_n'(k-3k_o,\omega-\omega_o)E_{om} + (1-\alpha)\,\chi_{\ell mn}(k-k_o,\omega-\omega_o;k_o,\omega_o;k-2k_o,\omega)\,E_n'(k-k_o,\omega-\omega_o)\,E_{om}^*;$$

$$(18)\quad \frac{\epsilon(k+2k_o,\omega)E_e'(k+2k_o,\omega)}{4\pi} = \alpha\,\chi_{lmn}(k+k_o,\omega-\omega_o;-k_o,\omega_o;k+2k_o,\omega)E_n'(k+k_o,\omega-\omega_o)E_m^* + (1-\alpha)\chi_{lmn}(k+3k_o,\omega-\omega_o;k_o,-\omega_o;k+2k_o,\omega)E_n'(k+2k_o,\omega)E_{cm}.$$

When $\alpha = 0$ or 1, and we have a travelling-wave pump, only equations (14) and (15) are necessary. That is, with a travelling-wave, a truncation in frequency also truncates the series of equations in wavenumber. This is a result of the fact that a travelling-wave can only couple modes in which the wavenumber and frequency are shifted by the same multiple of (k_o, ω_o). However, a standing-wave can couple modes a more complicated fashion. Equation (19) shows, in matrix form, the infinite set of equations generated like (14)-(18) by a standing-wave pump. These equations have been truncated in frequency, but not yet in wavenumber. An analogous truncation is possible for the shifts in wavenumber, since, for large enough k_o, $\epsilon(\underline{k}\pm\underline{k}_o, \omega-\omega_o)$ and $\epsilon(\underline{k}\pm 3\underline{k}_o, \omega-\omega_o)$ cannot both be on resonance simultaneously. That is, if we assume that $\epsilon(k-k_o, \omega-\omega_o)$ is very close to a resonance of the unpumped plasma, then the mode at $(\underline{k}\pm n\underline{k}_o)$ with frequency $(\omega-\omega_o)$ will be "near" this same resonance only if:

$$|Re\,\epsilon(\underline{k},\omega) - Re\,\epsilon(\underline{k}\pm n_a\underline{k}_o,\omega)| < |Im\,\epsilon(\underline{k},\omega)|,$$

or, in terms of the other mode:

$$|Re\,\epsilon(\underline{k}-\underline{k}_o,\omega-\omega_o) - Re\,\epsilon(\underline{k}+n_b\underline{k}_o,\omega-\omega_o)| < |Im\,\epsilon(\underline{k}-\underline{k}_o,\omega-\omega_o)|.$$

Our wavenumber and frequency matching conditions and equation (19) allow these equations to be written:

$$(20a)\quad |Re\,\epsilon(\underline{k}_a,\omega_a) - Re\,\epsilon[\underline{k}_a\pm(n-1)\underline{k}_o,\omega_a]| < |Im\,\epsilon(\underline{k},\omega)|$$

(19)

$$
\begin{pmatrix}
\vdots & \vdots & \vdots & \vdots & \vdots \\
\epsilon(\underline{k}-2\underline{k}_0,\omega) & (1-\alpha)\chi_{2mn}(\underline{k}-\underline{k}_0,\omega-\omega_0;\ \underline{k}_0,-\omega_0;\ \underline{k}-2\underline{k}_0,\omega)\times E_{0m}^{*} & 0 & 0 & 0\ \ldots \\
(1-\alpha)\chi_{2mn}(\underline{k}-2\underline{k}_0,\omega;\ -\underline{k}_0,\omega_0;\ \underline{k}-\underline{k}_0,\omega-\omega_0)\times E_{0m} & \epsilon(\underline{k}-\underline{k}_0,\omega-\omega_0) & \alpha\chi_{2mn}(\underline{k},\omega;\ \underline{k}_0,\omega_0;\ \underline{k}-\underline{k}_0,\omega-\omega_0)\times E_{0m}^{*} & 0 & 0\ldots \\
\ldots 0 & \alpha\chi_{2mn}(\underline{k}-\underline{k}_0,\omega-\omega_0;\ -\underline{k}_0,-\omega_0;\ \underline{k},\omega)\times E_{0m} & \epsilon(\underline{k},\omega) & (1-\alpha)\chi_{2mn}(\underline{k}+\underline{k}_0,\omega-\omega_0;\ \underline{k}_0,-\omega_0;\ \underline{k},\omega)\ E_{0m} & 0\ldots \\
\ldots 0 & 0 & (1-\alpha)\chi_{2mn}(\underline{k},\omega;\ -\underline{k}_0,\omega_0;\ \underline{k}+\underline{k}_0,\omega-\omega_0)\times E_{0m}^{*} & \epsilon(\underline{k}+\underline{k}_0,\omega-\omega_0) & \alpha\chi_{2mn}(\underline{k}+2\underline{k}_0,\omega;\ \underline{k}_0,\omega_0;\ \underline{k}+\underline{k}_0,\omega-\omega_0)\times E_{0m} \\
\ldots 0 & 0 & 0 & \alpha\chi_{2mn}(\underline{k}+\underline{k}_0,\omega-\omega_0;\ -\underline{k}_0,-\omega_0;\ \underline{k}+2\underline{k}_0,\omega)\times E_{0m}^{*} & \epsilon(\underline{k}+2\underline{k}_0,\omega) \\
\vdots & \vdots & \vdots & \vdots & \vdots
\end{pmatrix}
\times
\begin{pmatrix}
\vdots \\
E_n'(\underline{k}-2\underline{k}_0,\omega) \\
E_n'(\underline{k}-\underline{k}_0,\omega-\omega_0) \\
E_n'(\underline{k},\omega) \\
E_n'(\underline{k}+\underline{k}_0,\omega-\omega_0) \\
E_n'(\underline{k}+2\underline{k}_0,\omega) \\
\vdots
\end{pmatrix}
= 0.
$$

(20b) $$|Re\,\epsilon(\underline{k}_a-\underline{k}_o,\omega_b)-Re\,\epsilon(\underline{k}_a\pm n\underline{k}_o,\omega_b)|<|Im\,\epsilon(\underline{k}-\underline{k}_o,\omega-\omega_o)|.$$

Notice that the same integer, n, enters both (20a) and (20b). This reflects a physical property of (19), namely, that two conditions must be satisfied for a given mode to be excited (thus, not excluded by our truncation scheme):

1). The mode must be "near enough" to a resonance of the unpumped system (this is expressed in (20a)); and,

2). This mode must be coupled, in (19), to another mode that satisfies the first condition.

This second requirement is a result of the fact that the second-order susceptibilities can only couple modes shifted by $(\pm k_o, \omega_o)$ and both of these modes must be close to resonance. For example, in the EID instability (see Table I, page 6), when ω_a is a Langmuir mode and ω_b is an acoustic mode, the n_a and n_b may be different. We must pick the smaller of n_a and n_b, i. e., the one that satisfies (20a) and (20b) simultaneously (n_a and n_b are defined in the two inequalities immediately preceeding (20a) and (20b)). In the next section, we will show results from a numerical test of this second requirement, by evaluating (19) in the case when we use (20a) and (20b) to eliminate modes, and in the case when we evaluate (19) without taking the smaller of n_a and n_b.

Equations (20a) and (20b), then allow us to truncate (19) in wavenumber. Figure one b) shows the situation

where modes at $(k_a \pm k_o, \omega - \omega_o)$, (k_a, ω), and $(k_a - 2k_o, \omega)$ will be coupled together. The other modes shown, at $(k_a + 2k_o, \omega)$, $(k_a - 3k_o, \omega - \omega_o)$ are not "near enough" to a natural resonance of the system to be excited. In most problems of interest, all frequencies of the daughter waves will be functions of the wavenumber which are slowly varying, and so we can write (20a) and (20b) as:

$$(n-1)\, k_o \left.\frac{\partial \epsilon(\underline{k}', \omega)}{\partial k'}\right|_{k' = k_a + (n-1)k_o} < \left| \mathrm{Im}\, \epsilon(\underline{k}_a, \omega) \right|, \tag{21a}$$

$$n\, k_o \left.\frac{\partial \epsilon(\underline{k}', \omega)}{\partial k'}\right|_{k' = k_a \pm n k_o} < \left| \mathrm{Im}\, \epsilon(\underline{k} - \underline{k}_o, \omega - \omega_c) \right|. \tag{21b}$$

where, again, n is the largest positive integer for which both inequalities hold. Examining (21) or (20) we can determine the total number of modes that a pump with a given k_o can couple together:

1). If n = 1, and $\left| \omega_a(k_a) + \omega_b(k_a - k_o) - \omega_o \right| > \left| \mathrm{Im}\, \omega \right|$, we cannot satisfy the basic frequency matching condition. In the three-wave approximation, there are no parametric interactions possible for this pump (note that this case could also arise if there were no value of n, besides zero perhaps, which could satisfy (20a) and (20b) together).

2). If n = 1, and $\left| \omega_a(k_a) + \omega_b(k_a - k_o) - \omega_o \right| < \left| \mathrm{Im}\, \omega \right|$, we have two possibilities. If equation (20b) holds only for the upper sign, then the following modes are coupled:

$$\omega_a(\underline{k}),\ \omega_b(\underline{k} - \underline{k}_o).$$

This is the same couplings that exist in the usual travelling-wave pumped instability. If, however, (20b) is satisfied for both signs, then the following modes are coupled:

$$\omega_a(\underline{k}),\ \omega_b(\underline{k}-\underline{k}_o),\ \omega_b(\underline{k}+\underline{k}_o).$$

This is the simplest standing-wave coupling.

3). If $n > 1$ (for both signs of (20b)), then we couple together m modes, where $m = 2n + 1$.

Thus the inequalities (20) or (21) allow us to truncate the infinite matrix, (19) in wavenumber, keeping only an m x m matrix out of the center (the 2 x 2 matrix and 3 x 3 matrix described by case two above are marked by dotted lines on equation (19)). In the 2 x 2 case, we get immediately the determinental condition:

$$\epsilon(\underline{k},\omega)\,\epsilon(\underline{k}-\underline{k}_o,\omega-\omega_o) - \alpha^2\,\chi(\underline{k},\omega;\underline{k}_o,\omega_o;\underline{k}-\underline{k}_o,\omega-\omega_o)\,\chi(\underline{k}-\underline{k}_o,\omega-\omega_o;-\underline{k}_o,-\omega_o;\underline{k},\omega)\,|E_o|^2 = 0. \tag{22a}$$

When $\alpha = 1$, this is the result of the usual travelling-wave calculation. Notice that for a standing-wave pump, when $\alpha = \frac{1}{2}$, we have a lower effective pump field. The consequences of this will be examined in the next section. For the 3 x 3 determinant:

$$\begin{aligned}&\epsilon(\underline{k},\omega)\,\epsilon(\underline{k}-\underline{k}_o,\omega-\omega_o)\,\epsilon(\underline{k}+\underline{k}_o,\omega-\omega_o)\\ &-\alpha^2\,\chi(\underline{k},\omega;\underline{k}_o,\omega_o;\underline{k}-\underline{k}_o,\omega-\omega_b)\,\chi(\underline{k}-\underline{k}_o,\omega-\omega_o;-\underline{k}_o-\omega_b;\underline{k},\omega)\,|E_o|^2\,\epsilon(\underline{k}+\underline{k}_o,\omega-\omega_b)\\ &-(1-\alpha)^2\,\chi(\underline{k},\omega;-\underline{k}_o,\omega_b;\underline{k}+\underline{k}_o,\omega-\omega_b)\,\chi(\underline{k}+\underline{k}_o,\omega-\omega_b;\underline{k}_o,-\omega_o,\underline{k},\omega)\,|E_o|^2\,\epsilon(\underline{k}-\underline{k}_o,\omega-\omega_o) = 0.\end{aligned} \tag{22b}$$

This is the dispersion relation we will study in detail in the next section, applying it to the cases of the EID and

$2\omega_{pe}$ instabilities. One feature of this equation, which bears on the meaning of our truncation scheme, should be noted; (22b) implies (22a) whenever (20b) is not satisfied for both signs. That is, if $\epsilon(\underline{k}+\underline{k}_o, \omega-\omega_o) \gg \epsilon(\underline{k}-\underline{k}_o, \omega-\omega_o)$ which is equivalent to (20b) being violated for the upper sign, then (22b) simplifies to (22a). This is a result of the fact that our truncation scheme does not introduce any new physics; it only serves to make the problem mathematically tractable by giving us a method of predicting which modes will be important (i.e., coupled together) and which we can afford to ignore.

APPLICATIONS

We now apply our general formalism to specific situations in which a transverse pump decays into longitudinal waves. There are two possible three-wave processes in which this happens:

1). The $2\omega_{pe}$ instability. Here a pump wave near twice the plasma frequency decays into two Langmuir waves. We will show that the geometry and growth rates of this instability are changed considerably by a standing-wave pump. The qualitative changes are due to the superposition of two instabilities, each due to one component of the standing wave.

2). The EID instability. In this instability, the pump wave decays into an acoustic wave and a Langmuir

wave. As was noted before, this instability always has $k >> k_o$ and the effects of a standing wave are confined to a decrease in the effective power of the pump. Even so, an analysis of the EID instability in the interpretation of ionospheric modification experiments shows this effect to be significant. For both instabilities we examine the limit of small k_o to recover the standard travelling-wave results.

The $2\omega_{pe}$ Instability[6]

The $2\omega_{pe}$ instability can be visualized as the decay of the pump wave, here at near twice the plasma frequency, into two plasma waves. The approximate frequency matching condition for this decay process is:

$$\omega_o(\underline{k}_o) \approx \omega_L(\underline{k}) + \omega_L(\underline{k}-\underline{k}_o). \tag{22}$$

This matching condition and the results of inequality (20) determine the qualitative aspects of the instability. In the initial work on this instability, Goldman derived results for arbitrary k_o.[6] The $2\omega_{pe}$ instability, in fact, does not exist for a homogeneous pump. He found maximum growth when (22) is satisfied and $\hat{k}\cdot\hat{k}_o \approx 1/\sqrt{2}$. The only generalization our results offer is that of a standing-wave pump. We find two regimes in the effects a standing-wave pump produces. One is the regime in which the daughter waves pumped by each component of the standing-wave are independent; this results in two, travelling-wave instabilities, pumped, however, by a field of only half the

local amplitude. In this case we recover the geometry of the travelling wave, where $\hat{k}\cdot\hat{k}_o \simeq 1/\sqrt{2}$. In the other regime, the daughter waves interact. This results in a growth rate intermediate between the other standing-wave regime and the growth rate that would result from a travelling wave pump. The geometry is essentially unchanged. Finally, we use physical arguments to show that in the $k >> k_o$ regime, the standing-wave and travelling-wave results agree. Let us look at the simplest case of a standing-wave driving a $2\omega_{pe}$ instability, when m = 3, and our dispersion relation is given by (22b). In this case, we have the following three modes coupled:

$$(23)\qquad Re\,\omega(\underline{k}) \simeq \omega_r(\underline{k}); \quad Re\left[\omega(\underline{k}\pm\underline{k}_o)-\omega_r\right] \simeq -\omega_r(\underline{k}\pm\underline{k}_o)$$

and, from (20) we get the exact conditions on k_o:

$$(24)\qquad 3\,\underline{k}_o\cdot(\underline{k}_o+\underline{k}) < Im\,\epsilon(\omega,\underline{k}) < 6\,\underline{k}_o\cdot(k+2k_o).$$

Using the symmetry properties of the susceptibilities given in the Appendix, the equation describing the new normal modes of the plasma is (from (22b)):

$$(25)\qquad \begin{aligned}&\epsilon(\underline{k},\omega)\,\epsilon(\underline{k}-\underline{k}_o,\omega-\omega_o)\,\epsilon(\underline{k}+\underline{k}_o,\omega-\omega_o)+\alpha^2|E_o|^2\,|\chi(\underline{k},\omega;\underline{k}_o,\omega_o;\underline{k}-\underline{k}_o,\omega-\omega_o)|^2\times\\ &\qquad\times\epsilon(k+k_o,\omega-\omega_o)\\ &+(1-\alpha)^2|E_o|^2\,|\chi(k,\omega;-k_o,\omega_o;k+k_o,\omega-\omega_o)|^2\,\epsilon(k-k_o,\omega-\omega_o)=0.\end{aligned}$$

The Appendix gives the general form for these susceptibilities:

$$(26)\qquad \chi(k,\omega;\pm k_o,\omega_o;k\mp k_o,\omega-\omega_o)=\frac{i}{2}\left(\frac{T+1}{T}\right)^{1/2}W_e^{1/2}(\hat{e}_o\cdot\underline{k})\left[\frac{\mp 2\underline{k}\cdot\underline{k}_o+k_o^2}{k\,|\underline{k}\mp\underline{k}_o|}\right]\equiv\frac{2i\,\Gamma_\mp}{\omega_{pe}},$$

where:

$$T = \theta_e/\theta_i ,$$

$$W_0 = E_0^2/[4\pi n_e(\theta_e + \theta_i)] .$$

Since all the high-frequency modes are well-defined, we also make resonance approximations for all the dielectric functions;

(27a) $$\epsilon(\underline{k},\omega) = \frac{2}{\omega_{pe}}\left[\omega - \omega_L(\underline{k}) + i\gamma\right] ,$$

(27b) $$\epsilon(\underline{k}\pm\underline{k}_0, \omega-\omega_b) = -\frac{2}{\omega_{pe}}\left[\omega-\omega_0+\omega_L(\underline{k}\pm\underline{k}_0)+i\gamma\right] .$$

This reduces equation (25) to an algebraic equation, cubic in the frequency:

$$\begin{aligned}(28)\quad &\left[\omega-\omega_L(\underline{k})+i\gamma\right]\left[\omega-\omega_0+\omega_L(\underline{k}+\underline{k}_0)+i\gamma\right]\left[\omega-\omega_0+\omega_L(\underline{k}-\underline{k}_0)+i\gamma\right] \\ &-\alpha^2\Gamma_-^2\left[\omega-\omega_0+\omega_L(\underline{k}+\underline{k}_0)+i\gamma\right] \\ &-(1-\alpha)^2\Gamma_+^2\left[\omega-\omega_0+\omega_L(\underline{k}-\underline{k}_0)+i\gamma\right] = 0 .\end{aligned}$$

Although it is not necessary, we will also assume that the only damping of these modes is collisional, and, so not dependent on $\underline{k}$. This cubic equation is intractable in its full generality, but it can be solved approximately in two regimes where the instability exists. Defining the frequency mismatch factors:

$$\delta_\pm \equiv \omega_0 - \omega_L(\underline{k}\pm\underline{k}_0) ,$$

we have the following conditions under which the solutions to equation (28) will have a positive imaginary part and can be dealt with analytically:

A). Independently excited daughter waves. In

this case, one of the daughter waves is much nearer to being resonant than the second, or:

$$\mathrm{Im}\,\epsilon(\omega-\omega_0) > \epsilon(\underline{k}_0\pm\underline{k},\omega-\omega_0) \gg \epsilon(\underline{k}_0\mp\underline{k},\omega-\omega_0)$$

or:

$$|\omega-\delta_\pm| \gg |\omega-\delta_\mp| .$$

Equation (28) can be approximately written:

$$(29)\qquad [\omega-\omega_L(\underline{k})+i\gamma][\omega-\delta_\pm+i\gamma] + \left\{\begin{matrix}(1-\alpha)^2\\ \alpha^2\end{matrix}\right\}\Gamma_\pm^2 = 0.$$

This is the equation describing the usual, travelling-wave pumped instability, except that the coupling between the two Langmuir waves, $\Gamma_\pm$, is only one-quarter the coupling for a travelling wave pump; this is a result of the local amplitude of the effective pump being one-half E_0. In other words, only one component of the standing-wave pump drives the instability. The growth rate is then, solving equation (29):

$$(30)\qquad \mathrm{Im}\,\omega = -\gamma + \left[\left\{\begin{matrix}(1-\alpha)^2\\ \alpha^2\end{matrix}\right\}\Gamma_\pm^2 - \frac{[\omega_L(\underline{k})-\delta_\pm]}{4}\right]^{1/2},$$

which has its maximum value of:

$$\mathrm{Im}\,\omega\big|_{max} = \left\{\begin{matrix}(1-\alpha)\\ \alpha\end{matrix}\right\}\Gamma_\pm - \gamma .$$

when $\omega_L(k) = \delta_\pm$. Notice that the maximum growth occurs when equation (22) is satisfied; this is the condition that determines $\underline{k}$ for maximum growth, as a function of $\underline{k}_0$, and so we have deduced the frequency matching condition in a natural way out of the dispersion relation. In addition,

there is a regime, for values of $\Gamma_\pm$ very near the threshold value of $\Gamma_\pm^2 = 4\gamma^2$, at which the maximum growth rate is proportional to Γ^2 rather than Γ. Figures two and three show a numerical solution to equation (28) in the regime of case A. Figure two shows the real and imaginary parts of ω, with $\hat{k}\cdot\hat{k}_o = 45^o$, and Figure three is a plot in polar coordinates of the imaginary part of the frequency (the growth rate of the instability) as a function of $\underline{k}$. Notice that for this case, equation (20), which requires the modes at $\underline{k}\pm\underline{k}_o$ to be "close enough" to resonance, is at best, marginally satisfied; we have, physically, two, essentially uncoupled (except near 90^o) instabilities, each pumped by a travelling-wave.

B). Coupled excited daughter waves. When $\delta_+ = \delta_-$, both daughter waves can be near resonance for the same $\underline{k}$, and equation (28) becomes (for $\alpha = 1-\alpha$):

$$[\omega - \omega_L(\underline{k}) + i\gamma][\omega - \delta + i\gamma] + 2\alpha^2\Gamma^2 = 0 \tag{31}$$

where:

$$\delta = (\delta_+ + \delta_-)/2$$
$$\Gamma = (\Gamma_+ + \Gamma_-)/2 .$$

The maximum growth rate here is larger by $\sqrt{2}$ than for case A:

$$\mathrm{Im}\,\omega|_{max} = \sqrt{2}\,\alpha\Gamma, \quad \omega_L(\underline{k}) = \delta . \tag{32}$$

Figure four shows the real and imaginary parts of the solutions to equation (28) in this regime, and Figure five

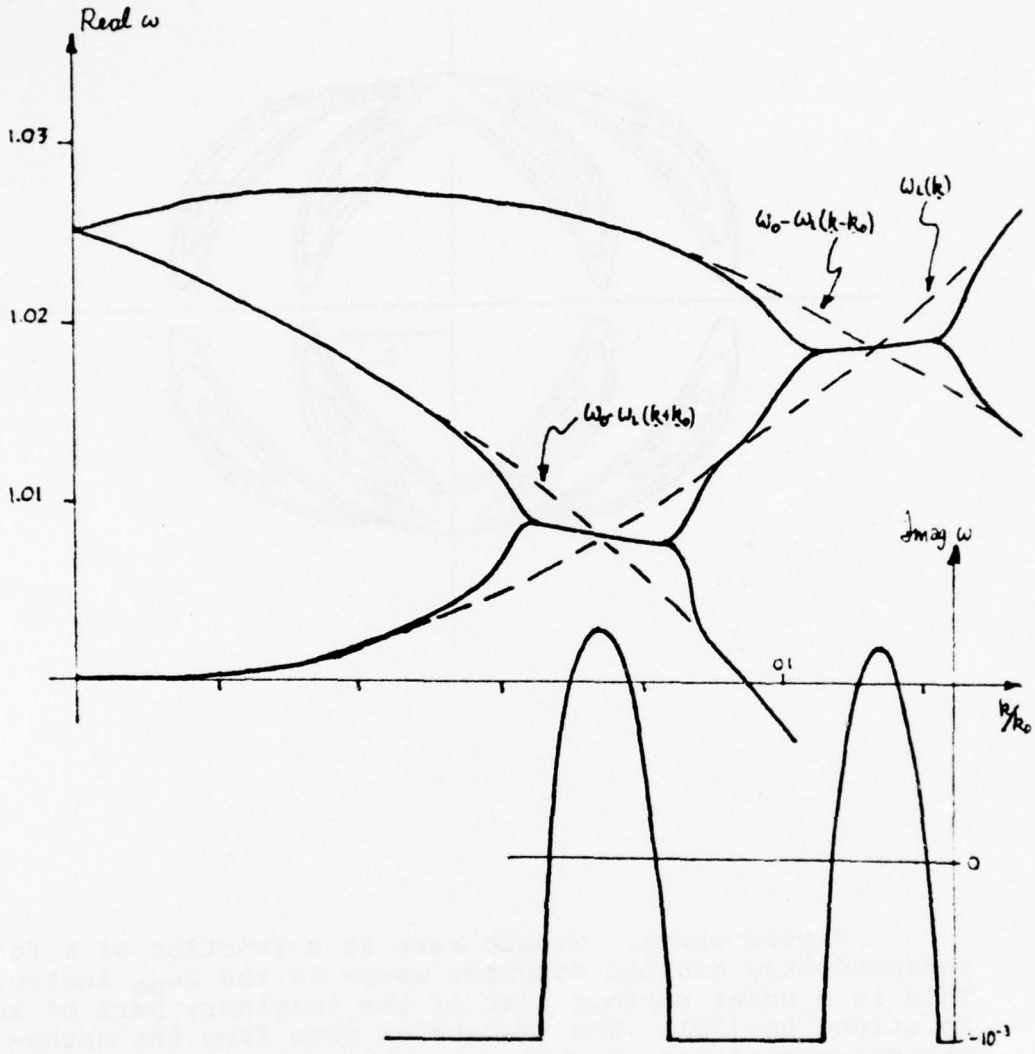

Figure two. Independently excited daughter waves driven by a standing-wave pump at $\hat{k}\cdot\hat{k}_o = 1/\sqrt{2}$. The real parts of the three roots of (28), given in the top solid lines, and the imaginary part of any root which greater taan the Langmuir damping, are shown on the same graph. The following parameters put this example in the regime of case A of the text for the $2\omega_{pe}$ instability: $k_o = .056$; $W_0 = 1.6\times10^{-4}$; $(v_e/c)^2 = 10^{-3}$; and $\gamma = 10^{-3}$. The maximum growth rate occurs when (23) is satisfied. In this regime, equation (29) is a good approximation to the above solution in the regions of growth.

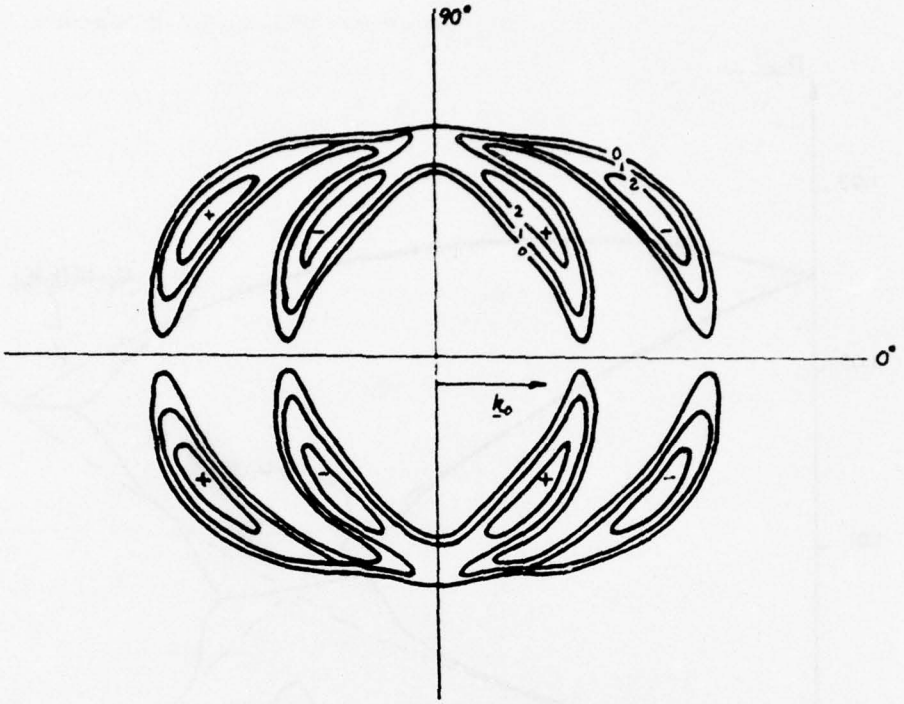

Figure three. Growth rate as a function of $\underline{k}$ for independently excited daughter waves in the $2\omega_{pe}$ instability. This is a polar contour plot of the imaginary part of the solutions to (28). The symmetries come from the mathematical properties of (29), such that, for example, inverting $\underline{k}$ changes the upper for lower sign in (29). The signs in the center of each region of the instability correspond to the appropriate sign in (29) and also indicate the wave coupling that produces the instability (± corresponds to $\omega(k)$ and $\omega(k\pm k_o)$ being coupled). The parameters for this graph are the same as in Figure two. The units in the contours are:

0 $-1\text{x}10^{-3}\ \omega_{pe}$
1 0
2 $+1\text{x}10^{-3}\ \omega_{pe}$.

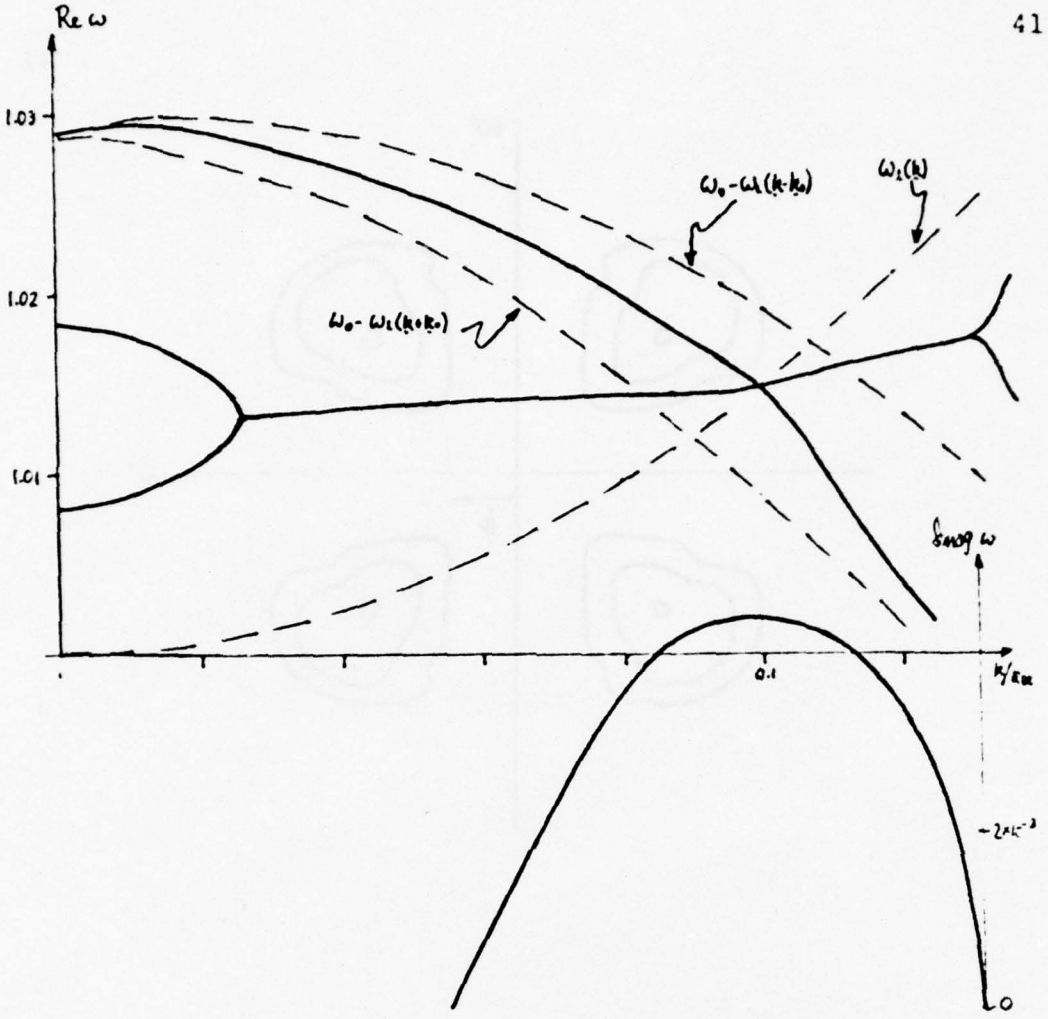

Figure four. Coupled excited daughter waves driven by a standing-wave pump at $\hat{k}\cdot\hat{k}_o = 1/\sqrt{2}$, the $2\omega_{pe}$ instability. The real roots of (29) are given on top, and the imaginary part of any root when it is positive, given in the lower curve. The following parameters put this example in the regime of case B: $k_o = .028$, $W_o = 1.6\times10^{-2}$, $(v_e/c)^2 = 2.5\times10^{-4}$, $\gamma_L = 10^{-2}$, $\hat{k}\cdot\hat{k}_o = \cos(45^o)$. For this smaller k_o, the disjoint structures of Figure two have coalesced. We can write the condition for this coalescence in terms of Γ and k_o:

$$3\underline{k}_m\cdot\underline{k}_o \lesssim 2\Gamma,$$

when $\omega_L(\underline{k}_m) - \delta(k_m) = 0$, from considerations of the width of the unstable regions and the distance between the regions of instability. Notice that when $\delta m\,\omega > \gamma_L$, that this is automatically guaranteed to be the case by (20). The broader region of instability is due to the larger value of γ_L used in this graph.

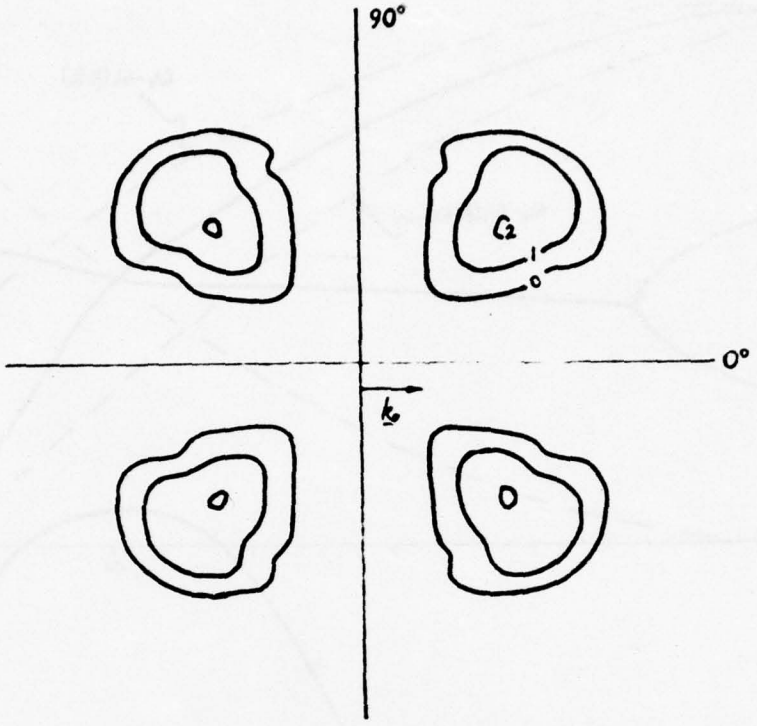

Figure five. The growth rate as a function of $\underline{k}$ for coupled excited daughter waves of the $2\omega_{pe}$ instability driven by a standing-wave pump. This is a polar, contour plot of the solutions to (28), with the parameters of Figure four. The symmetries are the same as in Figure three. The units on the contours are:

0	0
1	$2\text{x}10^{-3}\ \omega_{pe}$
2	$4\text{x}10^{-3}\ \omega_{pe}$.

shows a polar plot of the positive imaginary part of this solution.

Thus, the most important change that a standing-wave pump brings about is a change in the effective field strength that drives the instability. As we have seen above, when each component of the pump drives independent daughter waves, the effective pump field amplitude is down by one-half from the travelling-wave case, and, when both act simultaneously, the amplitude is down by a factor of $\sqrt{2}$. In this second case, the pump fields seem to add incoherently, with powers rather than amplitudes adding. The difference between cases A and B can be one of k_o getting smaller; as k_o decreases, and we approach a uniform pump, the effective field strength increases. The inequalities in (20) determine whether the daughter waves are "broad" enough to be pumped by both components of the pump simultaneously (see Figure one b), page 26).

Indeed, if we can solve the full equation (19) in the limit of $k_o = 0$, we should recover the travelling-wave results. The limit of (19), however, is subtle. Strictly speaking, the instability does not exist when $k_o = 0$, since all the susceptibilities are proportional to k_o when $k_o \ll k$. Thus, we can look at the limit $k_o \ll k$, but with k_o still non-zero. There are at least two ways of taking the limit:

1). In (11),

$$E_o = |E_o|\left[(1-\alpha)\sin(\underline{k}_o\cdot\underline{x}+\omega_o t+\varphi) - \alpha\sin(\underline{k}_o\cdot\underline{x}-\omega_o t+\varphi)\right],$$

let α go to one, followed by k_o getting small. This limit presents no problems; when $\alpha = \frac{1}{2}$, it easily gives the results for a standing-wave pump, and, when $\alpha = 1$ or 0, it gives the properly normalized amplitude for a travelling-wave.

2). If, we set $\alpha = \frac{1}{2}$, but take the limit $k_o \ll k$, the inequalities in (20) demand that more and more modes be coupled together. If we require that $nk_o \ll k$ for any n, then we must use an arbitrarily large matrix equation of the form of (19). In the limit, all the susceptibilities are the same, and we have to evaluate the following determinant, with the definitions:

(33) $$\chi = \frac{i}{2}\left(\frac{T+1}{T}\right)^{\frac{1}{2}} W_o^{\frac{1}{2}} (\hat{e}_o\cdot\hat{k})(\hat{k}_o\cdot\hat{k}),$$

(34) $$\epsilon(\omega) \equiv R = \frac{2}{\omega_{pe}}\left[\omega - \omega_L(\underline{k}) + i\gamma\right]$$
$$\epsilon(\omega-\omega_b) = -\frac{2}{\omega_{pe}}\left[\omega - \delta + i\gamma\right].$$

evaluated at the k for which $\omega_L(k) = \delta$, so that

$$\epsilon(\omega-\omega_o) = -R,$$

(35)
$$D_m = \begin{vmatrix} \vdots & \vdots & \vdots & \vdots & \vdots \\ \cdots\ R & \chi/2 & 0 & 0 & 0\ \cdots \\ \cdots\ \chi/2 & -R & \chi/2 & 0 & 0\ \cdots \\ \cdots\ 0 & \chi/2 & R & \chi/2 & 0\ \cdots \\ \cdots\ 0 & 0 & \chi/2 & -R & \chi/2\ \cdots \\ \cdots\ 0 & 0 & 0 & \chi/2 & R\ \cdots \\ \vdots & \vdots & \vdots & \vdots & \vdots \end{vmatrix} = 0$$

We have not been able to mathematically reduce this infinite determinant to the equation for a $2\omega_{pe}$ instability pumped by a travelling-wave with amplitude twice the amplitude of either component of the standing-wave (this is the limit that would be expected); however, we have been able on physical grounds, to derive a limit on the size of the determinant, and within this limit our large determinental condition reproduces the travelling-wave results. That is, an m x m determinant (m is the limit we are able to derive), for large m, gives the same results as the center 2 x 2 determinant (marked by dotted lines in (35)) does with E_o doubled. Physically, this describes the fact that as k_o becomes negligible compared to k, the two components of the standing-wave become indistinguishable, and the local amplitude of the field goes from:

$$[E_o(k_o,\omega_o) + E_o(-k_o,\omega_o)]/2 \text{ to } E_o(\omega_o)$$

In a straightforward, although tedious, calculation it is possible to derive recursive relations relating the determinants of different dimension, m.

(36) $$D_m = R D_{m-1} - (\chi/2)^2 D_{m-2} \quad , \quad \mathrm{mod}_4 m = 0,$$

(37) $$D_m = R D_{m-1} + (\chi/2)^2 D_{m-2} \quad , \quad \mathrm{mod}_4 m = 1,$$

(38) $$D_m = -R D_{m-1} + (\chi/2)^2 D_{m-2} \quad , \quad \mathrm{mod}_4 m = 2,$$

(39) $$D_m = -R D_{m-1} - (\chi/2)^2 D_{m-2} \quad , \quad \mathrm{mod}_4 m = 3.$$

where mod_4 m is the modulo, base 4, of m (i.e., the integer remainder upon division of m by 4). There are four relations because of the alternating sign of the diagonal elements in (35).

Keeping terms fourth order in E_o, but no higher powers, we can write the determinental conditions for the two cases of interest, mod_4 m = 1 or 3 (which have the same value to this order in E_o):

$$D_m = \left[R^4 + (m-1)\chi^2 R^2/4 - \left(\frac{m^2-5m-6}{2}\right)\chi^4/16\right] R_{m-4} = 0. \tag{40}$$

It is easy to factor this quadratic in R^2 and write its generally complex solutions in the form:

$$D_m \propto R^2 - \beta\,(\chi/2)^2. \tag{41}$$

For a travelling-wave pump we have, in this notation:

$$D_m \propto R^2 - 4\,(\chi/2)^2,$$

Our 3 x 3 results are that:

$$D_m \propto R^2 - 2\,(\chi/2)^2.$$

For m $\lesssim$ 9, we get the expected result, that β approaches four; at m = 9, β = 3.94. This is physically equivalent to the two components of the standing-wave field coalescing, doubling the local field amplitude and thus quadrupling χ. Numerical results showing this dependence of β on m are presented in the next section. However, after a gradual asymptotic-like approach to β = 4, β begins to increase as

$\sqrt{m}$.

We must look for a physical explanation for the breakdown of our matrix formalism. Physically, the problem seems to in our continuing to treat all the modes as distinguishable as k_o decreases, no matter how close they are to each other. That is, as k_o decreases, all the modes at $k \pm 2nk_o$ must coalesce with the mode at (k, ω) and all the modes with wavenumbers of $(k \pm (2n+1)k_o)$ must coalesce with the mode at $(k, \omega - \omega_o)$. Physically, this will not be a discontinuous process, obviously, collapsing an infinity of modes for any non-zero k_o to only two when k_o equals zero. Rejecting that possibility, we must examine the criteria for being able to distinguish modes which are close to each other.

Referring back to Figure one b) (page 26), it is clear that if k_o is small enough so that for $n \gg 1$, we have:

$$|\omega_a(\underline{k}_a) - \omega_a(\underline{k}_a - 2\underline{k}_o)| \ll |\omega_a(\underline{k}_a) - \omega(\underline{k} - n_a\underline{k}_o)|$$

and, then, in this case, it will be difficult to distinguish between $\omega_a(\underline{k}_a)$ and $\omega_a(\underline{k}_a \pm 2\underline{k}_o)$. Both of these modes will overlap entirely and so must, physically, be considered identical. This result puts a rough upper limit on n: $n \lesssim 10$, and on m, the size of the determinant, $m \lesssim 20$. This consideration gives an upper bound on the number of modes which can be put in this matrix formalism of (19) and still remain physically meaningful. That is to say, for m large enough, say greater than 10, we expect the linear

results for these modes to be meaningless, because the modes are no longer distinguishable. And, it is at this point that our mathematical results begin to give physically suspicious results. Another way of looking at this situation is to say that only on the order of ten modes with the same frequency can be excited, and the coupling of these ten modes is given by (34). When this many modes must be taken into account, we have the standing-wave pump duplicating the coupling given by a travelling-wave pump.

It is important to note that this argument is a physical and intuitive one. Mathematically, in an infinite, homogeneous plasma, there are no limits on the number of modes that can exist. If two modes have different wavenumbers, no matter how close these wavenumbers may be to each-other, they are distinguishable. For a reason that remains unclear, our matrix formalism does not mathematically allow us to take the limit $k_o \rightarrow 0$ and, by doing so, to reproduce the travelling-wave results.

THE ELECTRON-ION DECAY INSTABILITY[1,2]

In the case of the electron-ion decay instability, the decay of a high frequency electric field near the plasma frequency into a low frequency acoustic mode (or quasi-mode) and a high frequency Langmuir wave, the new mode coupling effects of a standing-wave pump are similar to those for the $2\omega_{pe}$ instability. The important differences between

the standing-wave treatment of these two instabilities come from the fact that the daughter modes for the decay instability are different resonances of the system. Thus, to begin with, we must interpret the inequalities in (20) differently. The number of modes of the acoustic branch which are close enough (in the sense above) is n_a:

$$2(n_a-1)(m_e/m_i)^{1/2} k_o < \partial m\, \epsilon(\omega_A, k_a) \tag{43}$$

and of Langmuir waves, is n_b:

$$\epsilon\, n_b \underline{k}_o \cdot (\underline{k} + n_b \underline{k}_o) > \partial m\, \epsilon(\omega_L, \underline{k} + n_b \underline{k}_o). \tag{44}$$

In the case where:

$$3k_o + 3k\cos\vartheta > (m_e/m_i)^{1/2}, \quad \vartheta = \cos^{-1}(\hat{k}\cdot\hat{k}_o), \tag{45}$$

these relations imply that the standing wave pump will couple together first modes at:

$$\omega_L(\underline{k}),\ \omega_A(\underline{k}+\underline{k}_o),\ \omega_A(\underline{k}-\underline{k}_o),$$

and then additional modes as allowed. When (45) holds, there cannot be a coupling of one acoustic wave and two Langmuir waves. This follows from the frequency matching condition:

$$\omega_o \approx \omega_A + \omega_L,$$

which, for a transverse pump, assures that k is always much greater than k_o. Thus for any value of k_o, n_a will be greater than n_b.

We have looked in some detail at this case, the simplest standing-wave coupling, that of $\omega_L(k)$ coupled

with $\omega_A(\underline{k}\pm\underline{k}_o) = \omega_o - \omega_L(\underline{k})$. Corresponding to equation (28) for the $2\omega_{pe}$ instability, we have (from (25)):

$$[\omega-\omega_i(\underline{k})+i\gamma][\omega-\omega_o+\omega_A(\underline{k}+\underline{k}_o)+i\gamma_A][\omega-\omega_o+\omega_A(\underline{k}-\underline{k}_o)+i\gamma_A]$$

$$-\alpha^2\Gamma_+^2[\omega-\omega_o+\omega_A(\underline{k}-\underline{k}_o)+i\gamma_A] \tag{46}$$

$$-(1-\alpha)^2\Gamma_-^2[\omega-\omega_o+\omega_A(\underline{k}+\underline{k}_o)+i\gamma_A]=0,$$

where (see (A.8) and (A.9)):

$$\Gamma_\pm^2 = -\frac{1}{4}\left(\frac{1+T}{T}\right)W_o\,\omega_A(\underline{k}\pm\underline{k}_o)\,(\hat{k}\cdot\hat{e}_o)^2 \quad . \tag{47}$$

This equation is valid as long as (using (43) and (44)), and $n_a = n_b = 1$:

$$(m_e/m_i)^{1/2}\,k_o < \gamma_A \tag{48a}$$

and:

$$Im\,\epsilon(\omega) < 6\,\underline{k}\cdot\underline{k}_o + 6k_o^2. \tag{48b}$$

Notice that as long as $\theta_e \approx \theta_i$, then $\gamma_A = O(m_e/m_i)^{1/2}k)$, so that (48a) is easily satisfied; (48b), however, is a restrictive condition on $Im\,\epsilon(\omega_L)$. It is always the case, furthermore, that:

$$|\omega_A(k-k_o)-\omega_A(k+k_o)| << \omega_o \quad .$$

This means there is no regime corresponding to case A for the $2\omega_{pe}$ instability, and it is always a valid approximation to write for (46), when $\alpha = 1/2$:

$$[\omega-\omega_i(\underline{k})+i\gamma][\omega-\omega_o+\omega_A(k)+i\gamma_A]-2(\Gamma/2)^2=0. \tag{49a}$$

That is, for the decay instability with a standing-wave pump and k_o in the range prescribed by (48a) and (48b), the coupling is half what it would be for a travelling-wave pump with the same local amplitude. The effective power is down by a factor of two. The formal solutions to this type of equation (49a) have been studied in detail elsewhere,[4-6] and the growth rate is gotten straightforwardly by solving (49a):

$$\mathrm{Im}\,\omega = -\frac{\gamma_A+\gamma_L}{2} \pm \frac{1}{2}\sqrt{2\left(\frac{\Gamma}{2}\right)^2+\left[i(\gamma_A-\gamma_L)+\Delta\right]^2}$$

where:

$$\Delta \equiv \omega_A(\underline{k}) + \omega_L(\underline{k}) - \omega_o .$$

This gives, with $\Delta = 0$:

$$\mathrm{Im}\,\omega\big|_{max} = \begin{cases} \Gamma^2/8\gamma_A , & \Gamma^2 \ll \gamma_A ,\ \gamma_L \ll \gamma_A , \\ (\Gamma^2/8)^{1/2} , & \Gamma^2 \gg \gamma_A ,\ \Gamma^2 \gg \gamma_L , \\ \Gamma^2/8\gamma_L , & \Gamma^2 \ll \gamma_L ,\ \gamma_L \gg \gamma_A . \end{cases} \tag{49b}$$

We note here only the consequences of a standing-wave pump. These changes all result from the factor of two in (49a). This halving of the effective power means that, given a local field amplitude, the threshold is doubled if this field is a standing-wave rather than a travelling wave. In the case of a travelling-wave with local amplitude E_o, the threshold for the decay instability is:

$$(\Gamma_c/2)^2 = \gamma\gamma_A \tag{50a}$$

and the maximum growth rate is:

$$(50b) \qquad \mathrm{Im}\,\omega\big|_{max} = \begin{cases} \Gamma^2/4\gamma_A\,, & \Gamma^2 \ll \gamma_A\,,\ \gamma_L \ll \gamma_A\,, \\ \Gamma/2\,, & \Gamma^2 \gg \gamma_A\,,\ \Gamma^2 \gg \gamma_L\,, \\ \Gamma^2/4\gamma_L\,, & \Gamma^2 \ll \gamma_L\,,\ \gamma_A \ll \gamma_L\,. \end{cases}$$

But if the pump field is a standing-wave with total, local amplitude, Γ_o, then the threshold is given by:

$$(51) \qquad (\Gamma_c/2)^2 = 2\gamma\gamma_A\,.$$

and the maximum growth rate is given by (49b).

Let us look at one situation where this factor of two may be important. In several ionospheric modification experiments, it has been claimed that the observed enhanced level of Langmuir waves is due to a non-equilibrium spectrum created by the decay instability.[3,10-15] Physically, the scenario is as follows: the relatively intense electromagnetic wave from the ground (a wave of ordinary polarization) travels upwards from the antenna through the ionosphere. The inhomogeneity of the ionosphere has three effects: it results in an Airy swelling factor in the amplitude of the modifier wave, in an absorption which becomes a function of altitude, and in a reflection of the modifier wave when the critical density is reached (when ω_{pe}(height) = ω_o). Since this absorption is usually small, the modifier wave has sufficient power to exceed the decay instability threshold at the reflection point and at altitudes somewhat lower. If this threshold is exceeded, part of the energy

from the modifier wave is transferred to Langmuir turbulence by the EID instability. The instability is driven by the sum of the incident and reflected waves, a standing-wave. The saturation of this instability then provides a steady state level of Langmuir turbulence that is measured from the earth using a second wave (which is scattered by this enhanced turbulence in the "modified" ionosphere).

Attempts to understand the experimental data on this scattering revolve around estimating the ratio of modifier intensity to the EID instability threshold, then calculating the enhancement of the Langmuir spectrum that would be created by such a pump, and finally, calculating the scattering that such an enhanced spectrum would produce. Our results will be relevant, since the modifier wave, is, in fact, a standing-wave whenever it is of sufficient intensity and satisfies the frequency matching condition for the instability.[3] In a detailed study of the problem, DuBois, et al. show that even with considerable absorption of the incident wave, a standing-wave field is set up considerable distances from the reflection point. Using the parameters of this paper,[3] which correspond to a height about 560 meters below the reflection point, we have: $k_o = 4 \times 10^{-5}$ (in units of the Debye wavenumber, which is here $220 m^{-1}$), the fastest growing mode's wavenumber, $k = 0.05$, and $\hat{k} \cdot \hat{k}_o = 0.85$. In addition, DuBois, et al,, calculate a local, average power flux of 800 W/m^2 at this

height, for an antenna inensity flux of 50 W/m^2. This is about five times the threshold of the EID instability, so that:

$$\mathrm{Im}\,\epsilon(\omega) = 2\,\mathrm{Im}\,\omega \approx 2\times10^{-5}$$

(in units of the plasma frequency). Thus, inequality (48b) is satisfied. Notice, however, that even for a slightly higher power, (48b) would not be satisfied, and we would have to solve a more complicated coupling of waves.

Thus equation (49) describes the decay instability in this case. The correct way to account for the reflected wave in the ionosphere is not to add amplitudes, but rather to add fluxes or powers of the two components of the standing wave (that is, consistent with our homogeneous approximation, we must "decompose" the actual Airy function amplitude modulation of the modifier wave and look at it as made up of two waves, with different relations betweeen ω_o and k_o for each). Thus, the estimates of the effective power in the papers referred to above are too high by a factor of two. Even given the large uncertainty in all the calculations of the ionospheric problem, a increase by a factor of two in the threshold is critical. Perkins, et al., for example, estimate the field at a value only twice the threshold,[14] and DuBois and Goldman use a figure of five times threshold.[3] In the graphs which DuBois and Goldman[15] show of total (saturated) Langmuir energy as a function of

pump power, a change by a factor of two in the effective pump power, from 5.0 to 2.5, results in a decrease in the peak Langmuir wave energy by a factor of 100, and in the integrated Langmuir energy by a factor of 20. Since all the calculations of the scattering that should be observed are several orders of magnitude too large, this changed threshold helps in accounting for the discrepancy. Certainly, this is not a conclusive demonstration of the effect of a standing-wave pump, but our interpretation of the ionospheric modification experiments does open up a means of testing the effect of a standing wave pump. This factor of two may be observable in the comparison of low power modification experiments (with flux densities of less than 50 W/m^2), which have the simplest coupling of three daughter waves described above, and higher power experiments, in which (48b) is no longer satisfied and more modes are coupled. The theory of the case when k_o is smaller, or the power greater, so that (48b) is no longer satisfied, is treated next.

As in the case of the $2\omega_{pe}$ instability, we have also looked at the problem of the travelling-wave limit of the decay instability. Rather than an analytic treatment, we have numerically solved the equivalent of equation (34) for the decay instability. Specifically, we tested each mode, at the k for perfect matching, to determine whether it was "close enough" to $\omega_\lambda(k)$ to be coupled. Thus, the results

of our calculations were based on Table III, where the number of modes of the form $\omega_i(k \pm nk_o)$, $\omega_o - \omega_a(k \pm nk_o)$ that are within $\delta\omega$ of $\omega_i(k)$ are listed. Thus, coupling three Langmuir modes means that there are 26 acoustic modes that are close enough to be coupled. We actually evaluated a 29 x 29 matrix equation in this case, rather than taking advantage of the inequalities (43) and (44) which would have allowed us to neglect 22 of these acoustic modes. This test of the assumptions in (43) and (44) showed, in fact, that these are good assumptions. Figure six shows the results of this numerical work, where we have graphed the growth rate of the instability as a function k_o. Here the growth rate for $k_o = .006$ has the value from by equation (49). As more modes are coupled together, the growth rate increases. It approaches the value that would obtain for the solution to:

$$(\omega - \omega_L(\underline{k}) + i\gamma)(\omega - \omega_0 + \omega_A(\underline{k}) + i\gamma_A) - \Gamma^2 = 0,$$

exactly the result for a travelling wave-pump with the same local amplitude as the sum of the amplitudes of the two components of the standing-wave pump. Figure seven presents the same results as a function of the number of modes coupled together. This shows the dependence on the smaller of n_a and n_b that we noted above; it is a result of our matrix equation which allows no coupling between waves which have wavenumber shifts which differ by more than

TABLE III

MODES COUPLED IN THE DECAY INSTABILITY AS $k_o \to 0$.

k_o	$2n_a$, Number of Acoustic Modes	$2n_b-1$, Number of Langmuir Modes	γ_{max}
.0062	1	1	$.76\times10^{-4}$
.0031	2	1	1.20×10^{-4}
.00041	8	1	1.34×10^{-4}
.00020	14	1	1.33×10^{-4}
.00016	18	1	1.34×10^{-4}
.00014	22	3	1.79×10^{-4}
.00012	26	3	1.81×10^{-4}

NOTE: n_a and n_b and the number of modes are calculated according to equation (19). The limit as $k_o \to 0$ was taken keeping ω_o constant. In this case, $\gamma_L = 10^{-4}$ and $\hat{k}\cdot\hat{k}_o = .6$.

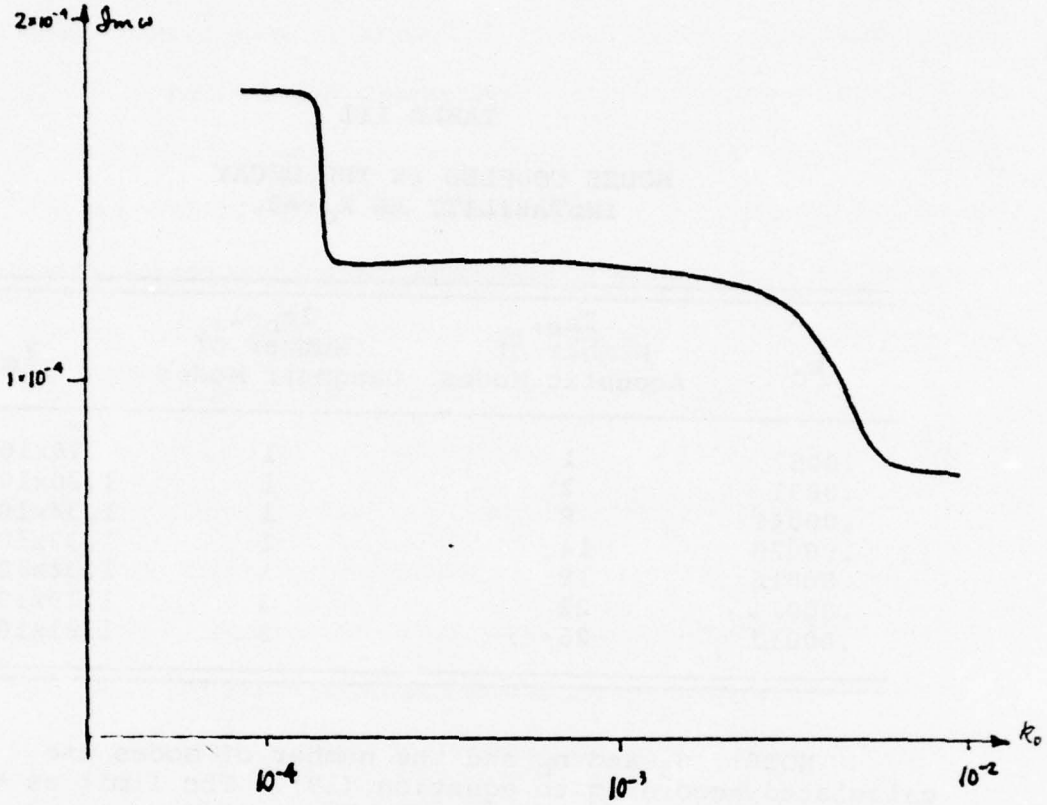

Figure six. The growth rate of the electron-ion decay instability, pumped by a standing-wave electromagnetic wave, as a function of the pump vavenumber. For this figure, $W_o = 4.x10^{-7}$, $(m_e/m_i) = 5.x10^{-3}$. The growth rate increases as the number of modes coupled together increases.

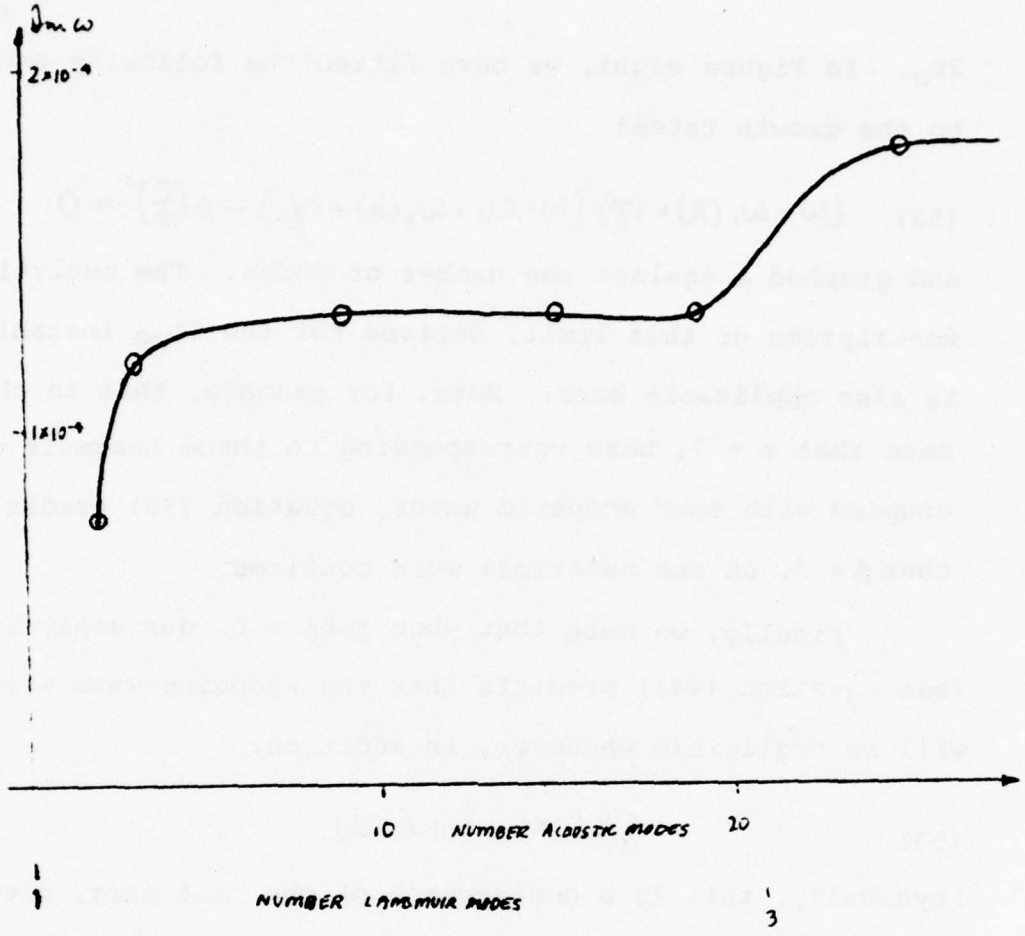

Figure seven. The growth rate of the electron-ion decay instability, pumped by a standing-wave electromagnetic pump, as a function of the number of waves that are coupled together; the parameters here are the same as in Figure six.

$2k_o$. In Figure eight, we have fitted the following equation to the growth rates:

$$(52) \quad (\omega - \omega_L(k) + i\gamma)(\omega - \omega_0 + \omega_A(k) + i\gamma_A) - \beta\left(\frac{\Gamma}{2}\right)^2 = 0.$$

and graphed β against the number of modes. The analytic description of this limit, derived for the $2\omega_{pe}$ instability, is also applicable here. Note, for example, that in the case that m = 7, here corresponding to three Langmuir waves coupled with four acoustic waves, equation (35) predicts that $\beta = 3$, as our numerical work confirms.

Finally, we note that when $\underline{k}\cdot\underline{k}_o = 0$, our analysis (see equation (44)) predicts that the standing-wave effects will be negligible whenever, in addition:

$$(53) \quad 6k_o^2 \ll \mathrm{Im}\,\epsilon(\omega)$$

Physically, this is a consequence of the fact that, given $k \gg k_o$, the variation of $\omega_L(\underline{k}\pm\underline{k}_o)$ with k_o comes almost entirely from the $\underline{k}\cdot\underline{k}_o$ term:

$$\omega_L(\underline{k}\pm\underline{k}_o) \approx (1 + \tfrac{3}{2}k^2 + \tfrac{3}{2}k_o^2 \pm 3\underline{k}\cdot\underline{k}_o).$$

If $k\cdot k_o = 0$, all the Langmuir waves at $\omega_L(\underline{k}\pm n\underline{k}_o)$ will be very close together, and $\beta \to 4$ as these modes are coupled.

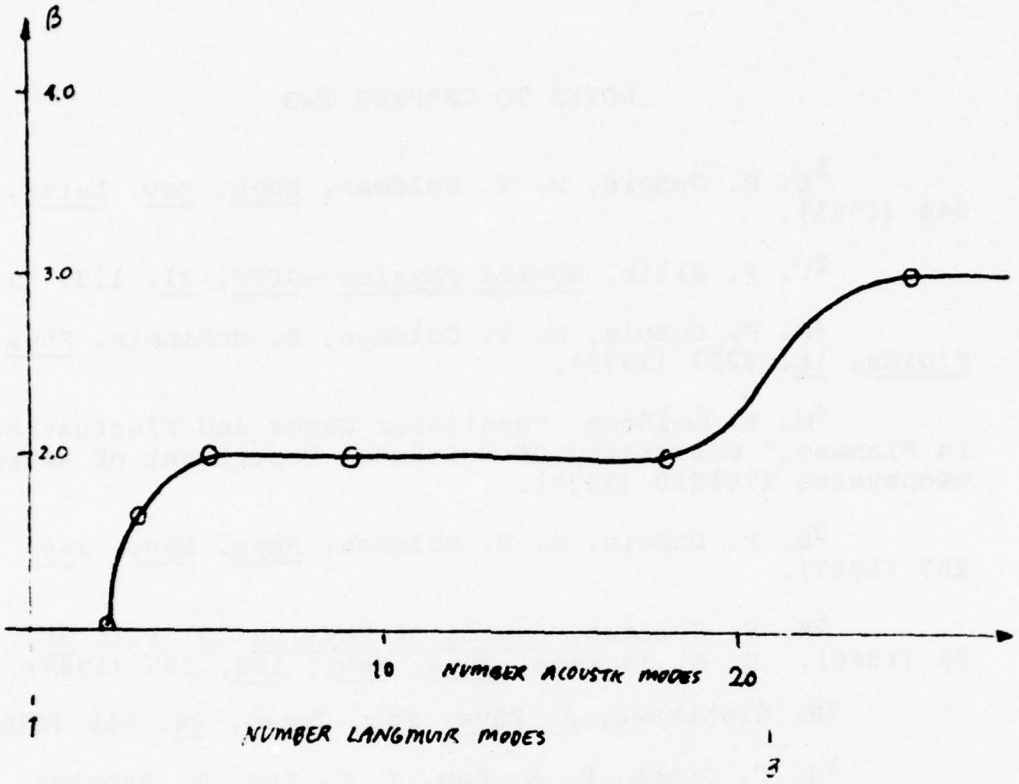

Figure eight. "Effective pump power," β, as a function of the number of modes coupled together. β is defined in equation (52). $\beta = 4$ corresponds to the amplitude of the field contributing as in the case of a travelling-wave.

NOTES TO CHAPTER TWO

[1]D. F. DuBois, M. V. Goldman, Phys. Rev. Lett., 14, 544 (1965).

[2]V. P. Silin, Soviet Physics--JETP, 21, 1127 (1965).

[3]D. F. DuBois, M. V. Goldman, D. McKinnis, Phys. Fluids, 16, 2257 (1973).

[4]M. V. Goldman, "Nonlinear Waves and Fluctuations in Plasmas," University of Colorado, Department of Astro-geophysics #CU1010 (1974).

[5]D. F. DuBois, M. V. Goldman, Phys. Rev., 164, 207 (1967).

[6]M. V. Goldman, Annals of Physics (N. Y.), 38, 95 (1966). L. A. Jackson, Phys. Rev., 153, 235 (1967).

[7]K. Nishikawa, J. Phys. Soc. Japan, 24, 916 (1968).

[8]J. F. Drake, P. K. Kaw, Y. C. Lee, G. Schmidt, C. S. Lin, M. N. Rosenbluth, Phys. Fluids, 17, 778 (1974).

[9]B. D. Fried, T. Ikemura, K. Nishikawa, G. Schimdt, UCLA preprint, PPG-246 (1975).

[10]A. Y. Wong, R. J. Taylor, Phys. Rev. Lett., 27, 644 (1971).

[11]D. F. DuBois, M. V. Goldman, Phys. Rev. Lett., 28, 218 (1972).

[12]F. W. Perkins, P. K. Kaw, J. Geophys. Res., 76, 282 (1971).

[13]J. A. Fejer, J. Geophys. Res., 76, 284 (1971).

[14]F. W. Perkins, C. Oberman, E. J. Valeo, J. Geophys. Res. 79, 1478 (1974).

[15]D. F. DuBois, M. V. Goldman, Phys. Fl., 15,919 (1972).

CHAPTER III

LANGMUIR PUMPED PARAMETRIC INSTABILITIES IN THREE DIMENSIONS

In this chapter we will study the four-wave processes which have longitudinally polarized Langmuir-like waves as both pump and daughter waves. These instabilities are well-known in one-dimension (for references see Table I, page 6, and II, page 8), when the daughter waves have wavevectors parallel to $\underline{k}_o$. These well known one dimensional instabilities for the Langmuir-to-Langmuir case are the oscillating two stream instability (OTS), which couples the high-frequency daughter waves with a zero frequency response of the plasma, and the modified EID instability, which couples the high frequency daughter waves with a resonant ion acoustic mode. In our analysis of these instabilities, we have derived a single dispersion relation wich includes all these instabilities, and which includes regimes where these instabilities exist for wavenumbers other than those parallel to k_o. We have, in addition, discovered another instability, the stimulated modulational instability (SM) which only appears in three dimensions. Our treatment for these instabilities includes the effects of an arbitrary wavevector pump and

an exact ion equation (rather than the usual fuild treatment).

As the kinetic theory derivation of the last chapter implied, we can express the susceptibility of the plasma in a power series in the fields, so that, at least formally, we have:

$$\chi(E) = \underline{\chi}_1 \cdot \underline{E} + \underline{E} \cdot \underline{\underline{\chi}}_2 \cdot \underline{E} + \underline{E} \cdot (\underline{E} \cdot \underline{\underline{\underline{\chi}}}_3 \cdot \underline{E}) + \ldots \quad (1)$$

Physically, based on an analogy with quantum mechanics, the higher order terms correspond to the plasma coupling with more than one pump field photon. In the last chapter, by restricting our work to phenomena involving only $\underline{\underline{\chi}}_2$, we were able to deal with only two daughter fields, a plasmon and photon, two plasmons, or two photons. However, important new effects occur with the couplings involved in $\underline{\underline{\underline{\chi}}}_3$, the so-called four-wave interactions. To treat the these interactions, we must include effects due to both $\underline{\underline{\underline{\chi}}}_3$ and arbitrary $\underline{k}_o$, since, in the case of a Langmuir or Langmuir-like wave (for both pump and daughter wave) one has a dispersion relation which allows daughter waves with wavenumbers comparable to the pump wavenumber. This follows since the dispersion of a Langmuir wave is proportional to v_e^2 rather than c^2, as in the case of an electromagnetic wave. The larger pump wavenumbers make three dimensional effects important. After a theoretical study of the linear stability of a Langmuir pump to

parametric growth, we will make specific applications of our results to the Langmuir spectra associated with electron beams in several parameter regimes: the solar corona, the ionosphere, and low density laboratory plasmas. Our general conclusion from these applications is that parametric processes do not greatly affect the dynamics of the beam plasm interaction (as has been theorized), but, even so, that these instabilities can account for a number of other phenomena associated with these beam plasma systems.

DERIVATION OF THE DISPERSION RELATION[1]

Using the formalism developed thus far, it is straightforward to write down the determinental condition describing the parametric processes induced by a pump made up of Langmuir waves, that is, a pump that is high frequency and longitudinally polarized, with frequency ω_o and wavenumber $\underline{k}_o$ (ω is a low frequency for all of this chapter):

$$(1)\quad \begin{pmatrix} \tilde{\epsilon}(\underline{k},\omega) & \chi(\underline{k}-\underline{k}_o,\omega-\omega_i;-\underline{k}_o,-\omega_i;\underline{k},\omega)E_o & \chi(\underline{k}+\underline{k}_o,\omega+\omega_i;\underline{k}_o,\omega_i;\underline{k},\omega)E_o \\ \chi(\underline{k},\omega;\underline{k}_o,\omega_i;\underline{k}-\underline{k}_o,\omega-\omega_i)E_o & \tilde{\epsilon}(\underline{k}-\underline{k}_o,\omega-\omega_o) & \chi(\underline{k}+\underline{k}_o,\omega+\omega_i;\underline{k}_o,\omega_i;\underline{k}_o,\omega_o;\underline{k}-\underline{k}_o,\omega-\omega_o)E_o^2 \\ \chi(\underline{k},\omega;\underline{k}_o,\omega_o;\underline{k}+\underline{k}_o,\omega+\omega_i)E_o & \chi(\underline{k}-\underline{k}_o,\omega-\omega_o;-\underline{k}_o,-\omega_i;-\underline{k}_o,-\omega_o;\underline{k}+\underline{k}_o,\omega-\omega_i)E_o^2 & \tilde{\epsilon}(\underline{k}+\underline{k}_o,\omega-\omega_o) \end{pmatrix} \begin{pmatrix} E(\underline{k},\omega) \\ E(\underline{k}-\underline{k}_o,\omega-\omega_o) \\ E(\underline{k}+\underline{k}_o,\omega+\omega_i) \end{pmatrix} = 0,$$

where, the entries in the first row and first column are the susceptibilities derived in the Appendix from the second order current, and the entries in the (2,3) and

(3,2) positions are the susceptibilities derived from the thrid-order current. These higher-order susceptibilities also enter into the definitions of the diagonal elements, "renormalizing" the dielectric functions:

$$\tilde{\epsilon}(\underline{k},\omega) \equiv \epsilon(\underline{k},\omega) + \chi(\underline{k},\omega;-\underline{k}_o,-\omega_o;\underline{k}_o,\omega_o;\underline{k},\omega)\, E_o^2 \cdot \tag{2}$$

Notice that the upper 2 x 2 matrix gives the usual decay instability, in which case, as is well-known, the higher-order susceptibilities are not necessary. However, when both the Stokes and anti-Stokes modes are coupled in the problem, they are each coupled (in first order) to the low frequency field at $E(k,\omega)$ and (in second order) to each other. Since we are dealing with Langmuir oscillations, these matrix elements must be evaluated for arbitrary $\underline{k}_0$; we cannot use the previously published results which assumed either $k \gg k_o$ or $\hat{k}\cdot\hat{k}_o = 1$.

The rather tiresome derivation of the susceptibilities is deferred to the Appendix. Even without the explicit form of these elements, we can use the following relations to write the determinate of (1) in a strikingly simple form (see (A.8), (A.10), and (A.11) from Appendix):

$$\chi(\underline{k}\pm\underline{k}_o,\omega\pm\omega_o;\underline{k}_o,\omega_o;-\underline{k}_o,-\omega_o;\underline{k}\pm\underline{k}_o,\omega\pm\omega_o) = k^2 \left|\chi(\underline{k}\pm\underline{k}_o,\omega\mp\omega_o;\pm\underline{k}_o,\mp\omega_o;\underline{k},\omega)\right|^2 , \tag{3}$$

and:

$$\chi(\underline{k}\pm\underline{k}_o,\omega\pm\omega_o;\pm\underline{k}_o,\pm\omega_o;\pm\underline{k}_o,\pm\omega_o;\underline{k}\mp\underline{k}_o,\omega\mp\omega_o) = k^2 \left|\chi(\underline{k}\pm\underline{k}_o,\omega\pm\omega_o;\pm\underline{k}_o,\pm\omega_o;\underline{k},\omega)\cdot \chi(\underline{k}\mp\underline{k}_o,\omega\mp\omega_o;\mp\underline{k}_o,\mp\omega_o;\underline{k},\omega)\right| . \tag{4}$$

With these relations, all terms third-order or higher in E_o cancel and we get, after rearrangement:

$$\left(\frac{k^2\epsilon(\underline{k},\omega)}{k^2\epsilon(\underline{k},\omega)-1}\right) + \frac{\chi(\underline{k}+\underline{k}_o,\omega+\omega_o;\underline{k}_o,\omega_o;-\underline{k}_o,-\omega_o;\underline{k}+\underline{k}_o,\omega+\omega_o)E_o^2}{\epsilon(\underline{k}+\underline{k}_o,\omega+\omega_o)}$$

$$+ \frac{\chi(\underline{k}-\underline{k}_o,\omega-\omega_o;\underline{k}_o,\omega_o;-\underline{k}_o,-\omega_o;\underline{k}-\underline{k}_o,\omega-\omega_o)E_o^2}{\epsilon(\underline{k}-\underline{k}_o,\omega-\omega_o)} = 0 . \tag{5}$$

This equation shows very clearly the coupling of the three resonances of the plasma, two with high frequency and one with low frequency, in a form characteristic of mode-coupling in non-linear optics, for example. Using the explicit expressions for the susceptibilities (equations A.8, A.10, and A.11, from the Appendix), we have:

$$-\frac{T}{T+1}\left(\frac{k^2\epsilon(\underline{k},\omega)}{k^2\epsilon(\underline{k},\omega)-1}\right) + \frac{W_o}{4}\left[\frac{\mu_+^2}{\epsilon(\underline{k}+\underline{k}_o,\omega+\omega_o)} + \frac{\mu_-^2}{\epsilon(\underline{k}-\underline{k}_o,\omega-\omega_o)}\right] = 0, \tag{6}$$

where:

$$T \equiv \theta_e/\theta_i ;$$

$$W_o \equiv \int \frac{d^3k \;\; E_o^*(\underline{k}_o)\cdot E_o(\underline{k})}{(2\pi)^3\left[4\pi n_e(\theta_e+\theta_i)\right]} ; \tag{7}$$

$$\mu_\pm^2 \equiv \left[\underline{k}_o\cdot(\underline{k}_o \mp \underline{k})\right]^2 \Big/ \left[k_o\,|\underline{k}_o \pm \underline{k}|\right]^2 .$$

Several aspects of equation (6) should be noted:

1). The two high frequency waves, the daughter (Langmuir-like) waves at $\underline{k} \pm \underline{k}_o$, are coupled together through a low frequency response of the plasma. As Tsytovich noted in his book, these couplings dominate all other Langmuir wave interactions.[2]

2). This low frequency response of the plasma is not given by the plasma dielectric function, except in the limit that $\epsilon(\underline{k}, \omega)$ goes to zero. Let us call:

$$D(\underline{k},\omega) \equiv -\frac{T}{T+1}\left[\frac{k^2\epsilon(\underline{k},\omega)}{k^2\epsilon(\underline{k},\omega)-1}\right] \tag{8}$$

At frequencies for which $k^2\epsilon(\underline{k}, \omega)$ is not small comapred to one (k is in units of k_{De}), the plasma's low frequency response is complicated. This "compensation" has been noted before,[3,4] and arises from the terms that the third-order current contributes. Figure one shows "diagrams" of the contributions to the wave-wave interactions from the second-order current (in Figure one a)) and the dominant contribution from the third order current (in Figure one b)). The terms that contribute from the third order current are essentially second order effects coupled together by a low frequency response of the plasma; the "four-wave" diagram can be viewed as two of the three-wave diagrams joined by a (virtual) low frequency response.

3). Equation (6) also comes out of a more careful analysis of the linear stability of an arbitrary Langmuir spectrum, if that spectrum, centered about $\omega_o(k_o)$, has a spread, Δk_o, in k-space about k_o, such that a condition on the narrowness of the spectrum is satisfied:

$$\frac{\partial}{\partial \underline{k}_o}\ln\left[\frac{\chi(\underline{k}\pm\underline{k}_o,\omega\pm\omega_o;\underline{k}_o,\omega_o;-\underline{k}_o,-\omega_o;\underline{k}\pm\underline{k}_o,\omega\pm\omega_o)}{\epsilon(\underline{k}\pm\underline{k}_o,\omega\pm\omega_o)}\right]\cdot\Delta\underline{k}_o \ll 1 . \tag{9}$$

This condition insures that the resonance is a broader function in k-space than the spectrum, so that the detailed shape of the spectrum can be ignored.

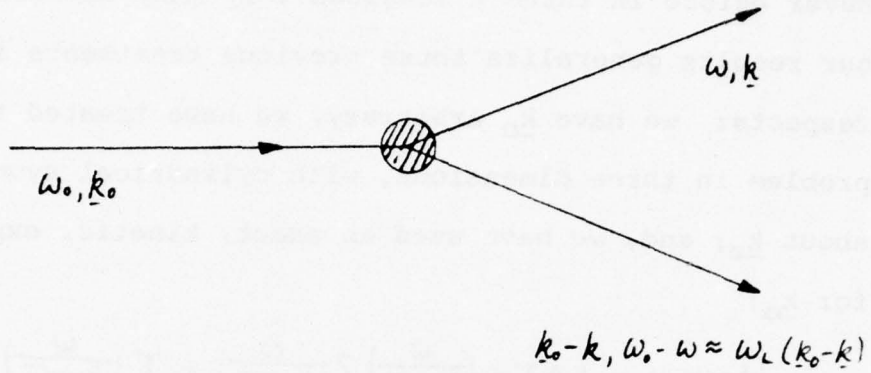

a).

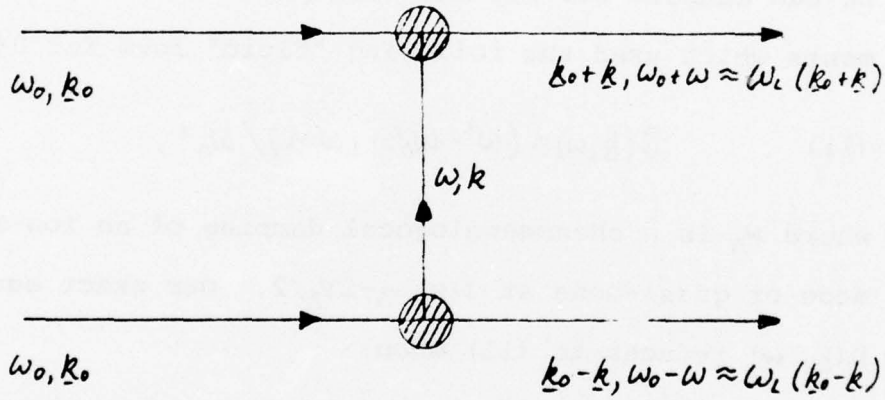

b).

Figure one. Three-wave (a) and four-wave (b) interactions. The pump wave has wavevector $\underline{k}_o$ and frequency ω_o; the low-frequency electrostatic disturbance has wavevector $\underline{k}$ and frequency ω; and, the Langmuir daughter waves have wavevectors $\underline{k}_o \pm \underline{k}$ and frequencies $\omega_o \pm \omega$. In the four-wave case both of these high frequency waves are excited and in the three-wave case, only one of them, the Stokes wave, at $\underline{k}_o - \underline{k}$, $\omega_o - \omega$. The wave at $\omega_o + \omega$ is called the anti-Stokes wave.

The question of the linear stability of a Langmuir pump has been treated, in various approximations (although never before in three dimensions), by many authors;[1,4-8] our results generalize these previous treatments in three respects: we have $\underline{k}_o$ arbitrary; we have treated the problem in three dimensions, with cylindrical symmetry about $\underline{k}_o$; and, we have used an exact, kinetic, expression for $\underline{k}_o$:

$$(10)\quad k^2\epsilon(\underline{k},\omega) = 1 + T + \left(\frac{\omega}{kv_e\sqrt{2}}\right) Z\left(\frac{\omega}{kv_e\sqrt{2}}\right) + T\left(\frac{\omega}{kv_i\sqrt{2}}\right) Z\left(\frac{\omega}{kv_i\sqrt{2}}\right),$$

where Z is the Fried-Conti plasma dispersion function.[9] We can connect our results with previous theoretical treatments which used the following "fluid" form for $D(\underline{k}, \omega)$:

$$(11)\qquad D(\underline{k},\omega) = (\omega^2 - \omega_A^2 + i\omega\nu_A)/\omega_A^2,$$

where ω_A is a phenomenologocal damping of an ion-acoustic mode or quasi-mode at $\omega = \omega_A - i\nu_A/2$. Our exact equation for $D(\underline{k}, \omega)$ reduces to (11) when:

$$kv_i \ll \omega \ll kv_e,$$

and we then can use the asymptotic forms for the Z-function:

$$\mathrm{Re}\ Z(\xi) = \begin{cases} -2\xi, & \xi \ll 1; \\ -\frac{1}{\xi} - \frac{1}{2\xi^3} - \frac{3}{4\xi^4}, & \xi \gg 1. \end{cases}$$

Substitution of these forms for Z into (10) and the definition of $D(\underline{k}, \omega)$ gives the real part of (11); the imaginary part can also be gotten similarly. However, the fluid

treatment goes on to use (11) for all values of ω. A specific problem arises with the zero frequency limit of (11). For $\omega = 0$, (11) gives the value -1. This is also the value of the static limit of the exact expression for $D(\underline{k}, \omega)$. In fact, (11) and the exact form for $D(\underline{k}, \omega)$ agree only when $\omega = 0$ and $\omega = O(\omega_A)$. As we shall see, this is not a severe limitation on the fluid expression, since it is only in these two regimes that interesting solutions exist for our dispersion relation, (6), and quantitatively satisfactory results can be obtained with a suitable choice of ω_A and v_A.

In the calculations presented here, we have made a resonance approximation for the high-frequency dielectric function:

$$\epsilon(\underline{k} \pm \underline{k}_0, \omega \pm \omega_0) = \pm 2 \left[\omega \pm \omega_0 \mp \omega_L (\underline{k} \pm \underline{k}_0) + i\gamma_L \right], \tag{12}$$

γ_L being phenomenological damping (either collisional or Landau) and an exact expression for the low frequency $\epsilon(\underline{k}, \omega)$ in terms of the Fried-Conti Z-function given in equation (9). Finally, in the frequently valid approximation that:

$$|\omega| \ll \left| \chi_0 + \delta \, \frac{\mu_+^2 + \mu_-^2}{\mu_+^2 - \mu_-^2} \right|,$$

(which is usually guaranteed because $\mu_+ \approx \mu_-$), (6) becomes:

$$D(\underline{k}, \omega) \left[(\omega - \chi_0 + i\gamma_L)^2 - \delta^2 \right] + \frac{W_0}{8} \left(\mu_+^2 \delta_- + \mu_-^2 \delta_+ \right) = 0, \tag{13}$$

where:

$$\delta_{\pm} = \omega_0 - \omega_L(\underline{k} \pm \underline{k}_0) = \mp\chi_0 - \delta,$$

$$2\delta = 2\omega_0 - \omega_L(\underline{k}+\underline{k}_0) - \omega_L(\underline{k}-\underline{k}_0) = -3k^2,$$

$$2\chi_0 = \delta_- - \delta_+ = 6\underline{k}\cdot\underline{k}_0 ,$$

in dimensionless units of wavelength in units of k_{De}^{-1} and frequency in units of the plasma frequency. $\mu_{\pm}$ is the cosine of the angle between the pump wavevector, $\underline{k}_0$, and the wavevector of the duaghter waves, $\underline{k}\pm\underline{k}_0$. The three deltas are different frequency mismatches: $\delta_{\pm}$ being the mismatch between the up- (or down-) shifted wave and the pump; and δ being the average of these mismatches.

Before proceeding to applications of equation (6), we need some way of systematizing the large number of regimes in k_0, W_0, ν_A, and γ_L in which qualitatively different solutions to (6) exist. We will restrict our results in this section on analytic results to the case that $\omega \ll k\mu$. This is almost always satisfied. We have organized our study of the analytic solutions to (6) as follows: we first divide the solutions with positive imaginary parts into three groups on the basis of the physical processes which account for the unstable solutions. Each of these physical processes has a group of parameters which determine its qualitative features.

1). Oscillating two-stream instabilities (OTS). There are a class of growing solutions to (6) characterized by their non-oscillatory nature, Re $\omega <$ Im ω. By

analogy with the well-known OTS instability,[4,10] we call these OTS-like instabilities, even though we will include a much larger class of behavior under this name, This is a four-wave interaction, schematically shown in Figure one.

2). Electron-ion decay instabilities (EID). These solutions occur when $\omega \approx \omega_A$, and only one of the high frequency dielectric functions is near resonance. This is a three-wave coupling, and is shown in Figure one.[11,12]

3). Stimulated modulational instabilities (SM). Also known as a "modified electron-ion decay instability," this is a four-wave interaction, in which both high frequency waves participate. Several special cases of the SM instability have been studied for an electromagnetic pump.[6,13]

OSCILLATING TWO STREAM INSTABILITIES

The character of this class of instabilities is sufficiently determined by W_o and k_o. For the OTS instability, both k and Im ω depend on W_o, and we have been able to solve (6) analytically in the following regimes:

A. $|\omega| \ll \omega_i$, $k \ll k_o$, or $W_o \ll 64\alpha/T$, $W_o \ll 10k_o^2$;

B. $|\omega| \ll \omega_i$, $k \gg k_o$, or $W_o \ll 64\alpha/T$, $W_o \gg 10k_o^2$;

C. $|\omega| \gg \omega_i$, $k \ll k_o$, or $W_o \gg 64\alpha/T$, $W_o \ll 10k^2$;

D. $|\omega| \gg \omega_i$, $k \gg k_o$, or $W_o \gg 64\alpha/T$, $W_o \gg 10k^2$;

where:

$$\alpha \equiv \frac{2}{3}(m_e/m_i)(T+1)/T$$

$$\omega_i = (m_e/m_i)^{1/2}\omega_p$$

In the intermediate regions, where k is on the order of k_o and $|\omega|$ on the order of ω_i, numerical solutions are found which connect the analytic solutions.

A). $|\omega| \ll \omega_i$, $k \ll k_o$. Under these conditions:

$$\epsilon(\underline{k},\omega) \approx \epsilon(\underline{k},0) = 1 + \frac{k_{De}^2}{k_{Di}^2 + k_{De}^2},$$

$$D(\underline{k},0) = -1,$$

so that (6) becomes:

$$(\omega + i\gamma_L - \chi_o)^2 - \delta^2 - \frac{W_o}{8}(\mu_+^2\delta_- + \mu_-^2\delta_+) = 0. \tag{14}$$

If we call $\omega = x + iy$, then an OTS solution exists when $\hat{k}\cdot\hat{k}_o \ll k/k_o$, and

$$\chi = \chi_o,$$

$$y = -\gamma_L + \sqrt{-\delta^2 - W_o(\delta_-\mu_+^2 + \delta_+\mu_-^2)/8}. \tag{15}$$

The threshold, maximum growth rate and wavenumber for maximum growth are easily gotten; solving for y = 0 in equation (15) gives the threshold value for W_o

$$W_o^c = 16\gamma_L\delta / (\mu_+^2\delta_- + \mu_-^2\delta_+).$$

To get the maximum growth rate by differentiation of (15), we need to deal with the angular dependence in $\mu_\pm$. We can write the angular factor in (15) as:

$$\mu^2 \equiv \frac{\mu_+^2\delta_- + \mu_-^2\delta_+}{2\delta} = 1 - \sin^2\psi\left\{\frac{k^2}{k_o^2}\left(\frac{1 + k^2/k_o^2 + 4\cos^2\psi}{1 + 2k^2/k_o^2 + k^4/k_o^4 - 4k^2\cos^2\psi/k_o^2}\right)\right\},$$

where:

$$\psi = \cos^{-1}(\hat{k}\cdot\hat{k}_o).$$

In the limit that $k^2 << k_o^2$:

$$\mu^2 = 1 - k^2 \sin^2\psi / k_o^2$$

and differentiation of (15) with respect to ψ gives a condition for maximum growth independent of k: $\psi = 90°$. Now, differentiating (15) with respect to k gives the k for which maximum growth occurs:

(16a) $$\delta \equiv -\frac{3}{2} k^2 = Im\,\omega|_{max} + \gamma_L = -\frac{W_o}{8}\left(1 + \frac{\sin^2\psi}{6k_o^2} W_o\right)^{-1},$$

and

(16b) $$Im\,\omega|_{max} = -\gamma_L + \frac{W_o}{8}\left(1 + \frac{\sin^2\psi}{6k_o^2} W_o\right)^{-1}.$$

In fact, differentiation of the general angular dependence of μ shows that the growth rate, in all regimes, has extrema at $\psi = 0°$ and $90°$. This is a general result as long as the growth rate has its only explicit angular dependence through μ. Our approximation requiring that:

$$Im\,\omega > Re\,\omega << \omega_i$$

demands that we choose the maximam at $90°$. The original assumption that:

$$|\omega| << \omega_i$$

gives the strictest upper bound on W_o and the lowest bound on k_o; for this case:

$$|\delta|^{1/2} << \alpha^{1/2},$$

or:

$$W_o \mu^2 << 64\alpha/T,$$

so that:

$$10 k_c^2 << W_o \mu^2 .$$

Figure two a shows numerical solutions of (6) in this regime. The OTS instability is the small, roughly circular feature perpendicular to the axis at the point $\underline{k}_o - \underline{k} = \underline{k}_o$.

B). $|\omega| << \omega_i$, $k >> k_o$. In this case, equation (14) also describes our results; however, when $k >> k_o$, then we must have $\hat{k}\cdot\hat{k}_o \approx 1$ (this is the other maximum of μ noted above). Thus, while x and y are again given by (15), the maximum growth occurs on axis. For this regime to be applicable:

$$y \gtrsim x$$

for the OTS generally. This, combined with the other conditions gives:

$$W_o << 64\alpha/T \quad , \quad 10 k_o^2 << W_o .$$

Figure three shows a case not strictly in this parameter regime, but which has the same qualitative features. The k for maximum growth is given by (16a), and we have the figure eight structure of the previous regime now on axis rather than perpendicular to the axis. More interesting is the transition from the $k >> k_o$ case, where growth occurs for $\hat{k}\cdot\hat{k}_o = 1$, to the $k << k_o$ case, where it occurs for $\hat{k}\cdot\hat{k}_o = 0$.

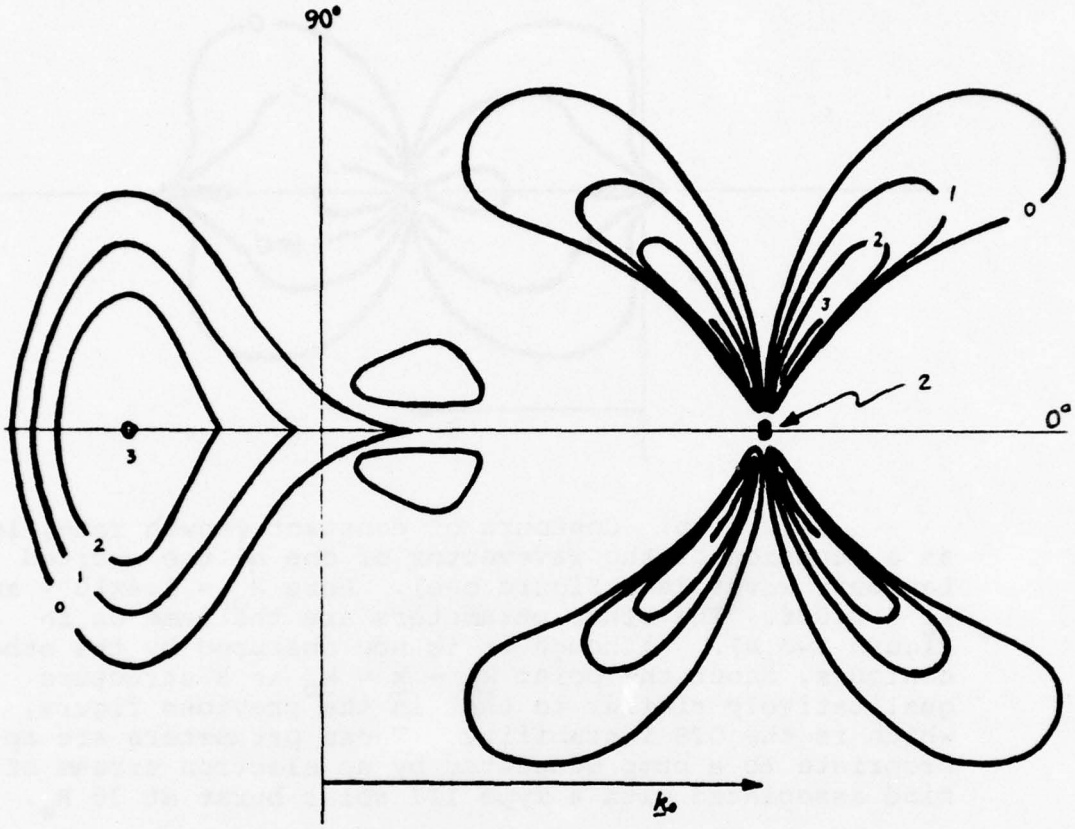

Figure two a). Solutions to the dispersion relation, equation (6), showing contours of constant growth rate, Im ω, as a function of the wavevector, $\underline{k}_o$-$\underline{k}$, of one of the excited daughter Langmuir waves. Here, $W_o = 4\times10^{-6}$. The pump wavevector is shown with an arrow, with magnitude, $k_o = 0.05$. Other parameters are: $\alpha = 7.3\times10^{-4}$, $\theta_e/\theta_i = 1$, and $\gamma_L = 10^{-9}$. The numbers on the contours give the growth rate in units of $2\times10^{-7}\,\omega_{pe}$. The feature on the left is the EID instability (here in the resonant backscattering regime). The butterfly-like pattern centered about the point $\underline{k}_o$-$\underline{k} = \underline{k}_0$, is the SM instability, and the small structure perpendicular to this same point is the OTS instability (here in the regime described under case A in the text). These parameters are appropriate to a pump generated by an electron stream associated with a Type III solar radio burst at 1 $R_\odot$ (about 7×10^5 km from the sun).

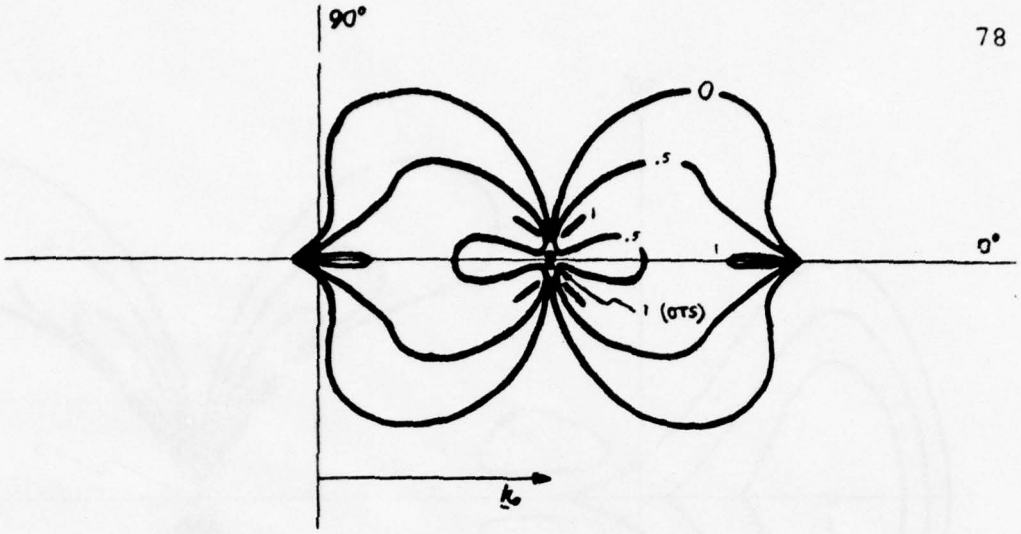

Figure 2b. Contours of constant growth rate, Im ω, as a function of the wavevector of one of the excited Langmuir waves (see Figure one). Here $W_o = 1.4 \times 10^{-6}$ and $k_o = 0.026$. The other parameters are the same as in Figure two a). Although it is now obscured by the other contours, about the point $\underline{k}_o - \underline{k} = \underline{k}_o$ is a structure qualitatively similar to that in the previous figure, which is the OTS instability. These parameters are appropriate to a pump generated by an electron stream of the kind associated with a Type III solar burst at 30 $R_\odot$.

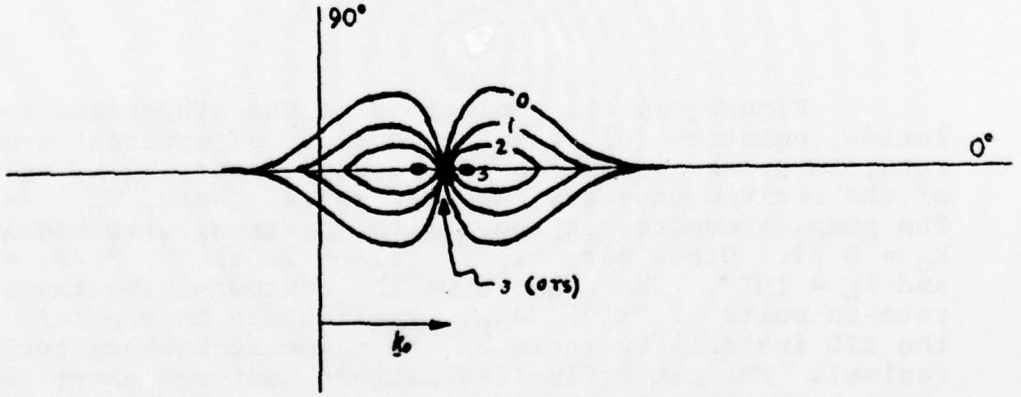

Figure 2c. Contours of constant growth rate, Im ω, as a function of the wavevector of one of the excited Langmuir waves (see Figure one). Here $W_o = 5 \times 10^{-6}$, and $k_o = 0.013$. The other parameters are the same as in Figure two a). The EID instability is here a resonant, forward scattering instability, marked by contour "3" on axis. These parameters are appropriate to a pump generated by an electron stream of the kind associated with a Type III solar radio burst at 215 $R_\odot$.

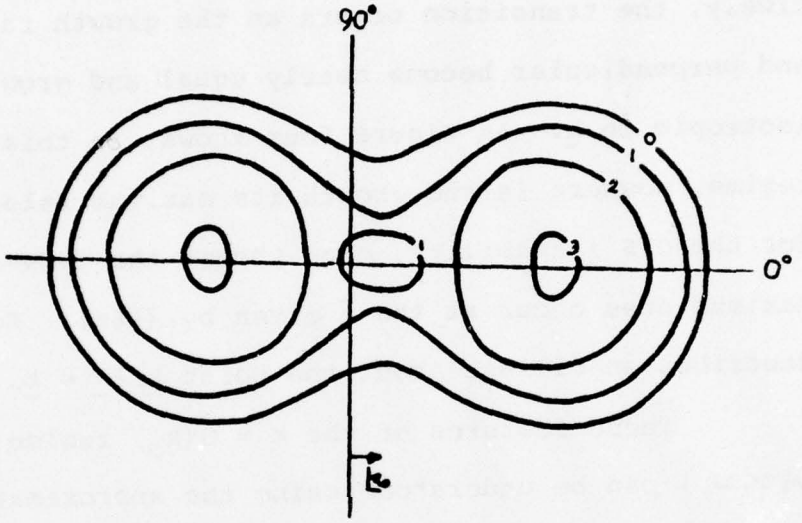

Figure three. Solutions to the dispersion relation, equation (6), showing contours of constant growth rate, Im ω, as a function of the wavevector of one of the daughter Langmuir waves, $\underline{k}_o - \underline{k}$. These solutions all occur in a regime intermediate between cases B and D for the OTS instability, where $10k_o^2 \ll W_o$ and $W_o = O(640\chi)$. Here $W_o = 0.04$ and $k_o = 0.0067$. The other parameters are given in Table V. These parameters are those of a pump generated by an auroral streamer. In this regime, the EID has disappeared and the the OTS instability is on axis. The numbers on the contours give the growth rate in units of $2.5 \times 10^{-4}\ \omega_{pe}$.

This occurs when $10k_o^2$ is on the order of W_o. A set of parameters in this transitional regime generated the solutions shown in Figure four. In this regime, the condition that $y > x$ is only marginally satisfied on axis. Qualitatively, the transition occurs as the growth rates on axis and perpendicular become nearly equal and growth is almost isotropic in $\underline{k}$. As Figure four shows, in this transitional regime, nowhere is the growth its maximum value of $W_o/8$ for the OTS instability, even though the (now-decreased) maximum does occur at the δ given by (16a). Equation (16a) describes an ellipse about the point $\underline{k}_o - \underline{k} = \underline{k}_o$.

These features of the $k = O(k_o)$ regime (with $|\omega| << \omega_i$) can be understood using the approximate expression for δ at maximum growth rate (from (16a) to first order in W_o):

$$\delta = -\frac{W_o}{8}\left(1 + \frac{2k^2\sin^2\psi}{k_o^2}\right)^{-1}.$$

As soon as $k_o = O(4k)$, the $\sin^2\psi$ term degrades the growth rate at $\psi = 90^o$. The increase in the growth rate for small $\sin^2\psi$, shown in (16), then competes with the decrease in growth rate that comes from the violation of the condition $y > x = 3kk_o(1-\sin^2\psi)^{\frac{1}{2}}$, that occurs when $\sin^2\psi$ is small. This regime is the transition among all four regimes considered here.

C). $|\omega| >> \omega_i$, $k_o >> k$. This limit occurs when $64\nu/\tau \ll W_o$ and $W_o << 10k_o^2$. In this case, we have:

AD-A031 292 COLORADO UNIV BOULDER DEPT OF ASTRO-GEOPHYSICS F/G 20/9
PUMP WAVENUMBER DEPENDENT EFFECTS IN THE PARAMETRIC INSTABILITI--ETC(U)
JUL 76 S J BARDWELL F44620-73-C-0003
UNCLASSIFIED CU-1019-A5 AFOSR-TR-76-1116-ATTACH-5 NL

2 OF 2
ADA031292

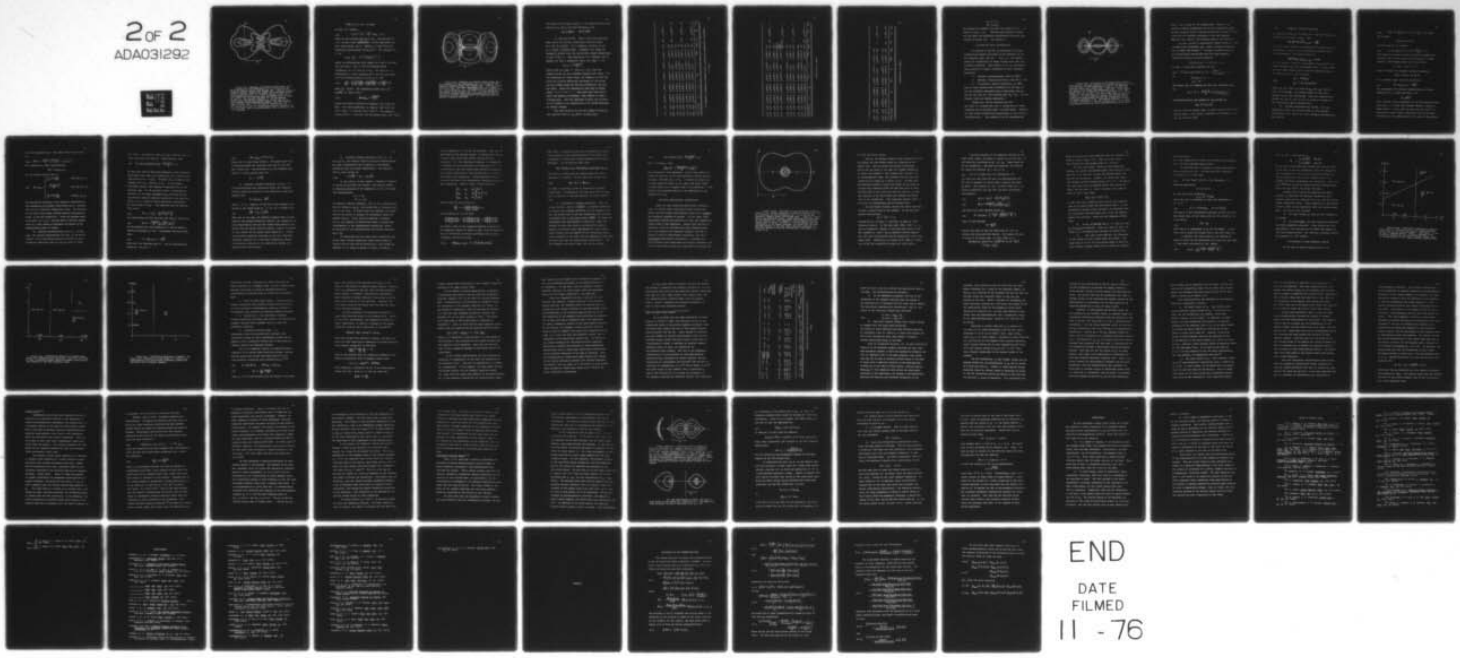

END

DATE
FILMED
11 - 76

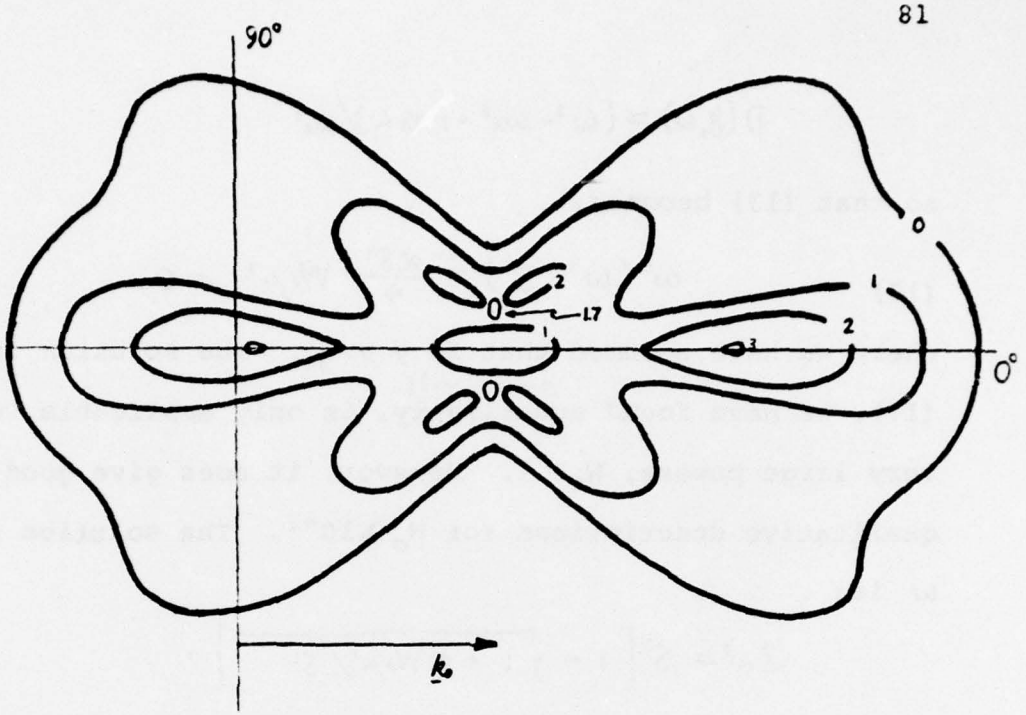

Figure four. Contours of constant growth rate, Im ω, as a function of the wavevector, $\underline{k}_o - \underline{k}$, of one of the daughter Langmuir waves (see Figure one). Here $W_o = 6.5 \times 10^{-4}$. 6.5×10^{-4} and k_o, shown by an arrow, has magnitude, 0.028. Other parameters are: $\alpha = 7.3 \times 10^{-4}$, $\theta_e/\theta_i = 1, \gamma_i = 10^{-9}$. The numbers on the contours give the growth rate in units of 3×10^{-5}. The contour labelled "3" is the maximum growth rate for the EID instability, which here is in the resonant forwardscattering regime. The four smaller lobes at acos $(\mu_s) = 15^o$ are the SM instability. The OTS instability here is intermediate between regimes A and C of the text, and its maximum growth rate is shown by the "1.7" contour.

$$D(\underline{k},\omega) \approx (\omega^2 - \omega_A^2 + i\nu_A\omega)/\omega_A^2$$

so that (13) becomes:

$$\omega^2(\omega^2 - \delta^2) - \frac{\alpha\delta^2}{4} W_o\mu^2 = 0, \tag{17}$$

where we have assumed that Im y >> γ_L. The solution to (17), we have found analytically, is only applicable for very large powers, $W_o > 1$. However, it does give good qualitative descriptions for $W_o \gtrsim 10^{-2}$. The solution for ω is:

$$2\omega^2 \simeq \delta^2\left[1 - \sqrt{1 + \alpha W_o\mu^2/\delta^2}\right].$$

Again, we differentiate with respect to μ and k, and get, for this limit, that $\mu = 90^o$ for maximum growth independent of k as long as $k \ll k_o$. The value of k is determined by a cubic equation for δ (or k^2) which comes from the differentiation of (17a) at $\mu = 90^o$:

$$\left(\frac{\delta}{\delta_o}\right)^3 - \frac{9}{8}\left(\frac{\delta}{\delta_o}\right)^2\left(\frac{\alpha W_o}{\delta_o^2}\right) + \frac{3}{2}\left(\frac{\delta}{\delta_o}\right)\left(\frac{\alpha W_o}{\delta_o^2}\right) - \frac{1}{2}\left(\frac{\alpha W_o}{\delta_o^2}\right) = 0, \tag{17b}$$

where $\delta_o = -3k_o^2/2$. The asymptotic growth rate, for $\delta \gg \sqrt{\alpha W_o}$ is (from (17a)):

$$\mathrm{Im}\,\omega|_{max} = \left(\frac{\alpha W_o}{4}\right)^{1/2} \tag{17c}$$

Figure five gives a solution to equation (6) in this regime. For these parameters, we predict, from (17b) and (17c), that k = 0.044 and Im $\omega = 6\times10^{-3}$. The numerical results give k = 0.038 and, for the growth rate, Im $\omega = 2\times10^{-3}$.

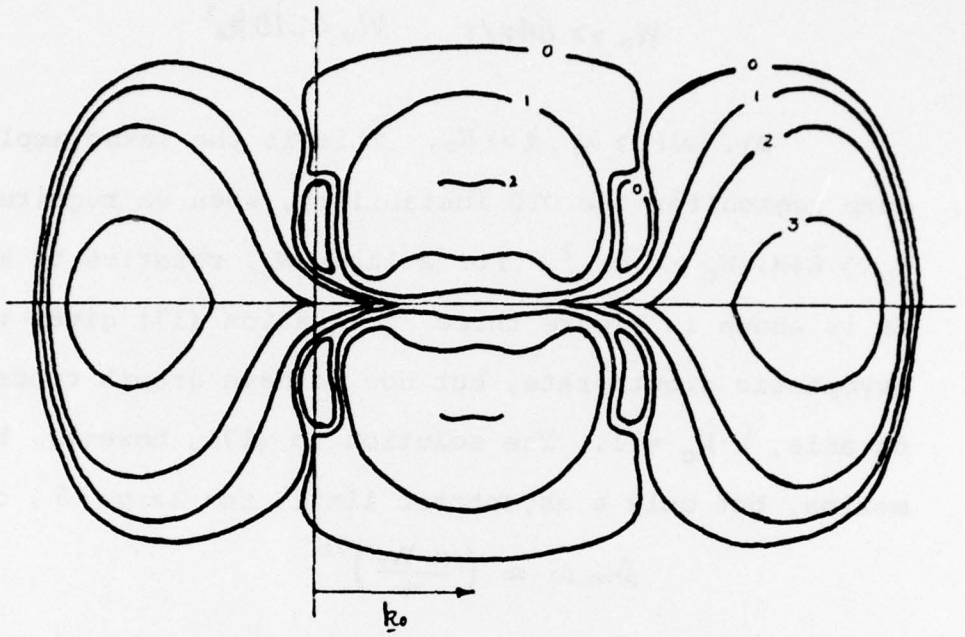

Figure five. Contours of constant growth rate, Im ω, as a function of the wavevector, $\underline{k}_o - \underline{k}$, of one of the daughter Langmuir waves (see Figure one). Here $W_o = 0.15$ and $k_o = 0.05$. The other parameters are; $\alpha = 7.3 \times 10^{-4}$, $\gamma_L = 10^{-9}$ and $\theta_e/\theta_i = 1$. The numbers on the contours give the growth rates in units of 10^{-3}. In this regime the OTS and SM instabilities have coalesced and the EID instability is still centered near the condition given by perfect frequency matching.

(See Table IV for these results.) The conditions that must obtain on k_o and W_o for self-consistency are:

$$W_o >> 64\alpha/T \ , \quad W_o << 10k_o^2 \ .$$

D). $|\omega| >> \omega_i$, $k >> k_o$. This is the large amplitude pump region for the OTS instability, when we require $W_o >> 64\alpha$, $W_o >> 10k_o^2$. For a large W_o, relative to k_o^2, as is shown in Figure three , equation (17) gives the asymptotic growth rate, but now we have growth concentrated on axis, $\hat{k}\cdot\hat{k}_o = 1$. The solution to (17), however, has no maxima, but only a asymptotic limit, for large δ, of:

$$\mathrm{Im}\,\omega \approx \left(\frac{\alpha W_o}{4}\right)^{1/2}$$

Notice that for large δ, that is $k >> k_o$, that the daughter waves set up a standing Langmuir wave field. For the parameters of Figure three, for example, we have computed the relative amplitudes and phases of the Stokes and anti-Stokes waves for the OTS instability, and they are equal. Since the frequency of each wave is almost equal: $\omega_o + \omega \approx \omega_o - \omega$, and since they have nearly equal and opposite wavenumbers, they combine to form a standing-wave. This has important effects, one of which we will examine in an application of the fields generated by auroral streams.

The lower bound on W_o for this regime is given by the condition that $k >> k_o$ and $|\omega| >> \omega_A$ which give:

TABLE IV

NUMERICALLY DETERMINED SOLUTIONS TO THE DISPERSION RELATION, EQUATION (6)

Fig.	W_o	k_o	Name	γ_{max}	x	ω_A	δ	k	$\lvert\omega-\delta_-\rvert$	$\lvert\omega+\delta_+\rvert$
2a	4.0×10^{-6}	.05	OTS	4.9×10^{-7}	$<10^{-8}$	1.8×10^{-5}	4.7×10^{-7}	5.6×10^{-4}	$=\sqrt{2}\delta$	$=\sqrt{2}\delta$
			SM	6.0×10^{-7}	2.4×10^{-4}	1.9×10^{-4}	5.4×10^{-5}	6.0×10^{-3}	10^{-5}	10^{-4}
			EID	6.1×10^{-7}	2.9×10^{-3}	2.3×10^{-3}	8.2×10^{-3}	7.4×10^{-2}	10^{-5}	10^{-2}
2b	1.4×10^{-6}	.026	OTS	1.7×10^{-7}	$<10^{-8}$	1.1×10^{-5}	1.7×10^{-7}	3.4×10^{-4}	$=\sqrt{2}\delta$	$=\sqrt{2}\delta$
			SM	2.0×10^{-7}	2.0×10^{-4}	2.0×10^{-4}	5.4×10^{-5}	6.0×10^{-3}	10^{-5}	10^{-4}
			EID	2.2×10^{-7}	1.0×10^{-3}	8.2×10^{-4}	9.4×10^{-4}	2.5×10^{-2}	10^{-5}	10^{-3}
2c	5.0×10^{-6}	.014	OTS	6.0×10^{-7}	$<10^{-8}$	2.0×10^{-5}	5.9×10^{-7}	6.3×10^{-4}	$=\sqrt{2}\delta$	$=\sqrt{2}\delta$
			EID	7.5×10^{-7}	7.6×10^{-5}	5.4×10^{-5}	4.0×10^{-6}	2.0×10^{-3}	10^{-6}	10^{-5}
3	4.0×10^{-2}	.007	OTS	7.7×10^{-4}	8.6×10^{-5}	5.9×10^{-4}	2.6×10^{-3}	4.2×10^{-2}	10^{-3}	10^{-3}

TABLE IV (continued)

Fig.	W_o	k_o	Name	y_{max}	x	ω_A	δ	k	$\lvert\omega-\delta_-\rvert$	$\lvert\omega+\delta_+\rvert$
4	6.5×10^{-4}	.028	OTS	5.6×10^{-5}	$<10^{-8}$	2.6×10^{-4}	9.6×10^{-5}	8.0×10^{-3}	10^{-4}	10^{-4}
			SM	6.6×10^{-5}	2.9×10^{-4}	3.3×10^{-4}	1.5×10^{-4}	1.0×10^{-2}	10^{-5}	10^{-4}
			EID	8.6×10^{-5}	1.1×10^{-3}	1.3×10^{-3}	2.3×10^{-3}	3.9×10^{-2}	10^{-4}	10^{-3}
5	1.5×10^{-1}	.05	OTS	1.9×10^{-3}	$<10^{-6}$	1.3×10^{-3}	2.5×10^{-3}	4.1×10^{-2}	10^{-3}	10^{-3}
			SM	1.9×10^{-3}	$<10^{-6}$	1.3×10^{-3}	2.5×10^{-3}	4.1×10^{-2}	10^{-3}	10^{-3}
			EID	3.4×10^{-3}	2.5×10^{-3}	3.4×10^{-4}	1.5×10^{-2}	1.0×10^{-1}	10^{-3}	10^{-4}
6	1.0×10^{-2}	.032	OTS $\hat{k}\cdot\hat{k}_o=0$	4.3×10^{-4}	$<10^{-7}$	6.0×10^{-4}	4.9×10^{-4}	1.8×10^{-2}	10^{-3}	10^{-3}
			OTS $\hat{k}\cdot\hat{k}_o=1$	5.6×10^{-4}	1.3×10^{-3}	8.3×10^{-4}	9.4×10^{-4}	2.5×10^{-2}	10^{-3}	10^{-3}
			EID	7.9×10^{-4}	1.5×10^{-3}	1.5×10^{-3}	3.3×10^{-3}	4.7×10^{-2}	10^{-4}	10^{-2}
7	4.0×10^{-6}	.005	OTS	6.0×10^{-7}	$<10^{-7}$	1.9×10^{-5}	5.0×10^{-7}	5.7×10^{-4}	10^{-5}	10^{-5}
			EID	1.6×10^{-7}	2.6×10^{-5}	7.3×10^{-5}	7.3×10^{-6}	2.2×10^{-3}	10^{-6}	10^{-4}

TABLE IV (continued)

Fig.	W_o	k_o	Name	y_{max}	x	ω_A	δ	k	$\lvert\omega-\delta_-\rvert$	$\lvert\omega+\delta_+\rvert$
11a	6×10^{-2}	.25	OTS	5.6×10^{-3}	4.5×10^{-2}	3.0×10^{-4}	9.6×10^{-5}	8.0×10^{-3}	10^{-2}	10^{-2}
			EID	1.4×10^{-3}	1.4×10^{-3}	1.9×10^{-3}	3.7×10^{-3}	5.0×10^{-2}	10^{-2}	10^{-2}
11b	6×10^{-2}	.1	OTS	2.6×10^{-2}	$< 10^{-6}$	6.8×10^{-5}	4.9×10^{-4}	1.8×10^{-2}	10^{-2}	10^{-2}
			EID	2.1×10^{-3}	3.4×10^{-2}	5.3×10^{-4}	2.9×10^{-2}	1.4×10^{-1}	10^{-2}	10^{-2}

$$W_o >> 10\, k_o^2,$$
$$W_o >> 64\alpha/\tau.$$

The transition between $k >> k_o$ and $k << k_o$ when $|\omega| >> \omega_A$, is shown in Figure six. The features evident in Figure two are again the qualitative determinants for this case, similar to Figure four for smaller ω.

ELECTRON-ION DECAY INSTABILITIES

In contrast to the OTS instabilities, the decay instabilities depend critically on the resonance of the low frequency mode, that is: Re $\omega \approx \omega_A$. Our general schema for classifying the decay instabilities uses this resonance condition; after Fried, et al. we distinguish three regions of k-space, depending on their resonance properties:

1). resonant, backscattering, when $k_o > \sqrt{2\alpha/3}$;

2). resonant, forward scattering, when $\sqrt{2\alpha/3} > k_o > \sqrt{\alpha/6}$,

3). nonresonant, forward scattering, $k_o < \sqrt{\alpha/6}$.

Each of these regions must be examined for the case of the low frequency resonance being a quasi-mode ($\theta_e \approx \theta_i$) and for the case of a well-defined mode ($\theta_e >> \theta_i$). We will examine these six regimes separately.

Physically, the EID instabilities are the decay of a plasma wave into a plasma wave at lower frequency and an acoustic mode (or quasi-mode). However, to treat these instabilities analytically is not entirely straightforward. The problem is one of approximating

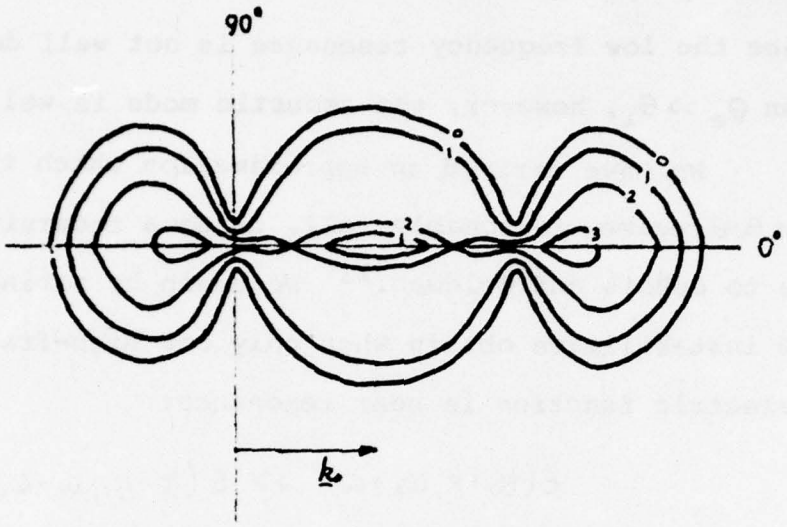

Figure six. Solutions to the dispersion relation, equation (6), showing contours of constant growth rate, Im ω, as a function of the wavevector of one of the daughter Langmuir waves (see Figure one). Here $W_o = 1 \times 10^{-2}$ and k_o, shown as an arrow, has magnitude 0.032. Other parameters are: $\alpha = 7.3 \times 10^{-4}$, $\gamma_i = 10^{-9}$, and $\theta_e/\theta_i = 1$. The numbers on the contours give the growth rate in units of 2.5×10^{-4}. In this large W_o regime, the OTS and SM instabilities have merged and the OTS instability itself is almost isotropic in $\underline{k}$. The maxima labelled "3" are the EID instability. The OTS instability is in a regime intermediate among the four cases described in the text.

$D(\underline{k}, \omega)$ for a range of ion temperatures. When $\theta_i \approx \theta_e$, particle effects predominate and the EID instability would be more properly called "induced scattering off ions,"[2,11,15] since the low frequency resonance is not well defined. When $\theta_e \gg \theta_i$, however, the acoustic mode is well-defined.

We have derived an approximation which treats the $\theta_e \approx \theta_i$ and $\theta_e \gg \theta_i$ regimes reasonably well, using a recursive approach due to DuBois and Goldman.[11] We begin by noting that the EID instabilities obtain when only one high-frequency dielectric function is near resonance:

$$\epsilon(\underline{k}_0+\underline{k}, \omega_0+\omega) \gg \epsilon(\underline{k}-\underline{k}_0, \omega-\omega_0)$$

so that we could write equation (6) as:

$$\epsilon^{NL}(\underline{k}-\underline{k}_0, \omega-\omega_0) \equiv \epsilon(\underline{k}-\underline{k}_0, \omega-\omega_0) - \frac{W_0 \mu_-^2 \delta}{\delta k^2 \epsilon(k,\omega)} = 0, \tag{18}$$

if:

$$k^2 \epsilon(k,\omega) \ll 1 ;$$
$$\mu_+^2 \approx \mu_-^2 .$$

The growth rate (or damping) of this new, non-linear mode is:

$$\gamma_{NL} = \gamma_L - \frac{W_0 \mu_-^2 \delta_+}{4} \operatorname{Im}\left[\frac{1}{k^2 \epsilon(\underline{k},\omega)}\right] .$$

The maximum growth rate depends on the maximum of:

$$\operatorname{Im}\left[k^2 \epsilon(k,\omega)\right]^{-1} .$$

We will treat the $\theta_e \approx \theta_i$ case, in which there is not a well-defined mode at the acoustic frequency by choosing ω_A' and ν_A' in the fluid form:

(18a) $$k^2\epsilon(\underline{k},\omega) = (\omega^2 - \omega_A'^2 + i\omega\nu_A')/\omega_A'^2$$

in such a way that the Im $k^2\epsilon(\underline{k}, \omega)^{-1}$ for the fluid case agrees with the exact result. Now:

$$\mathrm{Im}\left[k^2\epsilon(\underline{k},\omega)\right]^{-1}_{\text{fluid-max}} = \frac{\omega_A'}{2\nu_A'}$$

The fluid model attempts to approximate the bell-shaped k-dependence of $D(\underline{k}, \omega)$ near the acoustic frequency with a broad Lorentzian. The exact result is:

$$\mathrm{Im}\left[k^2\epsilon(\underline{k},\omega)\right]^{-1}_{\text{exact-max}} = 0.58.$$

We will attempt to use the fluid model by normalizing the fluid Lorentzian so that the maximum value of (18a) agrees with the exact result, and so that this maximum occurs at the same value of k; this requires:

(18b)
$$\nu_A' = 0.90\,\omega_A'$$
$$\omega_A' = 1.70\,(m_e/m_i)^{1/2}k.$$

These are the values (in units of ω_{pe} and k_{De}) which we will use if $\theta_e \approx \theta_i$. The results quoted in the first chapter can be used when $\theta_e \gg \theta_i$. With this approximation scheme for $D(\underline{k}, \omega)$, let us look at these six regimes for the electron-ion decay instabilities.

A). Resonant backscattering, $\theta_e \gg \theta_i$. For this temperature range, the acoustic mode is well-defined, Re $\omega_A \gg \gamma_A \equiv \nu_A/2$, and we can use a resonance approximation for $D(\underline{k}, \omega)$:

(20) $$D(k,\omega) \approx \frac{2}{\omega_A^2}(\omega^2 - \omega_A^2 + 2i\gamma_A\omega) \approx \frac{4}{\omega_A}(\omega - \omega_A + i\gamma_A),$$

and we have:

$$\epsilon(\underline{k}_o + \underline{k}, \omega_o + \omega) \approx 4\delta,$$

so that equation (6) becomes:

(21) $$(\omega - \omega_A + i\gamma_A)(\omega - \chi_o - \delta + i\gamma_L) + \frac{W_o \mu^2 \omega_A}{16} = 0.$$

This equation has been studied in detail by DuBois and Goldman,[5] and we note here only the simplest of their results. The maximum growth rate occurs when:

$$\omega = \omega_A = \chi_o + \delta = \delta_-.$$

which is merely the frequency matching condition:

$$\omega_o(\underline{k}_o) = \omega_A(k) + \omega_L(\underline{k}_o - \underline{k}).$$

For a Langmuir pump, this can be written:

(22) $$k = 2k_o \cos\psi - \sqrt{2\alpha/3}.$$

The requirement for resonant backscattering is then a condition on k_o, since here $\hat{k}\cdot\hat{k}_o = +1$:

$$k_o > \sqrt{2\alpha/3}.$$

Note, however, that in addition to the well-known solution with $\cos\psi = 1$, that (22) actually defines a locus in phase space; it will turn out that only the $\cos\psi = 1$ solution is truly a decay instability, and so we defer discussion of the other parts of the locus to the section

on the SM instabilities. The growth rate on this locus is:

$$(22a)\quad \mathrm{Im}\,\omega = -\frac{(\gamma_A+\gamma_L)}{2} + \sqrt{\frac{W_0\mu^2\omega_A}{16} - \frac{1}{4}(\gamma_A-\gamma_L)^2}\quad .$$

The threshold is, then, approximately:

$$W_0^c = 16\,\gamma_L\gamma_A/\omega_A\ ,$$

and the maximum growth rate is:

$$(23)\quad \mathrm{Im}\,\omega_{max} = \begin{cases} \frac{1}{32}\mu_-^2 W_0\left(\frac{\omega_A}{\gamma_A}\right) & , W_0 \ll \gamma_A,\ \gamma_L \ll \gamma_A\ ; \\ \left(\frac{\omega_A W_0 \mu_-^2}{16}\right)^{1/2} & , W_0 \gg \gamma_A,\ W_0\omega_A \gg \gamma_L\ ; \\ \frac{1}{32}\mu_-^2 W_0\left(\frac{\omega_A}{\gamma_L}\right) & , W_0 \ll \gamma_L,\ \gamma_A \ll \gamma_L\ . \end{cases}$$

The qualititive features of the resonant, backscattering EID instabiltty are evident from Figure two a), althouqh this is for a different temperature ratio. The structure on the left of the graph, showing growing backscattered waves, is the EID instability. Since the maximum growth is on axis, $\mu_-^2 = \mu_+^2$, and the detailed angular dependence of μ only serves to determine the spread of the backscattered region of growth.

B). Resonant backscattering, $T_e \approx T_i$. In this case, the resonant approximation for $D(\underline{k}, \omega)$ is not accurate; to get approximate analytic results, we use a normalized Lorentzian form for $D(\underline{k}, \omega)$ given by (18a)

and (18b). Our numerical work was done, however, with the exact expression for $D(\underline{k}, \omega)$. Approximately, then:

$$(24) \quad (\omega^2 - \omega_A'^2 + i\omega\nu_A')(\omega - \delta + i\gamma_L) - \frac{W_0 \omega_A'^2 \mu^2}{8} = 0.$$

We have been able to solve this equation in the frequently applicable limit that γ_L is negligible (i.e., much smaller than either Im ω or γ_A). To treat (24), we look at two regimes, Im $\omega \ll \gamma_A$, and Im $\omega \gg \gamma_A$. In the latter, high power regime, (24) reduces to equation (21) of the previous case. In the low power limit, a perturbation analysis, in the small parameter y/γ_A gives the following results (again we restrict ourselves to the case that $\hat{k} \cdot \hat{k}_0 = 1$, $\mu_+ = \mu_-$, which is easily satisfied a posteriori). To first order in y/γ_A, the imaginary part of equation (24) gives:

$$(25) \quad \text{Re } \omega = \delta_- \left[1 - \frac{y}{\nu_A'} \left(\frac{\delta_-^2 - \omega_A'^2}{\delta_-^2} \right) \right],$$

ans substitution of this into the real part of (24) gives:

$$(26) \quad \text{Im } \omega = \frac{\mu^2 W_0 \omega_A'^2}{8} \left[\frac{\delta_- \nu_A'}{(\delta_-^2 - \omega_A'^2)^2 + \nu_A'^2 \delta_-^2} \right].$$

We can maximize Im ω with respect to k, and we derive a condition analogous to (22), a wavenumber matching condition:

$$(27) \quad k = 2k_0 \cos\psi - .9\sqrt{\frac{2\kappa}{3}}.$$

From this, the imaginary part of can be calculated and maximized, when $\mu_-^2 = 1$:

(28) $$\mathrm{Im}\,\omega\big|_{max} = \mu^2 W_o / 7.51 \cdot$$

Figure two a) shows these results. The growth rate and k for maximum growth are predicted very well by (27) and (28) (within 5%). The condition on k_o for resonant backscatter is easily gotten from (27):

$$k_o > .9\sqrt{2\alpha/3}$$

C). Resonant, forward scattering, $\theta_e \gg \theta_i$. In the backscattering case considered above, the frequency matching condition resulted in the condition on the wavenumbers that:

$$k = 2k_c \cos\psi - \sqrt{2\alpha/3} \quad ,$$

and $k_o - k < 0$. However, we can still have resonant scattering in the regime where $k_o - k > 0$, or, in terms of k_o:

(29 $$\sqrt{2\alpha/3} > k_o > \tfrac{1}{2}\sqrt{2\alpha/3} \cdot$$

When this is the case, the daughter Langmuir wave is scattered in the forward direction; however, the instability is still described by (21) and the growth rates given by (23). Notice that the growth rates may differ, since k is smaller in this regime and the growth rates depend on k. Figure four presents numerical solutions to the full dispersion relation, equation (6) in the equal temperature regime. The numerical results for the regime here, $\theta_e \gg \theta_i$, are qualitatively very similar.

D). Resonant, forward scattering, $\theta_e \approx \theta_i$. As for $T_e >> T_i$, the analysis from the resonant backscattering for equal temperatures can be applied to the forward scattering case with equal temperatures. The condition that k_o must satisfy is:

(29a) $$0.9\sqrt{2\alpha/3} > k_o > 0.45\sqrt{2\alpha/3}.$$

At this point, we must examine a feature of equation (7) which we have thus far ignored. We begin by noting an important property of the symmetries in (6); if we make the transformation:

$$\underline{k} \longrightarrow -\underline{k}$$
$$\omega \longrightarrow -\omega^*$$

the equation remains unchanged. That is for a given growth rate at $(\mathrm{Re}(\omega_o-\omega), \underline{k}_o-\underline{k})$, the growth rate at $(\mathrm{Re}(\omega_o+\omega), k_o+k)$ will be the same. In Figure four this symmetry is evident, and the EID growth is present for wavenumbers larger and smaller than k_o. Thus, strictly speaking, in Figure two a), for example, we should have drawn a forward lobe corresponding to the backscattered instability, gotten by inversion of the backscattering lobe through the point $\underline{k}_o-\underline{k} = \underline{k}_o$.

To understand why this other decay instability only exists under certain conditions (whose exact nature is closely tied up with the SM instability), even though the symmetry in (6) seems to demand it always, we must go

back to equation (1), and ask the question: What are the amplitudes of the excited fields? To answer this, we use a result from normal mode theory, noting that the solution of (6), our dispersion relation, is essentially a solution for the eigenvalues of the matrix in (1). It is well-known that this normal mode analysis can predict the relative amplitudes of the excited waves, as well as the normal mode frequencies. These amplitudes will be given by the norm of the eigenvectors associated with the zero eigenvalue. That is, given a matrix equation:

$$\begin{pmatrix} \epsilon_1 & \partial_{12} & \partial_{13} \\ \partial_{12} & \epsilon_2 & \partial_{23} \\ \partial_{13} & \partial_{23} & \epsilon_3 \end{pmatrix} \begin{pmatrix} E_1 \\ E_2 \\ E_3 \end{pmatrix} = 0$$

then we know for non-trivial E_i:

$$\frac{E_2}{E_3} = \frac{\partial_{23}\partial_{13} - \epsilon_3 \partial_{12}}{\partial_{23}\partial_{12} - \epsilon_2 \partial_{13}} .$$

For the matrix in (1), we have:

$$\frac{E(\underline{k}-\underline{k}_0, \omega-\omega_0)}{E(\underline{k}+\underline{k}_0, \omega+\omega_0)} = \frac{\mu_- \epsilon(\underline{k}+\underline{k}_0, \omega+\omega_0)}{\mu_+ \epsilon(\underline{k}-\underline{k}_0, \omega-\omega_0)} \approx \frac{\epsilon(\underline{k}+\underline{k}_0, \omega+\omega_0)}{\epsilon(\underline{k}-\underline{k}_0, \omega-\omega_0)} .$$

As either a look at the frequency matching condition or the numerical results in Table IV show, only the branch of the EID instability involving the Stokes wave is near resonance, and for that case:

(30a) $$|E(\underline{k}-\underline{k}_0, \omega-\omega_0)| \gg |E(\underline{k}+\underline{k}_0, \omega+\omega_0)| .$$

When (30a) is satisfied, only the EID instability growth rates occuring on the left-hand side of our graphs will correspond to a wave with a large parametrically excited amplitude. In the opposite case, when:

$$|Re\ \epsilon(\underline{k}-\underline{k}_o, \omega-\omega_o) - Re\ \epsilon(k+k_o, \omega+\omega_o)| < Im\ \epsilon(\omega-\omega_o),$$

then both the Stokes and anti-Stokes modes may simultaneously be resonant. We can then write (using (11)):

$$|\delta_+ + \delta_-| \leq Im\ \omega. \tag{30b}$$

If (30b) is satisfied, then our three-wave treatment breaks down. A treatment of the case when (30b) is satisfied is taken up in the next section, on the SM instability.

E). Nonresonant, forward scattering. As k_o decreases further, and $k_o < \frac{1}{2}\sqrt{2\alpha/3}$, it becomes impossible to satisfy the resonance condition for the Langmuir wave, but, the growth rate of the EID instability does not drop off sharply once k_o decreases beyond $\frac{1}{2}\sqrt{2\alpha/3}$. To treat the nonresonant case analytically is difficult, since the equation we must then solve is intrinsically quartic. However, the growth rates (approximately), and a qualitative feeling for the depence of the instability on k_o, can be obtained in the limit that the dampings of the waves are much less than the growth rates, while $W_o\alpha \ll 1$. In this somewhat artificial limit, (6) can be written:

$$(31) \qquad (\omega^2 - \omega_A^2)(\omega - x_o)^2 - \frac{W_o \omega_A^2 \delta\mu^2}{4} = 0$$

Now, if $\mathrm{Re}\,\omega \ll x_o$, then:

$$(\mathrm{Im}\,\omega)^2 = \frac{W_o \omega_A^2 \delta\mu}{4}\left(\frac{1}{1 - x\delta}\right).$$

As k_o decreases, Im ω decreases. Figure seven shows solutions to equation (6) in the nonresonant forward scattering case, although here, $k < k_o$. It should be noted that a recent paper by Fried, et al. treats the decay instabilities driven by a Langmuir pump in one dimension.[7] They present very detailed results on the dependence of the growth rate on k_o.

STIMULATED MODULATIONAL INSTABILITIES

Under the name stimulated modulational instabilities, we include those interactions which require the Stokes and anti-Stokes high frequency waves and a resonant low frequency response be treated. In this case, three dimensional effects are critical; in fact, the instability cannot exist in one dimension. (Notice that the OTS instability, while it involved both high frequency waves, had a non-resonant low frequency response. The OTS is properly called a modulational instability, but not a stimulated modulational instability.) Inclusion of a third resonant wave complicates an analytic treatment, and we have been able to treat this case only in the very low

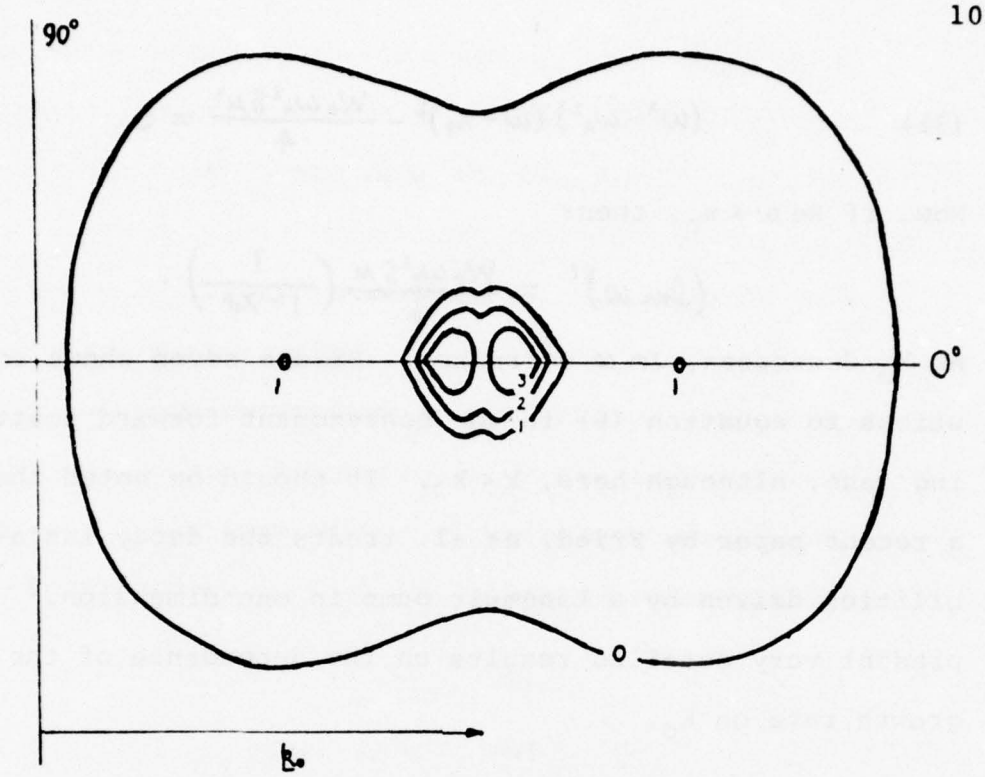

Figure seven. Solutions of the dispersion relation, equation (6), showing contours of constant growth rate, Im ω, as a function of the wavevector, $\underline{k}_o - \underline{k}$, of one of the daughter Langmuir waves (see Figure one). Here $W_o = 4 \times 10^{-6}$ and k_o has magnitude 0.005. Other parameters are the same as for Figure six. The numbers on the contours give the growth rate in units of 2×10^{-7}. In this regime, the EID instability is no longer resonant, and hence has the much degraded maxima at the two, small contours labelled "1." The other maxima is the OTS instability, here almost isotropic in $\underline{k}$.

and very high power limits.

Even so, the general result of the inclusion of both the Stokes and anti-Stokes waves is a lowering of the growth rate. This an effect well-known in nonlinear optics and was noted in the case of a plasma instability by DuBois and Goldman.[3] They showed that, in fact, for an electromagnetic pump, the threshold for the four-wave instability is higher by a factor $\omega_A/4\gamma_A$. We have used perturbation methods to study the effect of the coupling of both high frequency waves and have been able to show, directly that in the limit $y \ll \gamma_A$ and the limit $y \gg \gamma_A$ that the coupling of the anti-Stokes wave reduces the growth rate of the instability. This seemingly general result is essential in understanding the SM instabilities.

We have gotten analytic results for these four-wave, resonant instabilities in two regimes. In the low power regime, when we have:

$$\gamma_A \gg \mathrm{Im}\,\omega \gg \gamma_L$$

Figures two a), on page 77, and four, on page 81, give numerical results. In the high power limit, when $\omega \gg \omega_A$, the SM instability reduces to the high power limit of the OTS instability (case C and D); analytic results deduced for that case also describe the SM instability in the high power limit. Essentially, as Figure five (page 83) shows, the SM and OTS instabilities merge for large powers.

A striking feature of the numerical results for the lower power regime, as shown in Figures two a) and four, is the wing-like structures at $\underline{k}_o - \underline{k} = \underline{k}_o$. These lobes are the SM instability. We begin with equation (13) written as, using the ordering $\gamma_L << \mathrm{Im}\,\omega << \gamma_A$:

$$(32) \qquad (\omega^2 - \omega_A^2 + i\omega\nu_A)(\omega - \delta_-)(\omega + \delta_+) + W_o \delta \omega_A^2 \mu^2/4 = 0$$

(it turns out that even off axis the approximation that $\mu_-^2 = \mu_+^2$ is adequate to second order in γ/γ_A for the small W_o here). The solution to (32), to first order in y, is given by equations (25) and (26) and their anti-Stokes counterparts:

$$(33) \qquad \mathrm{Re}\,\omega = \pm \delta_\mp \left[1 - \frac{\gamma}{\nu_A}\left(\frac{\delta_\mp^2 - \omega_A^2}{\delta_\mp^2}\right)\right],$$

$$(34) \qquad \mathrm{Im}\,\omega = \frac{\mu^2 W_o \omega_A^2}{8}\left[\frac{\delta_\mp \nu_A}{(\delta_\mp^2 - \omega_A^2)^2 + \nu_A^2 \delta_\mp^2}\right],$$

and these have their maximum growth at:

$$(35) \qquad k = 2k_o \cos\gamma - \left[-\frac{\eta^2 - 2\alpha}{6} + \sqrt{\left(\frac{\eta^2 - 2\alpha}{6}\right)^2 + \frac{\alpha^2}{3}}\right]$$

where we have defined:

$$\eta = \frac{\nu_A}{k}\sqrt{\frac{3}{2}}.$$

Notice that when we take the upper sign in (34), we recover the three-wave EID results. The reason for this is clear if we notice that, to first order in y:

$$(\omega - \delta_-)(\omega + \delta_+) = [\pm\delta_\mp + i\gamma - \delta_- - \mathcal{O}(\gamma)][\pm\delta_\mp + i\gamma + \delta_+ - \mathcal{O}(\gamma)]$$
$$= 2\delta[i\gamma + \mathcal{O}(\gamma)].$$

which is putting one high frequency wave off resonance and fixed at $(k_o \pm k, w \pm w_o) = 2\delta$. That is to say, four-wave effects are also second order in y (or W_o).

We were able before, retaining only three-wave effects, to predict the maximum growth rate along the locus given by (35), and this is also the maximum growth rate for the SM instability. However, the three-wave treatment always predicts maximum growth for k = 0. Our numerical work shows that the maximum growth rate occurs for small, but non-zero, k. This is because, as k goes to zero, we have, from (30b):

$$|\delta_+ + \delta_-| = 2\delta \rightarrow 0,$$

so that both high frequency waves can be near resonance (and so we cannot ignore the anti-Stokes wave). As the interactions becomes truly four-wave, the threshold goes up, the growth rate goes down; and, we get the maximum growth rate off-axis. There are two competing effects here:

1). μ has its maximum when k = 0: that is, when $\underline{k}_o$ and $\underline{k}_o \pm \underline{k}$ are parallel. Thus, as k goes to zero, the effect is to increase μ and increase the growth rate;

2) But, when k gets smaller, the resonances of the Stokes and anti-Stokes waves get closer. This means that as $k \rightarrow 0$, the anti-Stokes modes is more and more strongly coupled, which has the effect of lowering

the growth rate.

It is the competition of these two effects which determines the k for which maximum growth occurs.

To calculate this k requires a second order perturbation analysis of (32). We have done this, beginning by writing (32) in the form:

$$(\omega^2 - \omega_A^2 + i\omega\gamma_A)(\epsilon + iy)(2\delta + \epsilon + iy) + W_0\delta\omega_A^2\mu/4 = 0, \tag{37}$$

using the definition:

$$\omega = \delta_- + \epsilon + iy .$$

We have four small parameters:

$$\epsilon, y, W_0, k^2W_0/k_0^2$$

since the last is necessary to treat the dependence of μ^2 on k:

$$\mu^2 = 1 - k^2\sin^2\psi/k_0^2 , \quad \psi = \cos^{-1}(\hat{k}\cdot\hat{k}_0) . \tag{38}$$

The result of this perturbation analysis is that the maximum growth rate, on the locus given by (35) occurs at the k for which:

$$2\delta = -\delta_\mp . \tag{39}$$

This result is independent of W_0 for low powers. It predicts the k values for Figures two a) and four within 5%.

In general, the locus given by (35) defines an angle at which the SM instability will occur for very small k, like those prescribed by (39), namely:

$$\cos\psi = \frac{1}{2k_0}\left[\frac{-\eta^2+2\alpha}{6} + \sqrt{\left(\frac{\eta^2-2\alpha}{6}\right)^2 + \frac{\alpha^2}{3}}\right] . \tag{40}$$

This is also a condition on k_o:

$$k_o > \begin{cases} 0.46\sqrt{2\alpha/3}\,, & \theta_e \approx \theta_i\,, \\ 0.50\sqrt{2\alpha/3}\,, & \theta_e >> \theta_i\,. \end{cases}$$

It was these conditions that assured (see (29) or (29a)) in the case of the EID instability, that the instability was a resonant one. For k_o less than this critical k_o, the SM instability, now on axis, becomes part of the forward scattering nonresonant EID instability. Thus, for $k_o < 0.45\sqrt{2\alpha/3}$ the SM and EID become identical instabilities, while for $W_o >> 64\alpha/T$, the SM and OTS merge.

Figures eight through ten summarize the above results, by labelling the dominate instability for a Langmuir spectrum as a function of k_o, W_o, and the ambient plasma temperature ratio. These diagrams give qualitative results, based on the instability with the largest growth rate. Two results are striking:

1). For small enough k_o, only the OTS instability is strong;

2). For large θ_e/θ_i, the EID instability dominates all other parametric processes. These results are only applicable to the case when we can ignore the damping of the high frequency modes. For large γ_L, different results are possible in a few regimes.

APPLICATIONS TO BEAM-GENERATED SPECTRA

We now turn to several applications of the

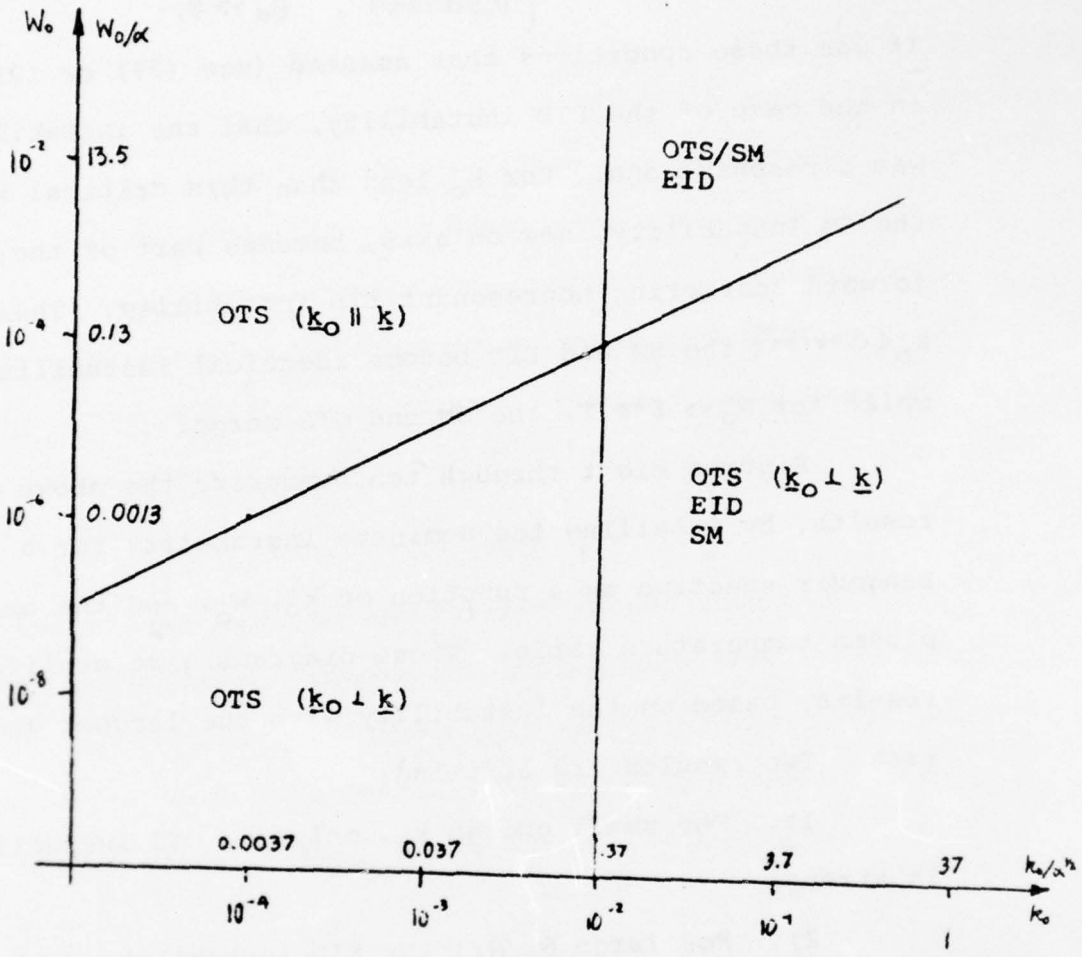

Figure eight. Qualitative features of Langmuir pump decay, as a function of W_o, the normalized pump power, and k_o, the pump wavenumber. Here $\theta_e/\theta_i = 1$ and we have a hydrogen plasma. There is assumed to be negligible damping of the high frequency waves. $\underline{k}_o - \underline{k}$ is the wavenumber of the fastest growing daughter wave.

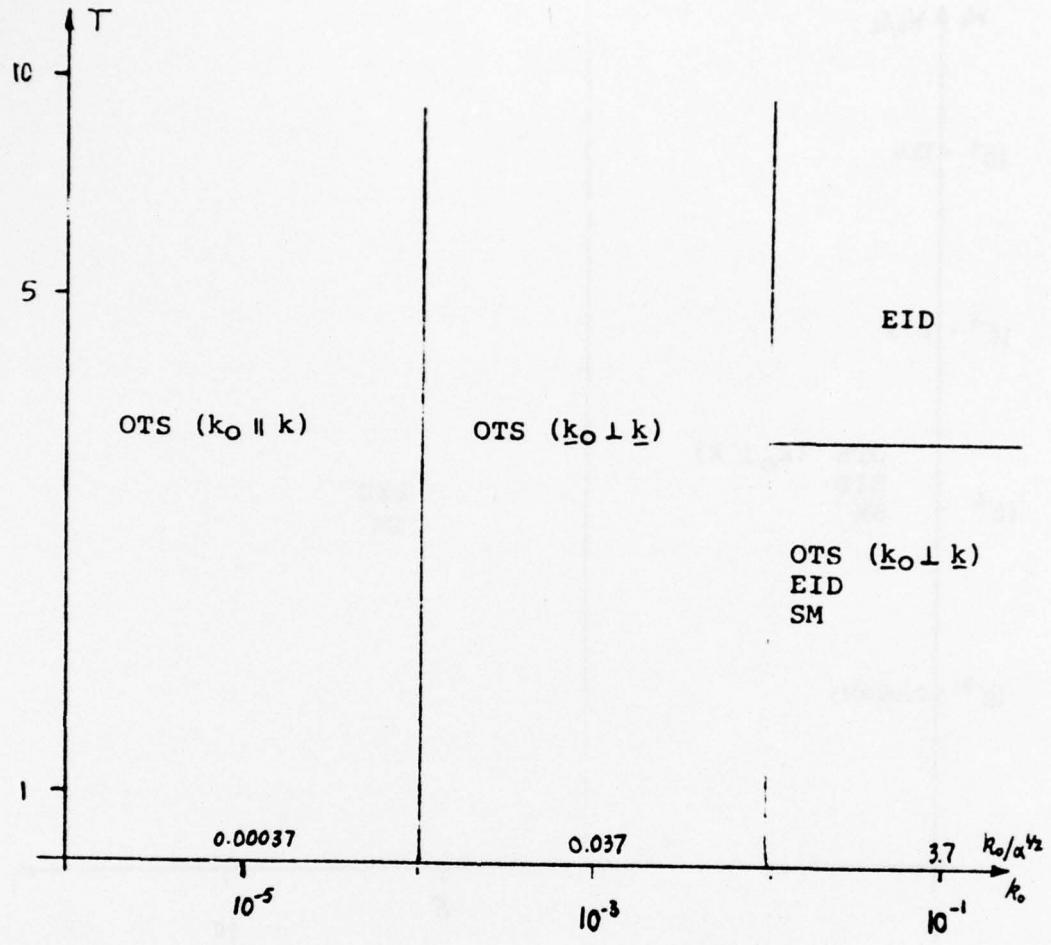

Figure nine. Qualitative features of Langmuir pump decay, as a function of k_o and θ_e/θ_i. Here $W_o = 10^{-6}$ and we have a hydrogen plasma, which we assume to have negligible damping of the high frequency waves.

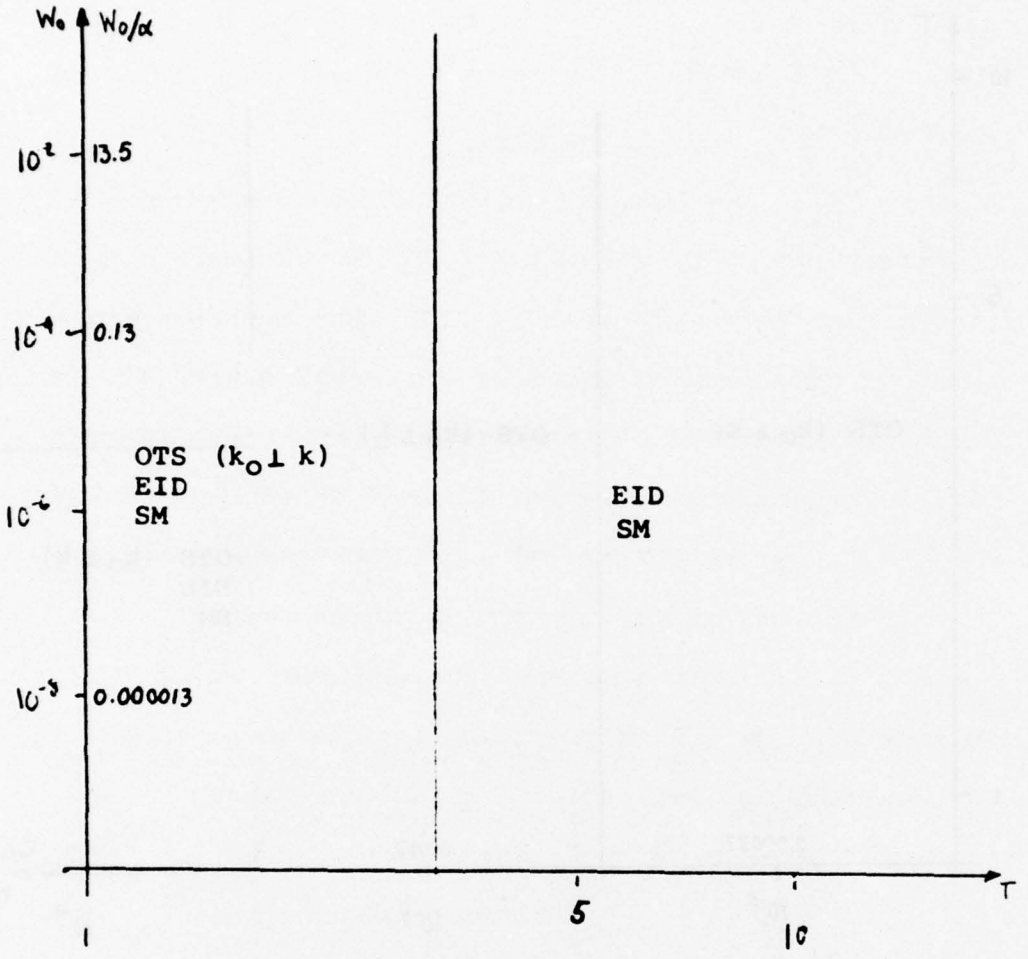

Figure ten. Qualitative features of Langmuir pump decay, as a function of W_o and $\Theta_e/\Theta_i = T$. Here k_o is approximately 0.05 and we have a hydrogen plasma with negligible high frequency damping.

dispersion relation, equation (6), which describes the linear stability of a Langmuir pump. We will examine three physical situations in which an enhanced spectrum of longitudinally polarized waves is created by an electron beam:

1). Type III solar radio bursts. These are radio signals associated with electron streams ejected from the sun which generate electromagnetic radiation through an intermediate step involving an enhanced Langmuir spectrum.

2). Auroral arcs. The ionospheric electron streams associated with these arcs create a non-equilibrium Langmuir spectrum which probably acts as a pump for parametric processes.

3). Laboratory electron beams. In experiments using a non-relativistic electron beam travelling through an almost homogeneous plasma with no magnetic field, parametric effects due to beam generated Langmuir spectra are sometimes evident.

One of the commonest sources of enhanced Langmuir radiation is an electon beam travelling through a plasma. Through quasilinear growth and stabilization,[16] this beam generates asspectrum with characteristics:[17-19]

$$k_0 = \omega_{pe}\,\hat{v}_b/v_b \quad , \quad \Delta k_0/k_0 \approx \Delta v_b/v_b , \tag{41}$$

$$W_0 \lesssim \frac{n_b}{2n_e}\,\frac{v_b\,\Delta v_b}{v_b^2} . \tag{42}$$

where v_b is the beam velocity, Δv_b the spread in the beam,

Δk_o is the spread in the spectrum, and n_b/n_e is the ratio of beam density to ambient plasma density. Equation (41) is a statement of the fact that the beam generates waves through a "resonant" wave-particle interaction, which requires the phase velocity of the waves to be the same as the velocity of the particles. Equation (42) is an upper bound on the energy that the beam can transfer to the wave spectrum.

Strictly speaking, the dispersion relation of these beam generated waves is not Langmuir-like; according to O'Neil and Malmberg, the dispersion relation of these "beam modes" is given by a product of the plasma dispersion relation and a factor due to the beam:[20]

$$\epsilon(\underline{k},\omega)(\omega - k_o v_b + ik\Delta v_b)^2 = n_b/n_e \ .$$

They have studied this equation in detail, and their results for weak beams may be summarized by noting that when the following inequality is satisfied:

$$\left(\frac{n_b}{2n_e}\right)^{-1/3} \frac{\Delta v_b}{v_b} \frac{v_b}{v_e} < 5 ,$$

then we can conclude that the dispersion relation of the waves is essentially that of Langmuir waves, with:

$$\omega = (1 + 3k_o^2)^{1/2} + O(n_b/n_e) .$$

This condition is satisfied for all of our applications except the last. Since it is also the case that:

$$\frac{3}{2} k_o^2 >> \frac{n_b}{n_e} ,$$

we have ignored beam corrections to the Langmuir dispersion relation of the pump in this limit.

We are making a further approximation in applying a single-mode pump theory, when we apply our dispersion relation, equation (6), to the case of a finite bandwidth pump. Mathematically, we are making an assumption about the narrowness of the Langmuir spectrum in k-space; we are requiring essentially, that the spectrum be narrower in k than the high frequency dielectric function (see equation (9) for an exact version of this). The effect of a broad pump in three dimensions is discussed in reference 8. Here, we only note the most important result, namely that the condition on the spectrum can be written:

$$|\omega \mp \tfrac{3}{2} k^2 - 3\underline{k}\cdot\underline{k}_o| >> |3\,\underline{k}\cdot\Delta\underline{k}_o|\,,$$

where it is important to realize that it is the spread of the spectrum in the direction of the fastest growing mode that appears in this equation. Note also that the left side of this inequality depends on the growth rate of the instability.

In the further approximation that the beam-wave interaction is unimportant, we can study the properties of the spectrum itself. This will be appropriate in a number of circumstances. If for example, the beam passes through the system quickly, but the Langmuir spectrum remains at a high level for times long compared to the beam duration, or, if the beam-wave interaction has characteristic times

much longer than the growth rates predicted by equation (6), then the predominant processes in the beam evolution will be parametric. In any case, given an assumed, enhanced spectrum, equation (6) gives growth rates and wavenumber shifts for the linear relaxation of the spectrum.

While our dispersion relation, equation (6), will describe the simplest, linear relaxation of the beam-enhanced spectrum, our formalism does not directly give any insight into the actual evolution of the beam-plasma system. Our methodology in the following applications is to use the properties of the daughter waves predicted by equation (6) to make qualitative statements about the importance of linear, parametric effects on the beam-plasma evolution. We can examine, for example, whether spectral evolution might be able to compete with quasilinear relaxation of the beam, if it turns out that the parametric growth rate is comparable to the quasilinear growth rate. Our theory of the linear relaxation of the spectrum offers important qualitative insights into features of these beam-plasma interactions, but it cannot make quantitative predictions of the detailed evolution of the beam or spectrum. Thus, our descriptions of these three applications only touches on the highly nonlinear processes that actually determine the physics; but, we apply (6) in an effort to find regimes where parametric effects most likely play a role in the total (nonlinear) interaction.

We take three cases of current interest and compare the results of numerical and analytic solutions of (6) with experimental data from the beam-generated spectra associated with Type III solar radio bursts, with auroral arcs, and with nonrelativistic electron beams (with no magnetic field). Table V summarizes the physical parameters of each of these beam generated spectra.

Type III Solar Radio Bursts[8,14,15,21-25]

It is believed that the radio discharges of solar origin, at 200 mH to 10mH, with durations of one to ten seconds and having a distinctive harmonic structure--Type III solar radio bursts--are due to high energy electron bursts ejected from the sun. These streams of electrons are then thought to interact quasilinearly with the surrounding plasma (either the solar corona, solar wind, or interplanetary plasma) to generate an enhanced Langmuir spectrum, which, in turn, is responsible for the observed radio signals. The role of the parametric instabilities in the evolution of this beam-spectrum system has been considered by several authors, the EID instability by Zheleznyakov and Zaitsev[15] and the OTS instability by Papadopoulos, et al.[22] and by Smith, et al.[26] The basic attack on the problem, from a suggestion by Kaplan and Tsytovich,[14] is to study the relaxation of the Langmuir spectrum and determine whether this relaxation

TABLE V

PARAMETER REGIMES FOR PHYSICAL APPLICATIONS

Plasma-beam system	Figure	n_e (cm^{-3})	v_e (cm/s)	T_e/T_i	n_b/n_e	v_b/v_e	$\Delta v_b/v_b$	γ_L	$\alpha=2c_s/3$	k_o	W_o
Type III solar burst											
at 1 $R_\odot$	2a	10^{8}	$10^{8.7}$	1	$10^{-7.}$	15.4	1/4	$10^{-9.}$	$10^{-3.1}$	.05	$10^{-5.4}$
at 30 $R_\odot$	2b	$10^{3.2}$	$10^{8.4}$	1	$10^{-6.9}$	10.9	1/2	$10^{-9.}$	$10^{-3.1}$	.026	$10^{-5.8}$
at 215 $R_\odot$	2c	$10^{0.9}$	$10^{8.1}$	1	$10^{-6.9}$	9.9	1/2	$10^{-9.}$	$10^{-3.1}$	.014	$10^{-5.3}$
Auroral streamer	3	$10^{3.3}$	$10^{7.5}$	1	$10^{-5.}$	150.	1/2	$10^{-8.}$	$10^{-3.9}$	.007	$10^{-1.4}$
Laboratory electron beam											
"slow"	11a	$10^{8.7}$	$10^{7.8}$	15	$10^{-1.3}$	4.	1/5	Landau $+10^{-5.5}$	10^{-5}	.25	$10^{-1.2}$
"fast"	11b	$10^{8.7}$	$10^{7.8}$	15	$10^{-1.3}$	10.	$\ll 1/5$	Landau $+10^{-5.5}$	10^{-5}	.1	$10^{-1.2}$

occurs in such a way as to affect the quasilinear decay of the beam. Two considerations are relevant:

1). Do the parametric processes involved in the relaxation of the Langmuir spectrum take the energy of the spectrum out of resonance with the beam (and so destroy the quasilinear beam-spectrum interaction); that is, are either of the following inequalities satisfied:

$$v_b - \Delta v_b > \underline{v}_{phase} \cdot \hat{v}_b \;;$$
$$v_b + \Delta v_b < \underline{v}_{phase} \cdot \hat{v}_b \;? \qquad (43)$$

2). Does this transfer energy occur rapidly enough to compete with the quasilinear processes?

The second of these questions has been answered partially by references 8 and 15, where it is shown that neither the OTS or EID instability occur fast enough to actually prevent quasilinear decay of the beam.

With our dispersion relation, (6), we have studied the behavior of the enhanced Langmuir spectrum and have found some parameter regimes in which the parametric processes can play an important role in the beam dynamics, even though they may not be able to actually prevent decay of the beam. We begin with a numerical solution to the beam-spectrum interaction in the case of solar bursts, recently done by Magelssen.[27] This numerical work solves the quasilinear equations in two dimensions, but assumes a one-dimensional spectrum and neglects the nonlinear relaxation of the

spectrum. From Magelssen's data we have taken the parameters necessary for a study of the spectrum, namely, k_o and W_o, as a function of the distance from the sun that the electron pulse has travelled (after it has left the surface of the sun). Table V includes the parameters for three distances from the sun, and Figure two (pages 57 and 58) shows contour plots of the parametric growth rates predicted by equation (6). We have used Magelson's data rather than the approximations from a homogeneous theory of the beam generated waves given by (41) and (42) for k_o and W_o.

Magelssen's results show that k_o is about 0.05 (in units of the Debye wavenumber) near the sun, and k_o decreases to 0.016 at the earth's orbit (about $215R_\odot$, where $1R_\odot$ is one solar radius, a distance of about $7x10^5$ km). His calculations of the Langmuir wave spectrum intensity, which include effects due to wave reabsorption and "pile-up"[2] give typical values of W_o of 10^{-6} to 10^{-5} (the wave intensity normalized to the thermal energy of the plasma).

The OTS instability, in this regime, always has its maximum growth for a $\underline{k}$ perpendicular to $\underline{k}_o$ and for values of k much less than k_o. Indeed, it would require stream densities higher by several orders of magnitude to result in the OTS instability having any growth on axis for even the smallest k_o given by Magelssen. This contradicts the

results of both references 22 and 26, both of which use the OTS instability to provide for energy transfers which satisfy (43)and so could account for beam stabilization. We believe that the OTS instability will have a minimal effect on the beam-spectrum system, because of the impossibility of satisfying (43) for the powers of the spectrum appropriate to Type III solar bursts.

However, as Zheleznyakov and Zaitsev noted, the EID instability can transfer energy to Langmuir waves with velocities sufficiently different from the velocity of the beam to satisfy (43) only when it is not a backscattering instability. For the values Magelssen gives, we find that, the EID instability from 1 $R_\odot$ to 80 $R_\odot$ is a backscattering instability. From 80 $R_\odot$ to 450 $R_\odot$, somewhat beyond the earth, the EID instability is a forward scattering instability. And beyond 450 $R_\odot$, k_o is so small that the condition obtained from combining (43) and (28a) is violated and the EID instability becomes a nonresonant forward scattering process. Note that for the low values of W_o for these spectra, that there is no possibility of satisfying the four-wave coupling condition, equation (20). Thus, if we accept Zaitsev and Zhelesnyakov's argument that multiple scattering, from the backscattering EID, prevents its being able to transfer energy to nonresonant waves (that is, waves not in "resonance" with the beam), we conclude that only between 80 and 450 $R_\odot$ can the EID instability

shift energy out of resonance with the beam. We also note that the SM instability occurs for all these sets of parameters for distances less than about 450 $R_\odot$, but at such small k-shifts as to violate (43).

Our conclusions here are dependent on two striking features of Magelssen's results:

1). The small values of W_o. Many authors have conjectured much larger values of W_o. If this were the case, the OTS instability, for example, could have growth on axis, if: $W_o \gg 10k_o^2$. In addition, at higher powers, the OTS instability will result in an angular spreading of the spectrum, even if k_o is not small enough to satisfy the above inequality (this effect is well shown in Figure five, page 83). However, to get into either of these regimes, even for the smallest of the k_o appropriate to the solar problem, $k_o = 0.013$ (in units of k_{De}), requires a power several orders of magnitude greater than Magelssen finds. If W_o were on the order of 0.1, it is even possible to use the dipole approximation for this problem, as Papadopoulos has done.[22]

2). The large values of k_o. Most recently, Smith, et al.[26] have presented a calculation using a value of k_o of 0.013. In this regime, the SM instability has merged with the now four-wave EID instability. While it seems that Smith, et al. have called this nonresonant forward scattering an OTS instability, their numerical results

show the interaction to important in the evolution of the beam and spectrum. They show numerically that this growth rate shifts energy out of resonance with the beam quickly enough to stabilize the electron beam. Magelssen's data, however, shows that the value of k_o that they use, as appropriate to the spectra that should exist near the earth, does not in actuality occur except for distances on the order of twice the earth's orbit (near 450 $R_\oplus$).

We have used Magelssen's data, in spite of these other considerations, because his results so closely mirror the best observations at this point; the essential effects that he includes are the inhomogeneity of the ambient plasma, and the finite size of the beam. The combination of a sharp beam front and an inhomogeneous plasma can stabilize the beam without the inclusion of mode-coupling effects. Even with his very low values of W_o, the observed shape of the spectra are nicely accounted for. What is necessary now to improve his numerical work, is the inclusion of these mode-coupling effects. Our results above give some guide to the regimes where these effects will be most important.

While our qualitative considerations seem to show that the parametric instabilities cannot stabilize the electron stream associated with Type III bursts (at least between the earth and the sun), it has been theorized that they be important in understanding the production of

electromagnetic radiation. The critical consideration in the conversion of Langmuir radiation to electromagnetic radiation, at the second harmonic, for example (the characteristic feature of Type III radiation is the presence of both the fundamental and second harmonic), is the angular relations between the Langmuir wavenumbers which can allow coalescence of two Langmuir waves to form a transverse, electromagnetic wave at twice the plasma frequency. (The electromagnetic ratiation at the plasma frequency is usually attributed to scattering by ion fluctuations.[23] We will not consider that process here.) Conservation of energy and momentum in this wave-wave process require that the wavenumbers of the Langmuir waves be approximately equal and opposite. Our results for the OTS and SM instabilities in this regime show that this is impossible to obtain for the daughter waves (contrary to the findings of Papadopoulos, et al.[22]). In addition, our results show that the EID instability is only a backscattering process in which $k_o - k = -k_o$ for distances within 16 $R_\odot$. Beyond this point, $k_o < 0.03$, and we have, from equation (27):

$$k_o - k = -k_o + 0.9\sqrt{2\alpha/3} \approx -0.01 .$$

making $k_o - k$ and k_o unsuitable for this process of generating radiation at $2\omega_{pe}$. Our analysis shows that the observed radiation at the second harmonic must be due to processes other than parametric ones.

Auroral Arcs[28,29]

Papadopoulos and Coffey have suggested the OTS instability as a mechanism involved in the production of another astrogeophysical phenomenon, the auroral arcs. In a situation similar to the Type III solar bursts, experimental data show distinctive electron distributions propagating along magnetic field lines in the ionosphere, which are associated with auroral discharges. There are two pieces of data that naive, homogeneous, quasilinear theory does not predict: the relative stability of these beams and the anomalous resistivity that they encounter along the magnetic field lines.

Our analysis of the linear stability of a spectrum of Langmuir waves enhanced by a stream typical of those associated with auroral discharges shows that, indeed, the OTS instability will have a profound effect on the resonance relations of the electron beam and the Langmuir spectrum. Figure three (page 77) shows the regions of highest instability for parameters associated with an auroral discharge and, given the fact that, $k \gg k_o$, we have a geometry with the fastest growing mode parallel to $\underline{k}_o$. The large value of k allows us to satisfy (43), even though the beam, and hence spectrum, are relatively broad; it appears that the OTS instability, in one dimension, for these parameters, can transfer energy from regions of the Langmuir spectrum in resonance with the beam to regions not

in resonance, and thus possibly stabilize the beam.

However, this is only a necessary condition for stabilization. As Kaplan and Tsytovich were the first to point out, these nonlinear processes also must proceed quickly enough to change the spectrum before the beam has relaxed. Zheleznyakov and Zaitsev give the following condition on the ratio of the rates of quasilinear relaxation and wave transfer:[15]

$$\epsilon \ln\left[\epsilon\, W_0(t)/W_0(t=0)\right] \ll 1, \quad \epsilon = \gamma_{q.l.}/\gamma_{p.t.} \tag{44}$$

Using the results for the wave transfer rate from equation (17b) and the usual quasilinear relaxation rate, we get the condition:

$$\frac{\Delta v_b}{v_b} >> 8\left(\frac{n_b}{n_e}\right)^{1/5} . \tag{45}$$

There is a discrepancy between (45) and the results of Papadopoulos and Coffey, which appears to come from their expression for the maximum growth rate, taken from Nishikawa, which is incorrect in this regime. Although data on the auroral plasma is approximate, we know that $\Delta v_b/v_b$ is on the order of 1/3 and that $n_b = 0.02\ cm^{-3}$, so that, (45) gives: $n_e > 2\times10^5\ cm^{-3}$. This is 100 times greater than the result of Papadopoulos and Coffey, and an examination of ionospheric electron densities shows that this condition is never satisfied in the ionosphere. The highest electron densities observed [30] are about 10^5, which occur at about 300km, much higher than the observed height

of auroral discharges. Thus, we conclude that are no parametric processes sufficiently fast to stabilize the beams associated with auroral discharges. However, the other important features of these discharges, the high anomalous resistivity and power law tails on the electron distributions, for example, may require the details of the linear stabiltiy of a Langmuir spectrum to be fully understood (and Papadopoulos and Coffey have examined a number of these questions), but in a situation where the OTS instability does not stabilize the beam. In recent paper,[29] Matthews, Pongratz, and Papadopoulos correct their formula for the growth rate and derive a formula similar to (45) for n_b/n_e. They also report new data which shows that $n_e \approx 2x10^5$.

We have developed a formalism sufficient to treat another aspect of the problem. The dynamics of the Langmuir spectrum, after an initial OTS instability transfers energy to large wavenumbers, $k_o \pm k \approx \pm 0.05$, will be determined by the instabilities of these daughter waves. The interesting feature of this situation is that the large wavenumber daughter waves form a standing wave field. It is straightforward to write down the 5 x 5 determinental condition that describes the coupling of the low-frequency response at (k, ω) and the high frequency waves at $(k_o \pm k, \omega_o \pm \omega)$ and $(k_o \pm k, \omega_o \mp \omega)$. The k_o is now the fastest growing mode in Figure three, and the W_o will

be determined by the saturation of the OTS instability in the auroral streamer. On this value of W_o, we can only speculate; the studies of the nonlinear saturation of the OTS instability, even in an homogeneous plasma (which the auroral plasma is not) are vague.[30,31] We have looked at a range of values of W_o from 1.6×10^{-6} to 4×10^{-2} (figured on the local amplitude of the field, that is, the sum of the amplitudes of both components of the standing wave).

At low powers, our numerical results are straightforward in that we get directly the travelling-wave results for a pump of one-quarter the power. For the k_o appropriate to the daughter waves of the auroral streamer, $k_o = 0.05$, the numerical work we have done for a travelling-wave pump of the same k_o (see Figure two a), page 77) gives the same results that would obtain for a standing-wave pump with $W_o = 1.6 \times 10^{-5}$. That is, as we saw was possible in Chapter II, only one component of the standing-wave pump is driving the instability. This means, most importantly, that the auroral streamer parameters generate a set of daughter waves which must be treated in three dimensions, even though the parent instability occurs all in one dimension. The relaxation of the spectrum of the auroral stream occurs in three dimensions.

At higher powers, $W_o > 1 \times 10^{-3}$, we have been unable to solve the dispersion relation. The exact reason for this is unclear, but there is evidence that our expansion

in E_o breaks down. The major difficulty is that the cancelation of third and fourth order terms in E_o, which occured in deriving our travelling-wave dispersion relation, equation (6), does not occur for the standing-wave case. This results in terms remaining in the dispersion relation which, as W_o gets larger, begin to dominate some second order terms. The conclusion we drew above about the importance of three dimensional effects does not seem to be affected by this difficulty in our formalism, but, for W_o greater than $1x10^{-3}$, a more careful study of the parametric processes driven by a standing-wave pump must be done.

Laboratory Electron Beams[33,34]

Quon, et al. have done a series of laboratory experiments involving nonrelativistic electron beams in which parametric processes in the beam-produced wave spectrum are evident. Their overall results show that the specific parametric interaction depends sensitively on the velocity of the electron beam, or equivalently, on the characteristic wavenumber of the enhanced spectrum of plasma waves that the beam drives up. The linear stages of the decay of the Langmuir spectrum that this beam produces should be described by the results we have derived.

We first note that the parameters of Quon's plasma are very different from the astrophysical plasmas; the mass

ratio is much smaller for the laboratory situation and the electron temperature is much greater than the ion temperature. The general results we have derived for this regime show that the LID backscattering instability will dominate, when parametric effects are evident.

In the experiments done by Quon, et al. two beam velocities are examined. In the case of the slower beam our analysis can be used directly; for the faster beam, hwwever, some modifications are required. In the case of the first beam, the growing solutions to equation (6) are shown in Figure eleven a). The large wavenumbers in this regime required our using Landau damping for the high frequency waves. As Quon suggests, the dominate process is the well-known decay instability, and the parametric part of the results he presents are described by the well-known theory. We note that it is only under conditions of small α and $T \gg |$ that the usual results (of a back-scattered wave at $-\underline{k}_o$ and ion fluctuations at $\underline{k}_i = 2\underline{k}_o$) obtain. The maximum growth rate that we predict from our analytic results (equation (23)) is 1.6×10^{-3}, which corresponds to the lowest value of W_o that Quon, et al. look at, with a beam density of 5% of background. We have introduced no phenomenological constants: the damping is purely Landau damping; the fields have been calculated from (41). In addition to the decay region, our numerical results predict another region of growth. This corresponds

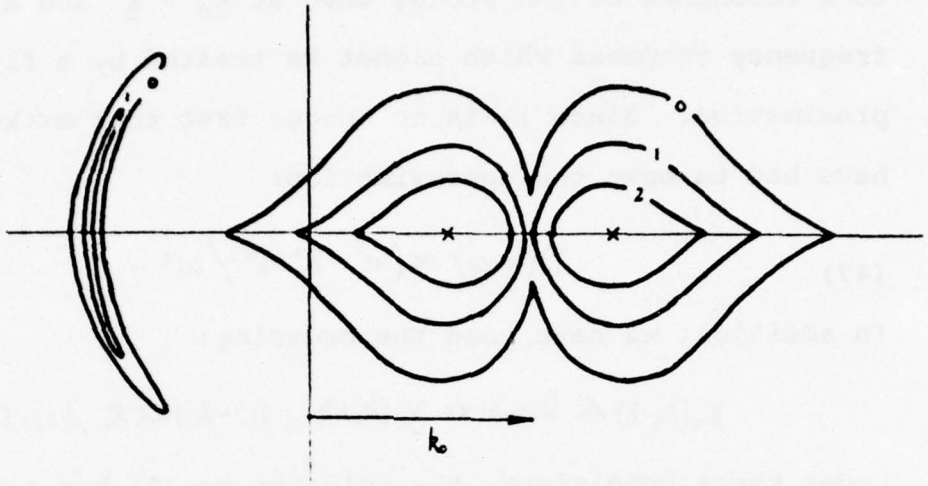

Figure eleven a). Solutions to the dispersion relation, equation (6), showing contours of constant growth rate, Im ω, as a function of the wavenumber of one of the daughter Langmuir waves, k_o-k. Here, W_o = 0.06; k_o = 0.25. Other parameters are; $\alpha = 9 \times 10^{-6}$, $\theta_e/\theta_i^o = 15$, and the high frequency damping is the sum of Landau damping and a collisional contribution equal to 3×10^{-6}. There parameters are appropriate to the pump generated by a typical laboratory electron beam passing through an argon plasma.

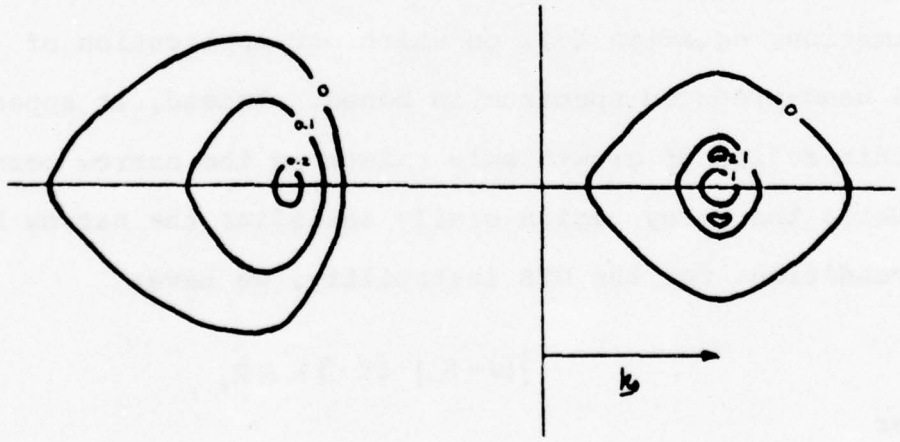

b). The same plasma as above, but with a beam which is now faster by a factor of 2.5. The pump this beam generates is here a beam mode with k_o = 0.1.

to a resonance of the Stokes wave at $\underline{k}_o - \underline{k}$ and a low frequency response which cannot be treated by a fluid approximation. Since it is no longer true that $\omega \ll kv_e$, we have had to make the approximation:

$$D(\underline{k},\omega) \approx (\omega^2 - k^2 v_e^2)/\omega^2 \quad . \tag{47}$$

In addition, we have used the ordering:

$$\gamma_L(k_o - k) \ll \mathrm{Im}\,\omega \ll \gamma_L(k_o + k)\,; \quad |\omega - \delta_-| \ll \delta_-\,; \quad |\omega + \delta_+| \approx 2\delta .$$

Under these conditions, the solution to (6) has a maximum growth rate:

$$\mathrm{Im}\,\omega = \frac{3W_o \delta_-^2 \delta}{8\,\gamma_L(k_o+k)(\delta_-^2 - k^2)} \quad .$$

The SM instability has disappeared because of the heavy damping of the anti-Stokes mode.

To understand why Quon, et al. do not observe this OTS-like structure, we must study the narrow beam approximation, equation (9), on which our application of (6) to a beam-produced spectrum is based. Indeed, it appears that this region of growth only exists in the narrow beam case, While the decay region easily satisfies the narrow beam condition, for the OTS instability, we have:

$$|\omega - \delta_-| \ll 3k\Delta k_{\parallel} \, ,$$

or

$$\mathrm{Im}\,\omega \gg 0.06 \, .$$

Since this is not the case for our parameters, the broad beam has washed out the OTS instability, so degrading the

growth rate that Quon, et al. do not observe it.

Two changes occur in this electron beam experiment when the beam velocity is increased, as in the second experiment by Quon et al.:

1). k_o becomes smaller. This is clear from the fact that the fastest growing mode of the beam instability has wavenumber:

$$k_o = \omega_{pe} \hat{v}_b / v_b .$$

2). There are electrostatic accelerations which cause the beam spread to decrease. This not only provides a relatively cold beam, but also generates a high frequency longitudinal wave with non-Langmuir dispersion, a beam mode as described above. For Wong's parameters, based on O'Neil and Malmberg's results for a narrow beam, we get:

$$\omega_o = 1.037 \ , \ k_o = 0.1 .$$

We have been able to treat the linear stability of this wave with equation (6), by merely using the above relation for $\omega_o(k_o)$ instead of the usual Langmuir dispersion. No other change in (6) is required, since its derivation depends only on the pump wave being high frequency and having longitudinal polarization. The numerical solution of (6) for these parameters is shown in Figure eleven b). This figure shows two parametric processes, a decay-like region to the left, and an OTS-like region near $\underline{k}_o - \underline{k} = \underline{k}_o$. The decay region is not, as Quon, et al., state, any more

difficult to excite than in the case of the slower beam. In fact, since the matching condition can be satisfied for somewhat smaller values of $k_o - k$, the Landau damping is smaller and the growth rates for this case slightly larger than for the previous experiment. Notice that perfect matching occurs when:

$$\omega_o - \omega_L(k_o - k) = \omega_A(k) .$$

This demands that $k = 0.26$ or $k_o - k = -0.16$. The growth rate is well accounted for by equation (23). Again, (47) must be used to account for the OTS-like region of growth, although here we have the ordering:

$$\mathrm{Im}\,\omega \gg \gamma_L(k_o \pm k);\ \chi_o = 0 .$$

so that the solution to (6) can be approximated:

$$\omega \approx i\sqrt{\omega_o|\delta|/4} ,$$

since here, $\delta = \delta_+ + \delta_- \approx 0.022$. Interestingly, Quon, et al. report neither of these kinds of plasma behavior. Since these are the results of a linear relaxation of the beam-induced spectrum, we have concluded that the effects that Quon,et al. do observe are due to non-parametric processes. The strongest parametric interactions possible are those that (6) predicts. That they are not observed points towards other effects, most probably trapping effects, being the processes that Quon, et al. observe in their second experiment.

CONCLUSIONS

We have developed a theory which allows us to treat the problem of linear relaxation of an enhanced Langmuir spectrum without approximation in $\underline{k}_o$ and taking into consideration multidimensional effects. Three new results of note come out of our analysis:

1). In a number of regimes, it is possible to have the Langmuir pump decay into daughter waves with wavenumbers larger than the pump wavenumber. Particularly, at equal temperatures, the SM instability, has daughter waves at $k_o + k \gtrsim k_o$. Thus, these waves have a phase velocity slightly greater than the phase velocity of the beam. These waves may be able to accelerate electrons, and, for a beam-induced pump, draw out a tail on the beam.

2). In every regime, there is significant three-dimensional structure, which will lead to a spreading of the spectrum in angle. The full problem of the three-dimensional, nonlinear relaxation of the spectrum has not been investigated, but our linear results show that this is essential. Especially, when the OTS instability is off-axis, large growth rates can occur at angles exceeding 20^o to $\underline{k}_o$. The angular spread of the spectrum, especially in the study of relativistic beams, is a critical parameter, and the wave effects that we have studied here

affect it greatly.

3). For a range of parameters with $\theta_e/\theta_i \gg 1$ and k_o in a critical range, the dominate process of decay is forward scattering. This result, coming uniquely from a study of the k_o dependence of the spectral decay, has immediate bearing on especially the theories relating to Langmuir-to-electromagnetic mode conversion. A whole new set of kinematic relations is possible with these daughter waves; the $k_o = 0$ result of daughter waves with equal and opposite wavenumbers to the pump is true only for values of k_o large compared to the root of the mass ratio.

To be sure, our results are only qualitative guides to the understanding of the real problem of Langmuir turbulence. What the linear theory we have presented here, offers is a physical understanding of the first stages of the process of relaxation of a narrow, Langmuir spectrum in a homogeneous, field-free plasma. The most important next step in this study is to extend our results to the case with a magnetic field, expecially since applications of our results to spectra enhanced by electron beams frequently occur in magnetized plasmas. And, of course, the full, nonlinear problem of the spectral decay, must be solved. Our results are only a beginning to that study.

NOTES TO CHAPTER THREE

[1]D. F. DuBois, M. V. Goldman, Phys. Rev., 164, 207 (1967). M. V. Goldman, "Nonlinear Waves and Fluctuations in Plasmas," University of Colorado, Department of Astro-geophysics, #CU1010 (1974).

[2]V. N. Tsytovich, Nonlinear Effects in Plasmas, New York, Plenum, (1970), page 244.

[3]D. F. DuBois, M. V. Goldman, Phys. Rev. Lett., 19, 1105 (1967).

[4]V. N. Tsytovich, Nonlinear Effects in Plasmas, p. 102.

[5]A. A. Vedenov, L. J. Rudakov, Dokl. Akad. Nauk. SSSR, 159, 738 (1964). N. E. Adreev, A. Yu. Kuri, V. P. Silin, ZHE. T. F., 57, 1024 (1970). V. E. Zakharov, Soviet Physics--JETP, 35, 908 (1972). V. P. Silin, Zhe. T. F., 7, 204 (1968).

[6]C. S. Lin, K. Nishikawa, P. K. Kaw, W. L. Kruer. Advances in Plasma Physics, volume 6, New York, Wiley--Interscience Pubs. (1975).

[7]B. D. Fried, T. Ikemura, K. Nishikawa, G. Schmidt, UCLA preprint, PPG-246 (1975).

[8]S. Bardwell, M. V. Goldman, Astrophys. J., in press.

[9]B. D. Fried, S. D. Conti, The Plasma Dispersion Function, New York, Academic Press, Inc. (1961).

[10]J. R. Sanmartin, Phys. Fluids, 13, 1533 (1970).

[11]D. F. DuBois, M. V. Goldman, Phys. Rev. Lett., 14, 544 (1965).

[12]V. P. Silin, Soviet Physics--JETP, 21, 1127 (1965).

[13]A. Hasegawa, Phys. Rev. A, 1, 1747 (1970).

[14]S. A. Kaplan, V. N. Tsytovich, Soviet Astr.--AJ, 11, 956 (1968).

[15]V. V. Zheleznyakov, V. V. Zaitsev, Soviet Astr.--AJ, 14, 47 (1970).

[16]R. C. Davidson, Methods in Non-Linear Plasma Theory, New York, Academic Press, Inc. (1972). Chapter 8.

[17]S. Kainer, J. M. Dawson, Phys. Fluids, 15, 2433 (1972).

[18]W. L. Kruer, J. M. Dawson, T. Coffey, Phys. Fluids, 15, 2419 (1972).

[19]W. L. Kruer, Phys. Fluids, 15, 2433 (1972).

[20]T. M. O'Neil, J. H. Malmberg, Phys. Fluids, 11, 1754 (1968).

[21]R. P. Lin, L. G. Evans, J. Fainberg, Astrophys. Lett., 14, 191 (1973).

[22]K. Papadopoulos, G. L. Goldstein, R. A. Smith, Astrophys. J., 190,175 (1974).

[23]D. F. Smith, Adv. Astr. and Phys., 2, 141 (1970).

[24]P. A. Sturrock, AAS-NASA Symposium on Physics of Solar Flares, ed. W. N. Hess (NASA-SP 50) (1962), page 357.

[25]V. V. Zaitsev, N. A. Mityakov, V. O. Rapoport, Solar Physics, 26, 444 (1972).

[26]R. A. Smith, M. L. Goldstein, K. Papadopoulos, "On the Theory of the Type III Burst Exciter," preprint (1975).

[27]G. Magelssen, "Inhomogeneous Quasilinear Theory of Electron Streams during Type III Radio Bursts," Ph.D. Thesis, University of Colorado (1976).

[28]K. Papadopoulos, T. Coffey, J. Geophys. Res., 79, 674 and 1558 (1974).

[29]D. L. Montgomery, M. Pogratz, K. Papadopoulos, J. Geophys. Res., 81, 123 (1976).

[30]Jon Frihagen (ed.), Electron Density Profiles in the Ionosphere and Exosphere, Amsterdam, North Holland Publishing, n. d.

[31]K. Nishikawa, Y. C. Lee, P. K. Kaw, Phys. Fluids, 16, 1380 (1973).

[32]E. Valeo, C. Oberman, F. W. Perkins, Phys. Rev. Lett. 28, 340 (1972).

[33]B. H. Quon, A. Y. Wong, B. H. Ripin, Phys. Rev. Lett., 32, 406 (1974).

[34]A. Y. Wong, B. H. Quon, Phys. Rev. Lett., 34, 1499 (1975).

BIBLIOGRAPHY

Bardwell, S., M. V. Goldman, Astrophys. J., in press.

Bloembergen, N., Nonlinear Optics, New York, W. A. Benjamin, Inc. (1965).

Davidson, R. C., Methods in Non-Linear Plasma Theory, New York, Academic Press, Inc. (1972).

Drake, J. F., P. K. Kaw, Y. C. Lee, G. Schmidt, C. S. Lin, M. N. Rosenbluth, Phys. Fluids, 17, 778 (1974).

DuBois, D. F., V. Gilinsky, M. G. Kivelson, Phys. Rev., 129, 2376 (1963).

DuBois, D. F., M. V. Goldman, Phys. Rev. Lett., 14, 544 (1965).

_____, Phys. Rev. Lett., 19, 1105 (1967).

_____, Phys. Rev., 164, 207 (1967).

_____, Phys. Rev. Lett., 28, 218 (1972).

_____, Phys. Fluids, 16, 2257 (1973).

Falk, L. R., V. N. Tsytovich, Physica Scripta, , (1975).

Faraday, M., Phil. Trans. Royal Soc., 121, 299 (1831).

Fejer, J. A., J. Geophys. Res., 76, 284 (1971).

Fried, B. D., S. D. Conti, The Plasma Dispersion Function, New York, Academic Press, Inc. (1961).

Fried, B. D., R. W. Gould, Phys. Fluids, 4, 139 (1961).

Fried, B. D., T. Ikemura, K. Nishikawa, G. Schmidt, UCLA preprint, PPG-246 (1975).

Frihagen, Jon (ed.), Electron Density Profiles in the Ionosphere and Exosphere, Amsterdam, North Holland Publishing, n. d.

Goldman, M. V., Annals of Physics (N. Y.), 38, 95 (1965).

Goldman, M. V., "Nonlinear Waves and Fluctuations in Plasmas," University of Colorado, Dept. of Astrogeophysics (1974).

Goldman, M. V., D. F. DuBois, Phys. Fluids, 8, 1404 (1965).

Gorbunov, L. M., Soviet Physics--JETP, 28, 1220 (1969).

Gorbunov, L. M., V. P. Silin, Tech. Physics, 14, 1 (1969).

Hasegawa, A., Phys. Rev. A, 1, 1747 (1970).

Kainer, S., J. M. Dawson, Phys. Fluids, 15, 2433 (1972).

Kaplan, S. A., V. N. Tsytovich, Svoiet Astr.--AJ, 11, 956 (1968).

Kruer, W. L., Phys. Fluids, 15, 2433 (1972).

Kruer, W. L., J. M. Dawson, T. Coffey, Phys. Fluids, 15, 2419 (1972).

Kuri, A. Yu., Soviet Physics--JETP, 31, 538 (1970).

Lin, C. S., K. Nishikawa, P. K. Kaw, W. L. Kruer, Advances in Plasma Physics, vo ume 6, New York, Wiley--Interscience Pubs. (1955).

Lin, R. P., L. G. Evans, J. Fainberg, Astrophys. Lett., 14, 1754 (1968).

Louisell, W. H., Coupled Modes and Parametric Electronics, New York, John Wiley and Sons, Inc. (1960).

Magelssen, G., "Inhomogeneous Quasilinear Theory of Electron Streams during Type III Radio Bursts," Ph.D. Thesis, University of Colorado (1976).

Melde, F., Ann. Physik Chemie, series 2, 109, 193 (1859).

Nishikawa, K., J. Phys. Soc. Japan, 24, 916, 1152 (1968).

Nishikawa, K., Y. C. Lee, P. K. Kaw, Phys. Fluids, 16, 1380 (1973).

O'Neil, T. M., J. H. Malmberg, Phys. Fluids, 11, 1754, (1968).

Papadopoulos, K, G. L. Goldstein, R. A. Smith, Astrophys. J., 190, 175 (1974).

Papadopoulos, K., T. Coffey, J. Geophys. Res., 79, 674 (1974).

Papadopoulos,K., T. Coffey, J. Geophys. Res., 79, 1558 (1974).

Perkins, F. W., P. K. Kaw, J. Geophys. Res., 76, 282 (1971).

Perkins, F. W., C. Oberman, E. J. Valeo, J. Geophys. Res., 79, 1478 (1974).

Quon, B. H., A. Y. Wong, B. H. Ripin, Phys. Rev. Lett., 32, 406 (1974).

Rayleigh, John William Strutt (Lord), Phil. Mag., series 5, 16, 50 (1883).

Sanmartin, J. R., Phys. Fluids, 13, 1533 (1970).

Silin, V. P., Soviet Physics--JETP, 21, 1127 (1965).

Smith, D. F., Adv. Astr. and Phys., 2, 141 (1970).

Smith, R. A., M. L. Goldstein, K. Papadopoulos, "On the Theory of the Type III Burst Exciter," preprint (1975).

Sturrock, P. A., AAS-NASA Symposium on Physics of Solar Flares, ed. W. N. Hess (NASA-SP 50) (1962).

Tsytovich, V. N., Nonlinear Effects in Plasmas, New York, Plenum (1970).

Valeo, E., C. Oberman, F. W. Perkins, Phys. Rev. Lett., 28, 340 (1972).

Vedenov, A. A., L. J. Rudakov, Dokl. Akad. Nauk. SSSR, 159, 738 (1964).

Wong, A. Y., R. J. Taylor, Phys. Rev. Lett., 27, 644 (1971).

Wong, A. Y., B. H. Quon, Phys. Rev. Lett. 34, 1499 (1975).

Zaitsev, V. V., N. A. Mityakov, V. O. Rapoport, Solar Physics, 26, 444 (1972).

Zakharov, V. E., Soviet Physics--JETP, 35, 908, (1972).

Zheleznyakov, V. V., V. V. Zaitsev, Soviet Astr.--AJ, 14, 47 (1970).

APPENDIX

DERIVATION OF THE SUSCEPTIBILITIES

The method used here to derive the susceptibilities is due to unpublished work by Martin V. Goldman. We begin with a fluid equation for $\underline{v}$ as a function of $\underline{E}$; all other fields and densities have been eliminated:

$$\begin{aligned}\underline{v}(K) = {} & \underline{\underline{T}}(K)\cdot\underline{E}(K) + \int dK_{12}\left(\frac{\underline{k}_2}{\omega_2}-\frac{\underline{k}}{\omega}\right)\cdot\underline{\underline{T}}(K)\cdot\underline{v}(K_1)\cdot\underline{E}(K_2) \\ & + \frac{im}{e}\int dK_{12}\,\underline{v}(K_1)\cdot\underline{k}_2\left[\underline{\underline{T}}(K)\cdot\underline{v}(K_2) + \frac{ie}{m\omega_2}\,T(K)\cdot E(K_2)\right] \\ & + \frac{im}{e\omega}\int dK_{12}\,\underline{k}\cdot\underline{\underline{T}}(K)\,\underline{v}(K_1)\cdot\underline{v}(K_2)\,\omega_2 \\ & + \frac{im}{e\omega}\,\underline{k}\cdot\underline{\underline{T}}(K)\int dK_{123}\,\underline{v}(K_1)\cdot\underline{v}(K_3)\;\underline{k}_3\cdot\underline{v}(K_2)\end{aligned} \tag{A.1}$$

where:

$$K \equiv k,\omega \quad ; \quad \underline{\underline{T}}(K) = -\frac{ie}{m\omega}\left(\underline{\underline{1}} + \frac{\underline{k}\,\underline{k}\,\gamma v_e^2}{\omega^2-\gamma v_e^2 k^2}\right);$$

$$dK_{12} = \frac{d^3k_1\,d\omega_1\,d^3k_2\,d\omega_2}{(2\pi)^8}\;\delta^3(\underline{k}-\underline{k}_1-\underline{k}_2)\,\delta(\omega-\omega_1-\omega_2);$$

$$dK_{123} = \frac{d^3k_1\,d\omega_1\,d^3k_2\,d\omega_2\,d^3k_3\,d\omega_3}{(2\pi)^{12}}\;\delta^3(\underline{k}-\underline{k}_1-\underline{k}_2-\underline{k}_3)\,\delta(\omega-\omega_1-\omega_2-\omega_3).$$

The strategy is now to calculate the various terms in the expansion of the velocity in terms of the field, use that in the integral for the current, and then group terms by powers of E to find the various susceptibilities:

$$\underline{v}^{(1)}(K) = \underline{\underline{T}}(K)\cdot E(K)\,; \tag{A.2}$$

$$\underline{v}^{2}(K) = \frac{\underline{k}\cdot\underline{T}(K)}{2}\int dK_{12}\left\{\frac{2mi}{e}\left[\underline{T}(K_1)\cdot\underline{E}(K_1)\right]\cdot\left[\underline{T}(K_2)\cdot\underline{E}(K_2)\right]\right.$$

(A.3)

$$\left. - \frac{\underline{E}(K)}{\omega}\cdot\left[\underline{T}(K_1)+\underline{T}(K_2)\right]\cdot\underline{E}(K_2)\right\}$$

Now:

$$\underline{j}^{(2)}(K) = -e\int dK_{12}\left[n^{(0)}(K_1)v^{(2)}(K_2) + n^{(1)}(K_1)\,v^{(1)}(K_2)\right]$$

$$= -\frac{en_e}{2}\int dK_{12}\left\{\frac{im}{e}\,\underline{k}\cdot\underline{T}(K)\underline{E}(K_1)\cdot\left[2\underline{T}(K_1)\cdot\underline{T}(K_2)+\frac{ie}{m\omega}\left(\underline{T}(K_1)+\underline{T}(K_2)\right)\cdot\underline{E}(K_2)\right.\right.$$

(A.4)

$$+\underline{T}(K_1)\cdot\underline{E}(K_1)\left[\frac{\underline{k}_2}{\omega_2}\cdot\underline{T}(K_2)\cdot\underline{E}(K_2)\right]$$

$$\left.\left.+\underline{T}(K_2)\cdot\underline{E}(K_2)\left[\frac{\underline{k}_1}{\omega_1}\cdot\underline{T}(K_1)\cdot E(K_1)\right]\right.\right.\,.$$

Comparing this with the definition:

(A.5) $$j_{\ell}^{(2)}(K) = -i\omega\int dK_{12}\;\chi(K,K_1,K_2)\cdot E_m(K_1)\cdot E_n(K_2)\,\hat{e}_{\ell}$$

we get:

$$\chi(K,K_1,K_2) = \frac{4\pi i e^3 n_e}{2m^2\omega\omega_1\omega_2}\left\{\frac{i\underline{k}\cdot\underline{T}(K)\cdot\hat{e}_m}{e\omega}\left[-\frac{2\omega\omega_1\omega_2\,\hat{e}_1\cdot\underline{T}(K_1)\cdot\underline{T}(K_2)\cdot\hat{e}_2\,m^2}{e^2}\right.\right.$$

(A.6)

$$\left.-\frac{i\omega_2\omega_1\,\hat{e}_1\cdot\underline{T}(K_1)\cdot\hat{e}_1 m}{e}-\frac{i\omega_1\omega_2\,\hat{e}_1\cdot\underline{T}(K_2)\cdot\hat{e}_2}{e}\right]$$

$$\left.-\frac{m^2k_1\cdot T(K_1)\cdot\hat{e}_1\,\hat{e}_k\cdot\underline{T}(K_2)\cdot\hat{e}_2}{e^2}-\frac{i\omega_1 m^2 k_2\cdot T(K_2)\cdot\hat{e}_2\,\hat{e}_k\cdot T(K_1)\cdot\hat{e}_1}{e^2}\right\},$$

and since two of these frequencies will always be high, we have for any instability:

$$\chi(K,K_1,K_2)\Big|_{\substack{\omega_1\gg v_e k_1\\ \omega_2\gg v_e k_2}} = \frac{4\pi i e^3 n_0}{2m\,\omega\omega_1\omega_2}\left\{\frac{k\cdot\hat{e}_k\,\hat{e}_1\cdot\hat{e}_2}{\omega}\,\frac{1}{1-\gamma v_e^2k^2/\omega^2}\right.$$

(A.7)

$$\left.+\frac{k_1\cdot\hat{e}\,\hat{e}_k\cdot\hat{e}_2}{\omega_1}+\frac{k_2\cdot\hat{e}_2\,\hat{e}_k\cdot\hat{e}_1}{\omega_2}\right\}.$$

Where the $\hat{e}_i$ are the polarization vectors of the fields $E(k_i)$. For the case when one of the fields is a low

frequency field, only one term contributes:

$$\chi(K \pm K_0, \pm K_0, K) = \frac{e^3 n_0 4\pi i}{2m^3 \omega \omega_b (\omega_b \pm \omega)} \left\{ \frac{k\,\omega}{k^2 v_e^2} \right\} \left\{ \frac{\underline{k}_0 \cdot (\underline{k} \pm \underline{k}_0)}{k_0 |k \pm k_0|} \right\} . \tag{A,8}$$

The third-order velocity is gotten similarly and consists of seven integrals, which must be then substituted in the expression for the third-order current. The integrals which are dominant for the case of two high frequency waves are:

$$\begin{aligned} \underline{j}^{(3)}(K) = -\frac{ie^3 n_0}{4m} \Bigg\{ \int dK_{123} \; & \frac{T(K_3)\cdot E(K_3)\,(k-k_3)\cdot T(K-K_3)\cdot(k-k_3)\,E(K_1)\cdot E(K_2)}{\omega_2(\omega-\omega_3)} \\ & + \frac{T(K_3)\cdot E(K_3)\,(k-k_3)\cdot T(K-K_3)\cdot(k-k_3)\,E(K_1)\cdot E(K_2)}{\omega_1(\omega-\omega_3)} \\ & + \frac{T(K_1)\cdot E(K_1)\,(k-k_1)\cdot T(K-K_1)\cdot(k-k_1)\,E(K_2)\cdot E(K_3)}{\omega_2(\omega-\omega_1)} \\ & + \frac{T(K_1)\cdot E(K_1)\,(k-k_1)\cdot T(K-K_1)\cdot(k-k_1)\,E(K_3)\cdot E(K_2)}{\omega_3(\omega-\omega_1)} \\ & + \frac{T(K_2)\cdot E(K_2)\,(k-k_2)\cdot T(K-K_2)\cdot(k-k_2)\,E(K_3)\cdot E(K_1)}{\omega_3(\omega-\omega_2)} \\ & + \frac{T(K_2)\cdot E(K_2)\,(k-k_2)\cdot T(K-K_2)(k-k_2)\,E(K_1)\cdot E(K_2)}{\omega_1(\omega-\omega_2)} \Bigg\} . \end{aligned} \tag{A.9}$$

Comparing this expression with the definition of the third-order susceptibilities, and using a travelling wave pump, we find:

$$\begin{aligned} & \chi(K \pm K_0, K_0, \mp K_0, K - K_0) \\ & \quad = \frac{4\pi i e^4 n_0}{4m^3(\omega_b \pm \omega)(\omega - \omega)\omega_b^2 v_e^2}\; \hat{e}_0 \cdot \hat{e}_\pm\, \hat{e}_0 \cdot \hat{e}_- \end{aligned} \tag{A.10}$$

and:

$$\begin{aligned} & \chi(K \pm K_0, K_0, \mp K_0, K + K_0) \\ & \quad = \frac{4\pi i e^4 n_0}{4m^3(\omega_0 \pm \omega)(\omega_0 + \omega)\omega_b^2 v_e^2}\; \hat{e}_0 \cdot \hat{e}_\pm\, \hat{e}_0 \cdot \hat{e}_+ \end{aligned} \tag{A.11}$$

We also note here some symmetry properties of these susceptibilities, which can be derived from either the integral definitions of the susceptibilities, or from the explicit forms we found for them:

(A.12) $$\chi_{lmn}(K,K_1,K_2) = \chi_{lnm}(K,K_2,K_1)$$

(A.13) $$\begin{aligned}\chi_{lmnp}(K,K_1,K_2,K_3) &= \chi_{lmpn}(K,K_1,K_3,K_2)\\ &= \chi_{lmnp}(K,K_2,K_1,K_3)\\ &= \chi_{lpnm}(K,K_3,K_2,K_1)\,.\end{aligned}$$

And, using the these relations:

(A.14a) $$\chi_{lmn}(-K,-K_1,-K_2) = \chi^{*}_{lmn}(K,K_1,K_2) = \chi_{nml}(K_2,-K_1,K);$$

(A.14b) $$\chi_{lmn}(-K,K_1,K_2) = \chi_{nml}(-K_2,K_1,K) = \chi_{mln}(-K_1,K,K_2).$$